SSD 102.3

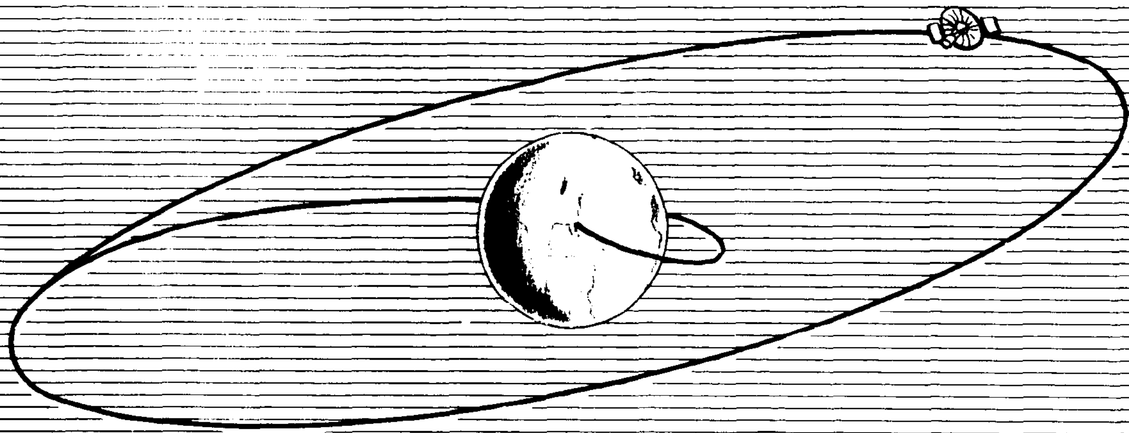

FACILITY FORM 602

N67-24607
(ACCESSION NUMBER)

139
(PAGES)

CR-81599
(NASA CR OR TMX OR AD NUMBER)

1
(THRU)

(CODE)

31
(CATEGORY)

VOLUME 4 OF 8

Final Report

ATS-4

PREPARED BY

FAIRCHILD HILLER
SPACE SYSTEMS DIVISION

FOR

NASA
Goddard Space Flight Center

DECEMBER 1966

SSD 102.3

ATS-4 STUDY PROGRAM

FINAL REPORT

(Contract NASW-1411)

VOLUME FOUR OF EIGHT

prepared by

FAIRCHILD HILLER SPACE SYSTEMS DIVISION

Sherman Fairchild Technology Center

Germantown, Maryland

for

GODDARD SPACE FLIGHT CENTER

NATIONAL AERONAUTICS AND SPACE ADMINISTRATION

December 1966

TABLE OF CONTENTS

VOLUME ONE

TABLE OF CONTENTS

VOLUME TWO

TABLE OF CONTENTS

VOLUME THREE

TABLE OF CONTENTS

VOLUME THREE (Continued)

TABLE OF CONTENTS

VOLUME FOUR

TABLE OF CONTENTS

VOLUME FOUR (Continued)

TABLE OF CONTENTS

VOLUME FIVE

TABLE OF CONTENTS

VOLUME SIX

TABLE OF CONTENTS

VOLUME SEVEN

TABLE OF CONTENTS

VOLUME SEVEN (Continued)

LIST OF ILLUSTRATIONS

VOLUME ONE

LIST OF ILLUSTRATIONS

VOLUME TWO

LIST OF ILLUSTRATIONS

VOLUME THREE

LIST OF ILLUSTRATIONS

VOLUME THREE (Continued)

LIST OF ILLUSTRATIONS

VOLUME THREE (Continued)

LIST OF ILLUSTRATIONS

VOLUME THREE (Continued)

LIST OF ILLUSTRATIONS

VOLUME FOUR

LIST OF ILLUSTRATIONS

VOLUME FOUR (Continued)

LIST OF ILLUSTRATIONS

VOLUME FIVE

LIST OF ILLUSTRATIONS

VOLUME FIVE (Continued)

LIST OF ILLUSTRATIONS

VOLUME SIX

LIST OF ILLUSTRATIONS

VOLUME SIX (Continued)

LIST OF ILLUSTRATIONS

VOLUME SIX (Continued)

LIST OF ILLUSTRATIONS

VOLUME SEVEN

LIST OF ILLUSTRATIONS

VOLUME SEVEN (Continued)

LIST OF ILLUSTRATIONS

VOLUME SEVEN (Continued)

PREFACE

This report covers the efforts of Fairchild Hiller Corporation and its team of subcontractors on NASA Contract (NAS-W-1411). The team organization and responsibilities during the study effort are shown on the accompanying chart. The report is divided into eight volumes, as follows:

Volume 1	Summary
Volume 2	Systems Analysis
Volume 3	Vehicle Engineering
Volume 4	Power System
	Orbital Analyses, Propulsion and Guidance
Volume 5	Stabilization and Control
Volume 6	Communication Experiments
Volume 7	Radio Interferometer Experiment
	Telemetry and Command Systems
Volume 8	Program Budgetary Costs and Schedules

ATS-4 TEAM ORGANIZATION

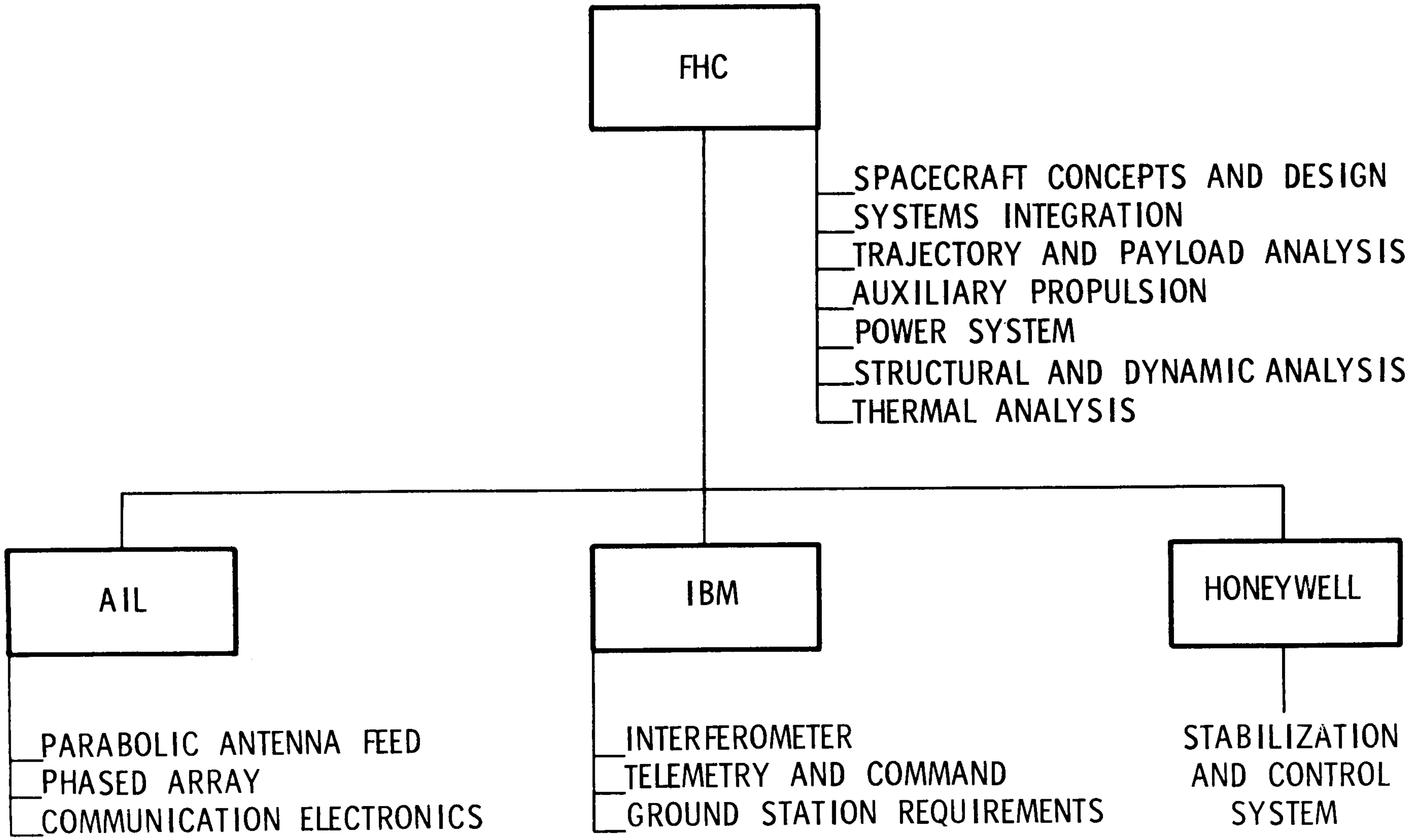

A-1

4.0 POWER SUBSYSTEM

Spacecraft power requirements in terms of magnitude, duration, and sequence determine the type and configuration of the most suitable system. At the outset, it may be stated that implementation of the concept experiments is easily accommodated by a solar power system.

Should the experiment mission demands be scaled upward in the future, such as addition of high power communications transmitters, SNAP power might be required. It is evident that the impact of such a change on spacecraft design would be considerable. Up to peak power demand on the order of 1 kw, solar power is likely to remain the best choice from the standpoints of weight, cost, and development time.

The concept solar power system discussed in Section 4. 5 is based on consideration of battery and solar panel characteristics, which are reviewed in Section 4. 1 through 4. 4. Load duty factor effects are briefly discussed in Section 4. 5.

4.1 SOLAR PANEL CONFIGURATION STUDY

A study of several solar panel configurations to determine their power output vs time characteristics over the orbital period has been completed. (Figures 4.1-1 through 4.1-9). The analysis is based on purely geometrical considerations. Results expressed in terms of the normalized power output per unit panel area (array factor) allow comparison of the arrangements. While shadow effects are not included, the results are meaningful in interpreting panel area requirements as a function of gross configuration.

The general configurations considered are compared on a per unit area basis; the per unit effective area figure on the following graphs is the array factor for that configuration. Both oriented and fixed panels are considered. Only the flat plate is included in the oriented array since deviations from this are compromises due to vehicle packaging limitations. One and two degrees of freedom were considered and it was found that two degrees of freedom provide very little added capability over a single degree of freedom. The fixed panel plots for this earth oriented synchronous orbit vehicle are shown in the graphs and in general have an array factor of 0.3. The effect of solstice is shown by the dash curves. Increasing of the number of panels reduces the swing between maximum and minimum and increases the frequency of this cycling. Since a constant power availability is desirable, the multi-face version of the fixed panels is favored.

From a power system standpoint, the most desirable of the configurations is the single degree of movement flat plate, which requires an orienting system with a long lifetime (undesirable). The best of the fixed configurations for this orbit is a cylinder. It is realized that a cylindrical configuration presents fabrication problems and thus flat plates become the practical solution. The number of flat plates utilized is greatly

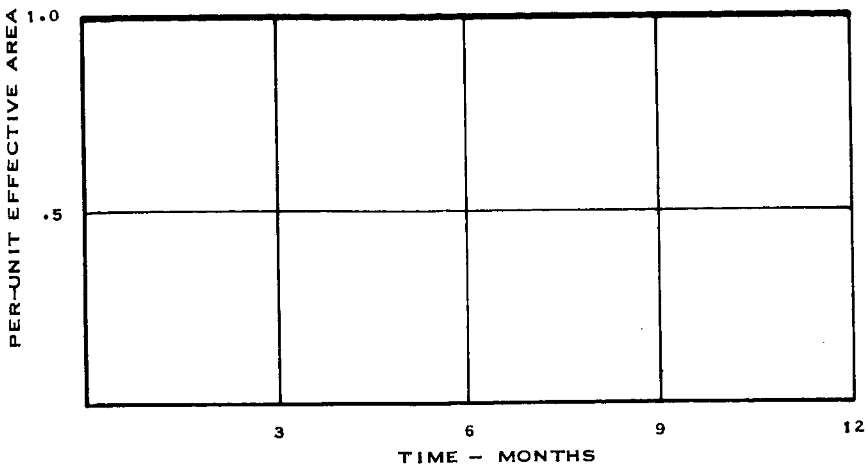

Figure 4.1-1 Flat Plate Array 2 Degrees of Freedom

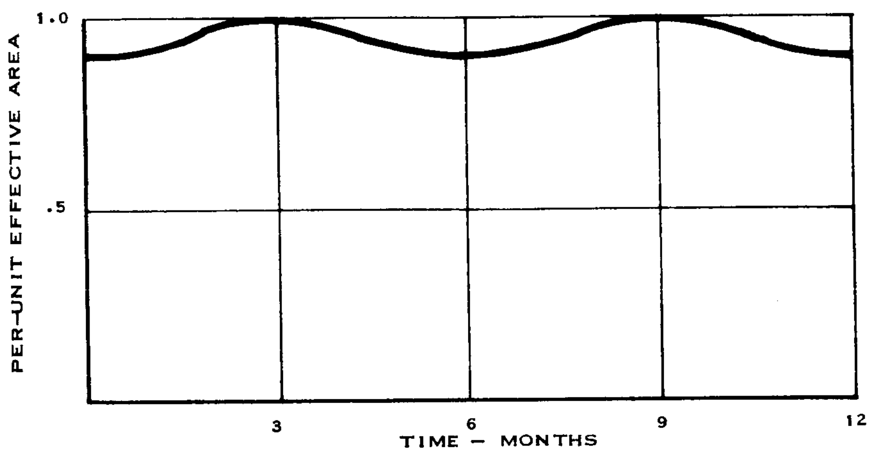

Figure 4.1-2 Flat Plate Array 1 Degree of Freedom

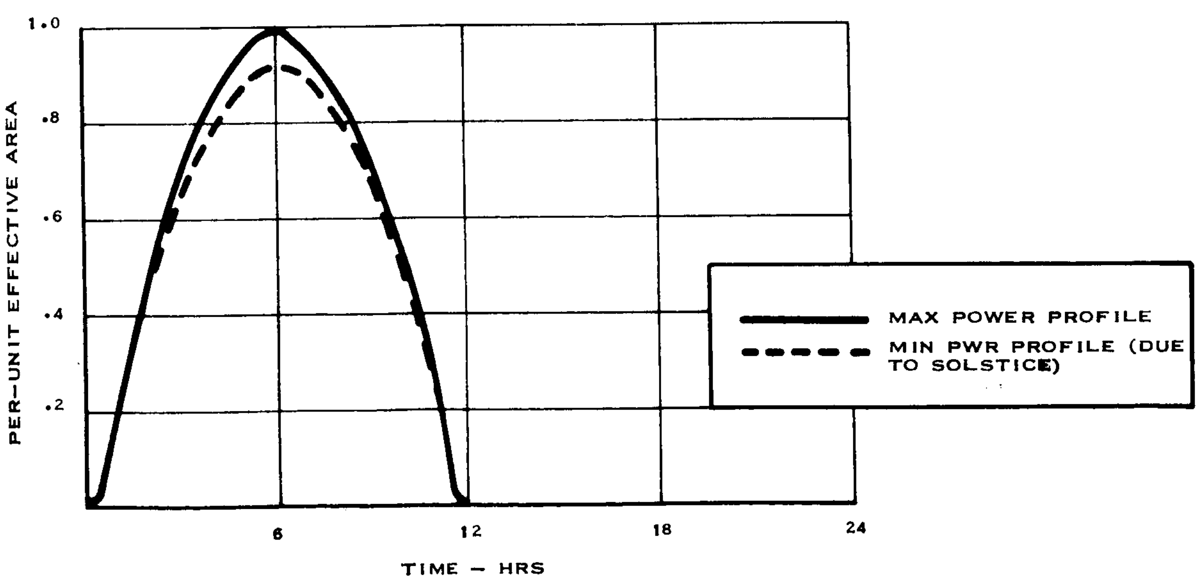

Figure 4.1-3 Fixed Flat Plate Array

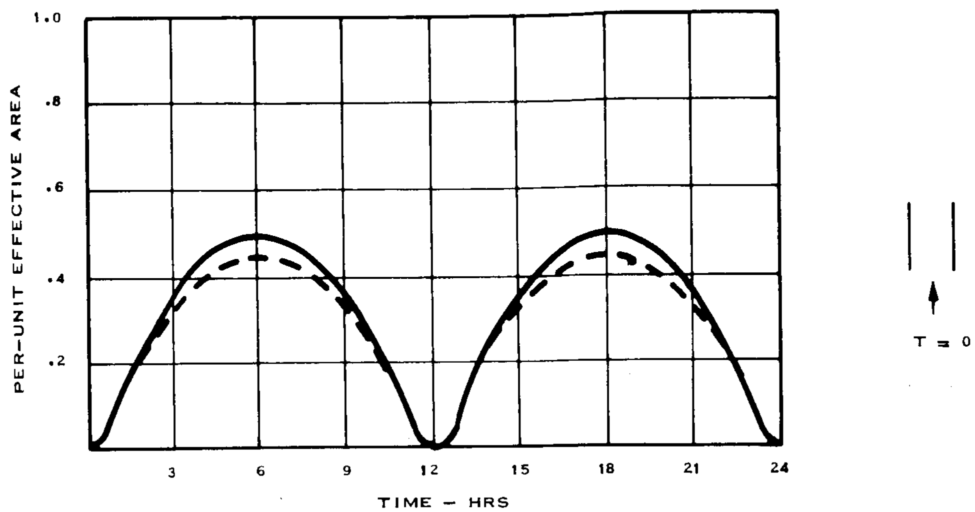

Figure 4.1-4 Two Flat Plate Arrays-Fixed

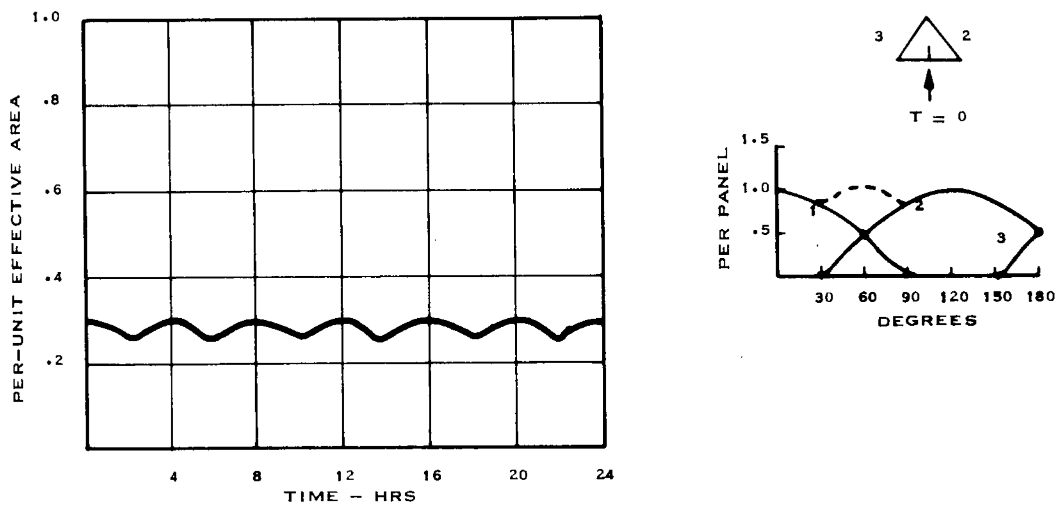

Figure 4.1-5 Three Flat Plate Arrays-Fixed

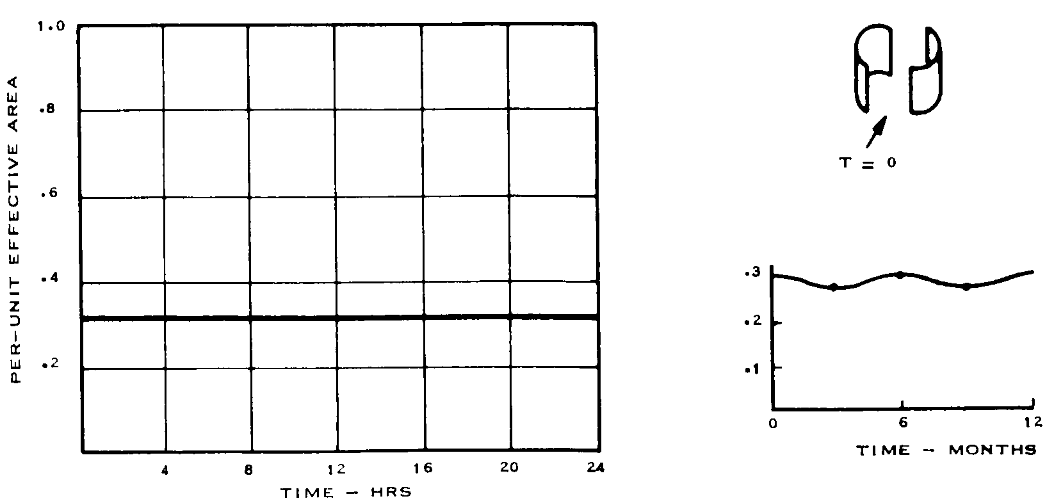

Figure 4.1-6 Fixed Cylindrical Array

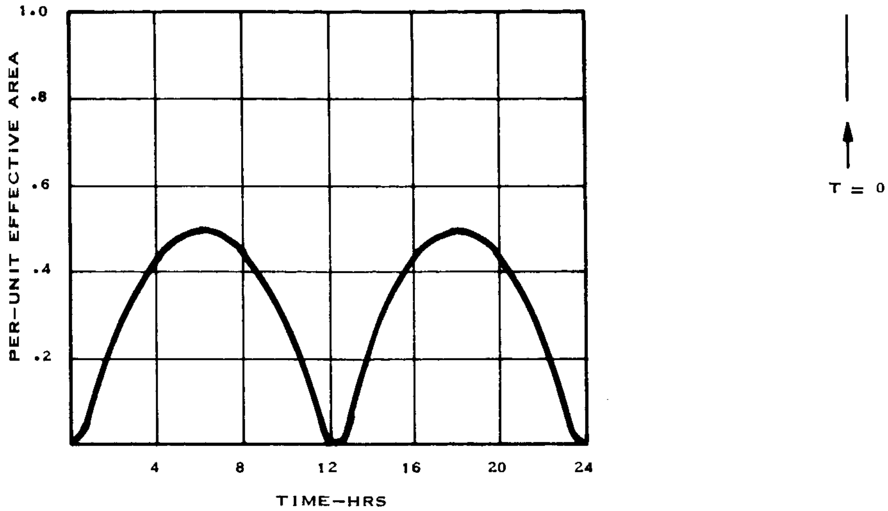

Figure 4.1-7 Double Faced Flat Plate Array

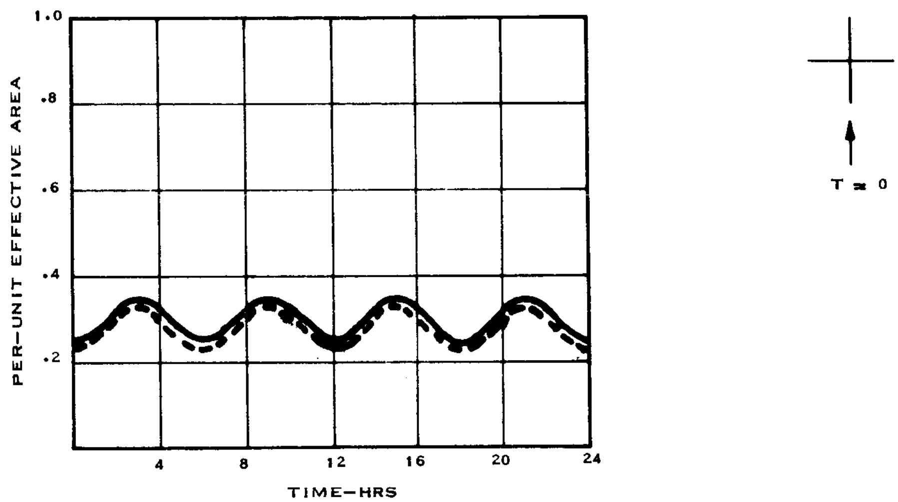

Figure 4.1-8 Double Faced Flat Plate Array

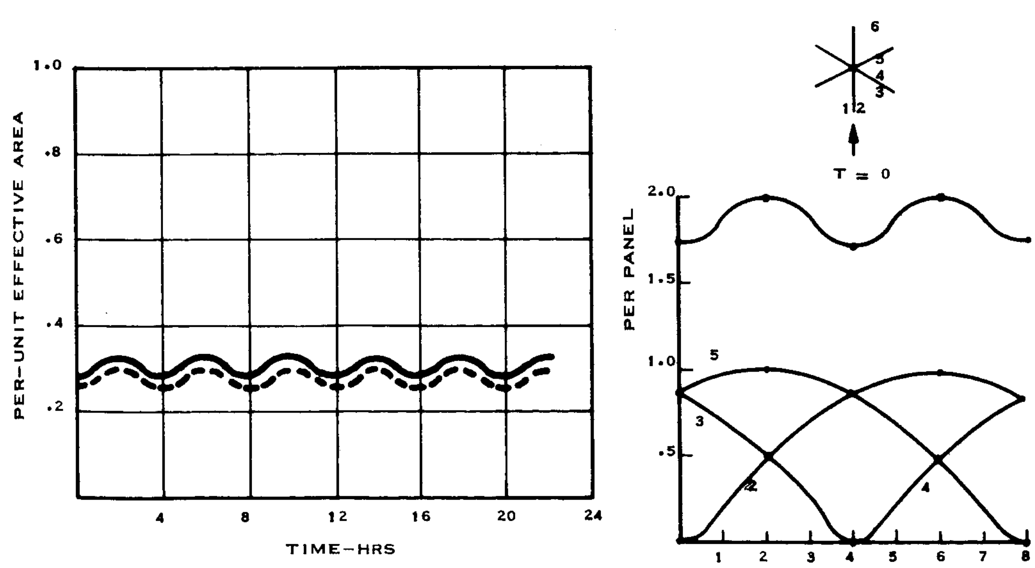

Figure 4.1-9 Double Faced Flat Plate Array

dependent upon vehicle configuration but three faces appear to be a minimum to reduce the variation in power availability thus reducing the waste area due to this variation. The array factor of approximately .3 holds for both faced cylindrical and double faced crossed panels and approaches $1/\pi$ as the number of panels is increased.

A selection of solar panel configuration (the cruciform: two double-faced panels) has been made based upon power requirements, vehicle configuration and maximum system flexibility for possible future power increase with minimum weight, volume and configuration changes. The selected array configuration is discussed in Section 4.5 Concept Power Subsystem.

4.2 SOLAR CELL RADIATION DEGRADATION

Cell output decreases with time as a function of total radiation damage. Figure 4.2-1 illustrates this effect for 10 ohm - cm, N on P, silicon cells subject to 1 Mev electron irradiation. Total particle radiation is composed of natural background and solar flare activity. A conservative estimate of the worst degradation occuring over a two year period must be based on the integrated background flux, and the highest estimate of flare activity during the period.

4.2.1 Radiation Environment Marked differences in the radiation environment for synchronous orbit in the 1969 - 1970 time period have been noted for various projects. The Large Aperture Antenna RFP GSFC No. 733-85037/235 estimates the environment as follows:

Particle	Particle Energy Electron Volts	2 Year Integrated Flux, Particles/cm^2
Electrons	$\geq 1.6 \times 10^6$ $\geq 40 \times 10^3$	2×10^{11} 2×10^{15}
Protons	0.1×10^6 to 5×10^6 $\geq 30 \times 10^6$	2×10^{15} 4×10^8

"Radiation Due to Solar Flares. It is expected that during the two year period in orbit, solar flares of 3+ magnitude, yielding an integrated flux of 5 x 10^9 particles/cm^2/event, will occur. Over this two year period, the total flux of protons having energies greater than 12 x 10^6 electron volts is expected to be 1.3 x 10^{12} protons/cm^2."

"The Natural Environment at Synchronous Orbital Altitude", a special technical report prepared for the Space Systems Division, AFSC as part of RFP No. 04-695-66-208 dated June 20, 1966 presents the radiation environment as follows:

Particle	Energy Range Electron Volts	Flux Particles/in^2/sec	2 Yr. Flux Particles/in^2
Electron	>1.6 x 10^6	3 x 10^5	1.9 x 10^{13}
	>40 x 10^3	3 x 10^7	1.0 x 10^{15}
Proton	$0.1 \leq E_p \leq 5 \times 10^6$	10^7	6.3 x 10^{14}
	$\geq 40 \times 10^6$	10^2	6.3 x 10^9

The solar flare activity during the two year period is predicted as yielding a proton flux as follows:

> 100 MEV	5.6 x 10^8	protons/in^2/yr.
> 30 MEV	4 x 10^9	protons/in^2/yr.
> 0 MEV	1.06 x 10^{10}	protons/in^2/yr.

The difference between these references in solar flare proton flux level alone is two orders of magnitude. These differences may be due in part to a variation in desired design margins.

4.2.2 Background Flux

The trapped radiation environment used for this study is based upon the work of J. Vette; figures employed correspond to integrated rates

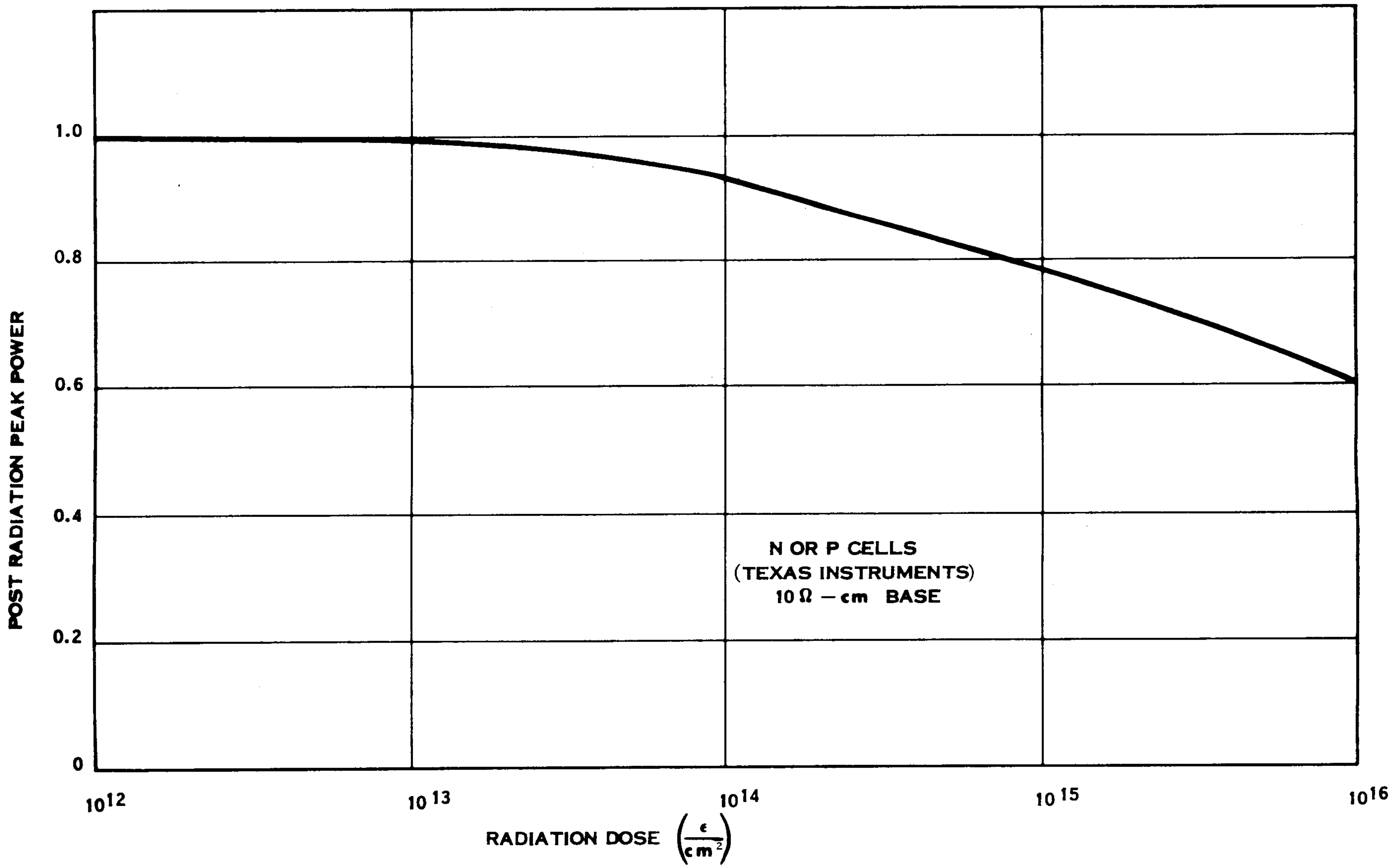

Figure 4.2-1 Solar Cell Radiation Degradation

at 2.9 earth radii. Based upon this altitude the dose rate should be sufficiently conservative since the trapped radiation decreases beyond this point. At 2.9 earth radii the electron flux is found to be less than $10^5 \frac{e}{cm^2 \ sec}$ (1), which corresponds to a two year dose of $6.3 \times 10^{12} \frac{e}{cm^2}$. The proton dose is about $6.3 \times 10^8 \frac{p}{2}$ (2) which produces an equivalent damage of $1.3 \times 10^{12} \frac{e}{cm^2}$ (3).

Solar Flares - - Projecting 1969 - 1970 activity based on the 11 year cycle, a total of about 15 flares is expected to occur in those two years. Flare activity will produce a total dose of about 8.3×10^9 p/cm^2 per flare, equivalent to 1.7×10^{13} e/cm^2 per flare.

Worst Case Degradation Estimate - - Use of the 2.9 earth radii altitude background radiation figures at synchronous altitude (5.6 earth radii) is conservative. Assuming the cumulative flare activity will be 5-each on day 1, 10 on day 365, and 15 on day 730, renders a worst case estimate of power output early in the period. (See Table 4.2.1). Figure 4.2-2 illustrates the drop in power output resulting from the "worst case" particle radiation conditions above.

4.2.3 Power Margin

The power margin available for operation of secondary experiments, or increasing the frequency with which primary experiments can be operated, is also shown in Figure 4.2-2. Virtually all of the initial panel output is available up to 6 months, decreasing by 4% at one year and 13% at two years. Initial output of 8.9 watts/ft^2 is reduced to 7.8 watts/ft^2 at two years. Power conditioning further reduces this to 6.6 watts/ft^2 at the load bus.

---

(1) (2) Models of the Trapped Radiation Environment, NASA SP-3024 dated 1966 by J. Vette and direct correspondence with J. Vette of Aerospace Corporation

(3) Conversion figures based upon Handbook of Space-Radiation Effects on Solar Cells, NASA SP-3033, Cooley & Janda.

TABLE 4.2-1 SOLAR ACTIVITY

Day	Background		Flares		e/cm^2 Total Dose	Real Power
	electrons	protrons	no.	Electron Equiv.*		
1	$8.6 \times 10^9 e/cm^2$ Day	$1.72 \times 10^9 e/cm^2$ day $8.6 \times 10^5 p/cm^2$ day	5	8.5×10^{13}	8.5×10^{13}	.94
180	$1.55 \times 10^{12} e/cm^2$	$3.1 \times 10^{11} e/cm^2$	5	8.5×10^{13}	8.7×10^{13}	.93
365	$3.14 \times 10^{12} e/cm^2$	$6.28 \times 10^{11} e/cm^2$	10	1.7×10^{14}	1.74×10^{14}	.90
730	$6.28 \times 10^{12} e/cm^2$	$1.25 \times 10^{12} e/cm^2$	15	2.6×10^{14}	2.67×10^{14}	.87

* Indicated dosage due to flare activity is between that indicated for ASFC RFP No. 04-695-66-208 (June 1966) and GSFC RFP No. 733-85037/235.

4.3 BATTERY CHARACTERISTICS

Uninterrupted operation of ATS-4 electrical equipment is required, therefore, energy must be stored during sun-lit periods for use during darkness. Even with the nearly continuous illumination of the ATS-4 synchronous orbit, a storage system is necessary to accommodate periodic changes in power demand. Several types of secondary batteries may satisfy the energy storage required, but depending upon many other factors (i.e. life duration, number of cycles, weight and volume available, temperature, charge and discharge rate, etc.), only one will best satisfy all of the requirements. Table 4.3-1 is a comparison of different battery systems. Primary and secondary batteries are both included for comparison although not all are applicable to the spacecraft for different reasons, such as non-rechargeable, not sealable, low current only, etc. Three secondary battery types are considered as possibilities: nickel-cadmium, silver-cadmium, and silver-zinc.

It is concluded that the ATS-4 life and cycling requirement (4000 maximum over two years) is most conservatively met in the 1969-70 period by the nickel-cadmium battery. Confidence is enhanced by the considerable amount of experience accumulated with this type in space application, and by

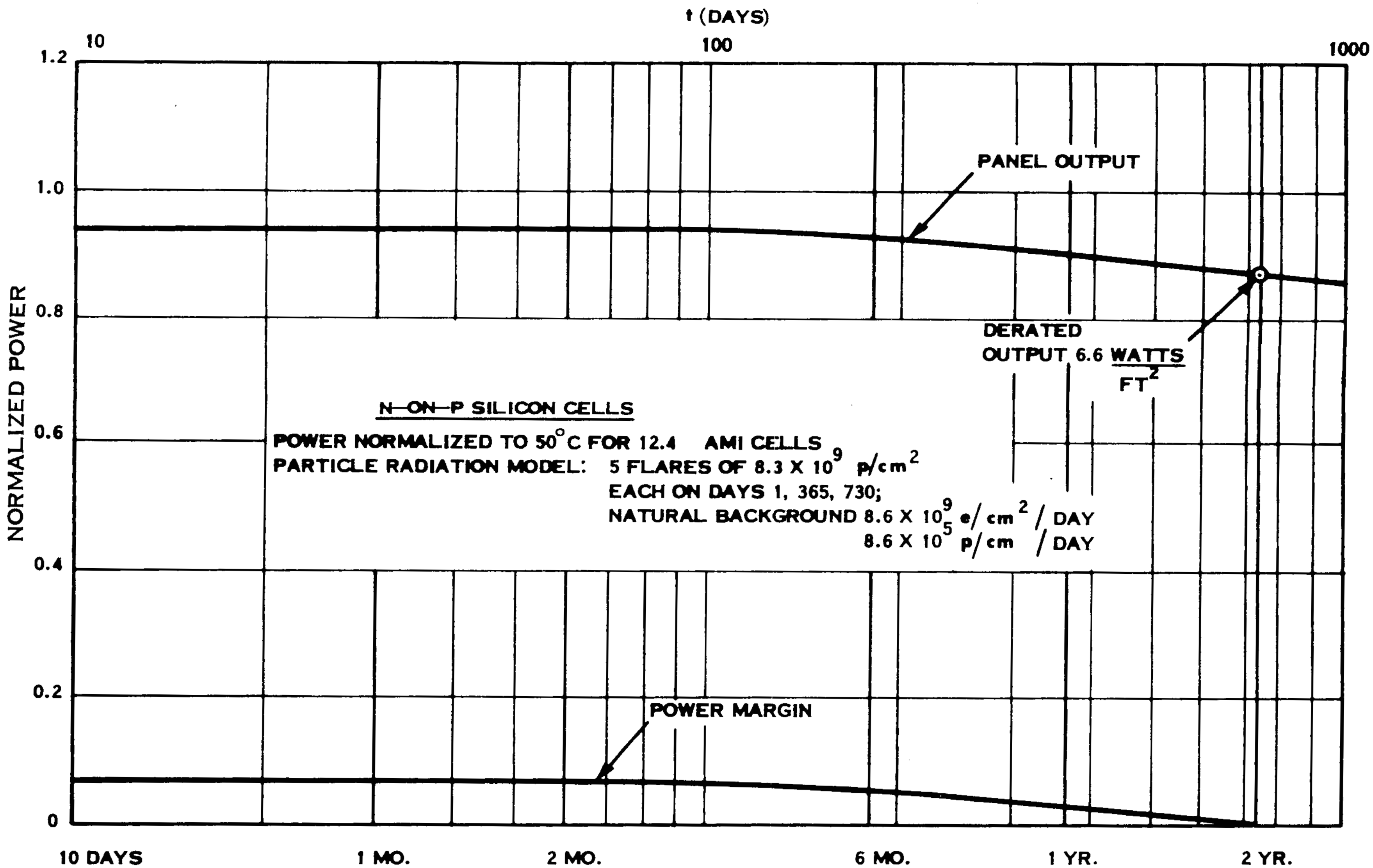

Figure 4.2-2 Power Loss Due to Radiation Effects

TABLE 4.3-1
BATTERY STORAGE SYSTEMS

		Type	Anode	Electrolyte	Cathode	Nominal Voltage of Basic Cell	Watt-hours/lb *	Watt-hours/cu-in. *	Voltage Regulation	Service Duty	Discharge Rate	Service Temperature (Dry Cells)	Cycle Life (Secondary Cells)	Watts-hours/dollar
PRIMARY	Ready (dry)	Leclanche'	Zn	$ClNH_4$ MnO_2 Cl_2Zn	C	1.5	10	1	Fair	Interm't	Low	30 to 90F		2-50
		Mercury	Zn	KOH	HgO C	1.34	30	5.0	Good	Interm't	Low	50 to 160F		0.7-14
		Alkaline dry cell	Zn	KOH	MnO_2	1.5	47	2.2	Good	Light	Low	40 to 90F		33
		Magnesium cell	Mg	MgBr	MnO_2	2.0	50	3.3	Fair	Light	Low			28
	Reserve (wet)	Lalande	Zn	NaOH CuO	CuO	0.8	20	0.94	Good	Light	Low			57
		Air cell	Zn	NaOH O_2-C	CuO	1.4	20	2.0	Good	Light	Low			75
		Water-activated cuprous-chloride	Mg	Water CuCl	CuCl	1.2	21	2.1	Good	Light	Low			
		Water-activated silver-chloride	Mg	Water AgCl	AgCl	1.4	47	5.0	Good	Heavy	High			
		Silver-zinc	Zn	KOH	AgO	1.5	70	5.6	Good	Heavy	High			
SECONDARY		Lead-acid	Pb	H_2SO_4 H_2O	PbO_2	2.0	12	1.1	Fair	Light	Med		200-2000	20
		Nickel-iron (Edison)	Fe	KOH	NiO_2	1.2	13	0.7	Good	Medium	Med		over 2000	5.7
		Nickel-cadmium (Jungner)	Cd	KOH	NiO_2	1.25	17	1.9	Good	Heavy	High		over 2000	2
		Silver-zinc	Zn	KOH	AgO	1.5	59	4.4	Good	Heavy	High		10-400	
		Silver-cadmium	Cd	KOH	AgO	1.1	32	2.6	Good	Heavy	High		300-1000	2

Energy/weight and energy/volume ratios correspond to 10-hr discharge rate for secondary batteries.

its successfully exceeding the ATS-4 performance requirements.

4.3.1 Nickel-Cadmium Battery

The nickel-cadmium cell is manufactured in two types of construction: pocket plate and sintered plate. The pocket plate is used in heavy duty batteries employed for terrestrial applications, whereas the sintered plate cell is capable of high rate cycling, lower in weight and more rugged in mechanical design which make it preferable for space use. In the sintered plate construction, the active materials (nickel oxide anode, cadmium metal cathode) are held in a highly porous thin flat plate made by sintering powders onto a screen or onto a perforated flat plate support. These flat plates are then rolled for the cylindrical type cell. Cellulose or polymeric woven or unwoven sheets are used as separator material between the closely packed sintered plates. Hermetic sealing of this battery and maintaining good overcharge characteristic is possible due to oxygen evolved at the nickel anode during overcharging migrating to the cadmium cathode where it is recombined. The cycle life of a sealed nickel cadmium battery, by comparison, is high, depending upon temperature and percentage of discharge. Figure 4.3-1 shows the cycle life of sealed nickel-cadmium cells as related to percent of discharge and cell temperature. Failure modes are overheating, separator and electrode degradation, electrode corrosion contamination, structural defects and leaks.

4.3.2 Silver-Cadmium Battery

The silver-cadmium secondary battery consists of a silver oxide cathode, a cadmium metal anode and an electrolyte of aqueous potassium hydroxide. The major advantage of the silver-cadmium system is its increased specific energy. Although the theoretical energy capability is 150 watt-hours per pound, 26 watt-hours per pound can be achieved in practical sealed units. The major disadvantages of the silver-cadmium system are

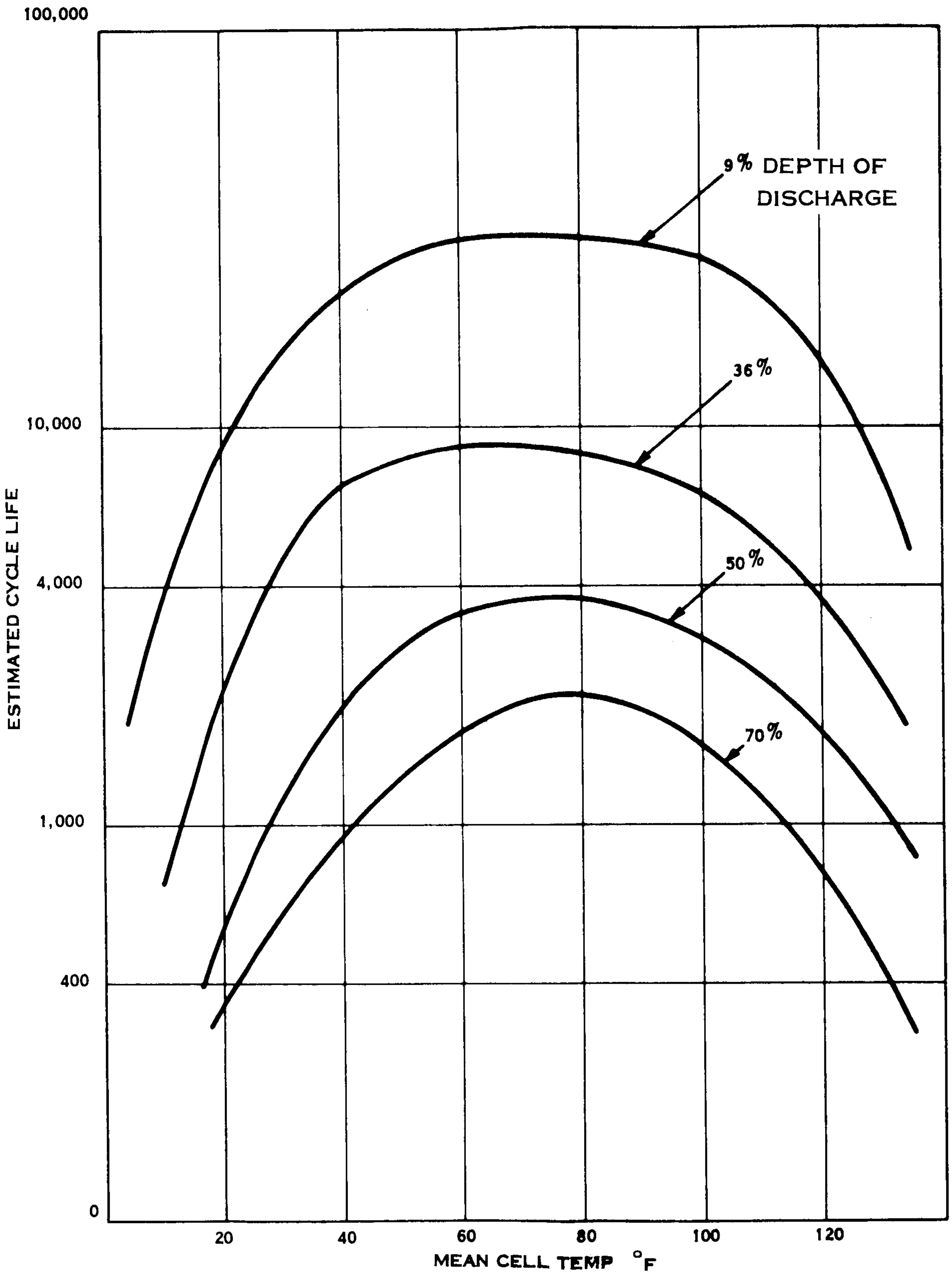

Figure 4.3-1 Ni-Cd Battery Life vs Discharge Depth and Temperature

limited cycle life, and deterioration of separators at elevated temperatures.

4.3.3 Silver-Zinc Battery

The silver-zinc rechargeable battery provides the greatest energy per unit weight and volume of the rechargeable types. Components of the silver-zinc secondary battery are similar to those of the silver-zinc primary battery: silver oxide cathode, zinc metal anode with an electrolyte of aqueous potassium hydroxide, except that the separator must be considerably thicker to inhibit migration of silver, and to prevent shorts caused by separator deterioration associated with an extended wet-life requirement. Hermetic sealing for space use is difficult because the zinc reacts with the electrolyte to form hydrogen, and, in addition, recombination of the oxygen evolved is not complete. Sealed cells, however, have been manufactured that can be operated at low charge-discharge rates, but they will not tolerate overcharge.

4.3.4 Battery Comparison

A capacity summary chart of the three types of batteries discussed is shown in Table 4.3-2. The automotive lead acid battery is included for comparison. The same type of information is presented in graph form in Figures 4.3-2, -3 and -4. The data presented in Table 4.3-2 and the following charts are based upon existing state-of-the-art. This information is considered a valid basis for conclusions applicable to a system for the late 1960s (67 - 70) due to the battery technologies steady rate of performance improvement. It can be readily seen from the graphs that for all of the battery types, high charge-discharge rates and elevated temperatures are disadvantageous to optimum battery utilization. Cycle life is a function of depth of discharge among many other factors, but maintaining these factors constant and varying only the depth of discharge, the variations in life for each of the three battery types are shown in Figures 4.3-5, -6, and -7.

TABLE 4.3-2
SECONDARY CELL TEMPERATURE-DISCHARGE CHARACTERISTICS

	Temperature (°F)	Discharge Rate (hours)	Lead-Acid	Nickel-Cadmium (Pocket Plate)	Nickel-Cadmium (Sintered Plate)	Edison (Nickel-Iron)	Silver-Zinc	Silver-Cadmium
Watt-hours per pound (Based on an Allowable Voltage Drop of 20 percent)	80	5	11.4	6	15	15	52.8	24.6
		1	8.4	4.8	11.6	9.5	45.8	19.8
		0.25	6.8	2.9	9.9	---	39	15.6
	0	5	5.4	4.2	11.5	---	39.4	20.9
		1	3.9	3.1	9.9	---	33	16.6
		0.25	2.9	1.7	8.7	---	24.6	12.1
	-40	5	3.7	3.2	9	---	---	10.7
		1	2.5	2.4	8.4	---	---	7.7
		0.25	1.5	0.9	5.3	---	---	---
Watt-hours per cubic inch (Based on an Allowable Voltage Drop of 20 percent)	80	5	0.83	0.47	1.08	1.16	3.36	1.57
		1	0.61	0.38	0.84	0.73	2.92	1.26
		0.25	0.49	0.23	0.72	---	2.48	0.99
	0	5	0.39	0.33	0.83	---	2.51	1.33
		1	0.28	0.24	0.72	---	2.1	1.06
		0.25	0.21	0.13	0.63	---	1.67	0.77
	-40	5	0.27	0.25	0.65	---	---	0.68
		1	0.18	0.19	0.61	---	---	0.49
		0.25	0.11	0.07	0.38	---	---	---

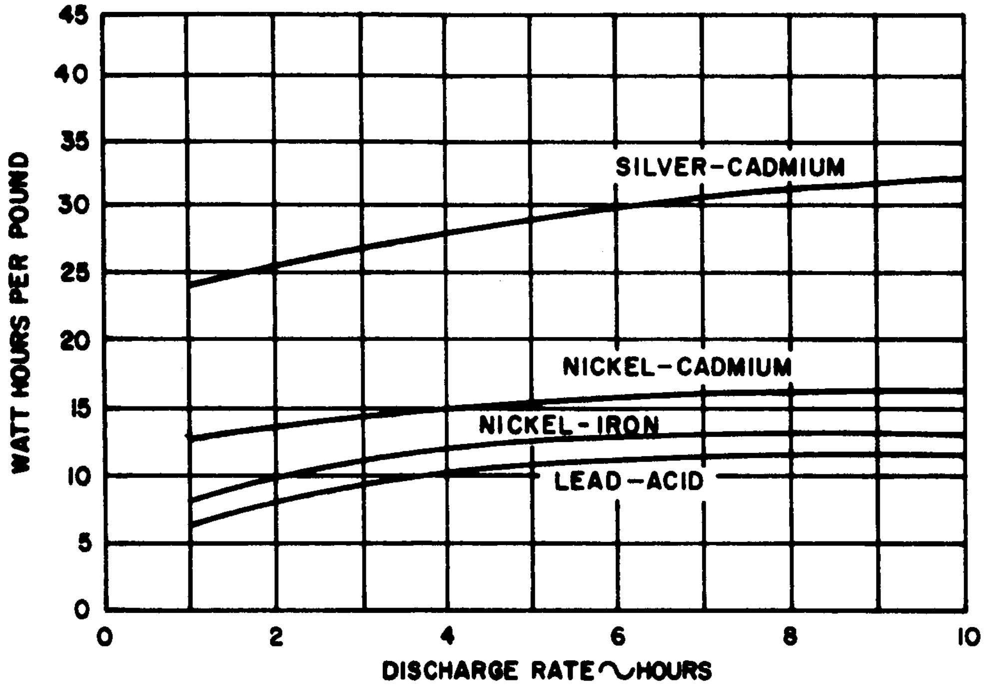

Figure 4.3-2 Energy vs Unit Weight for Various Batteries

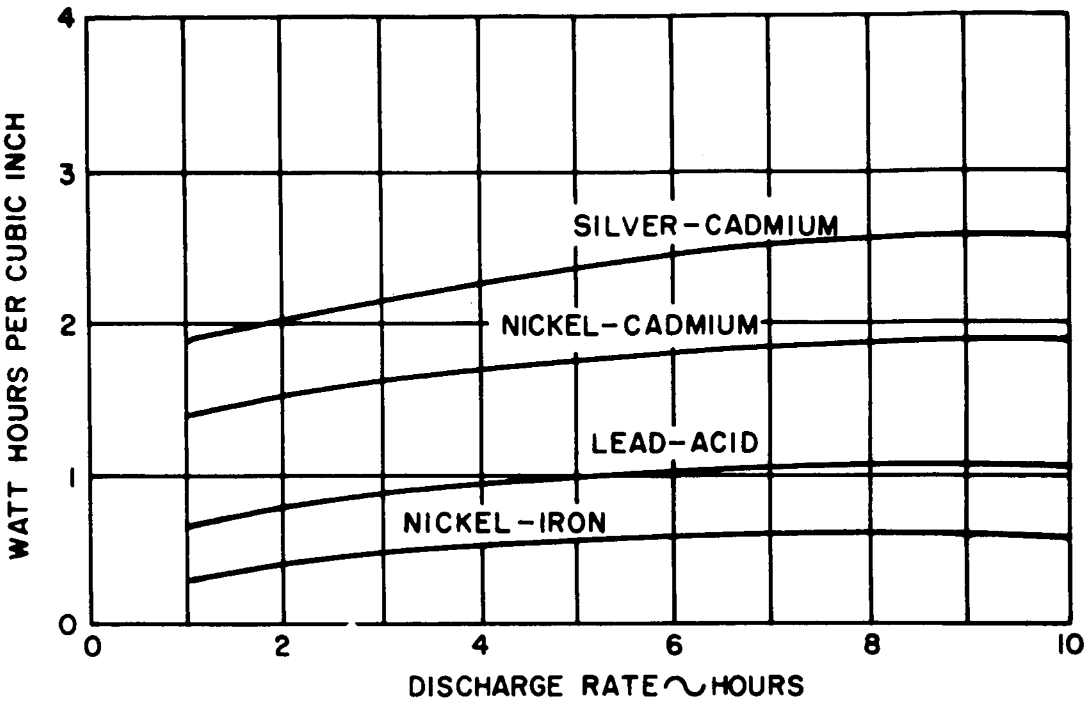

Figure 4.3-3 Energy vs Unit Volume for Various Batteries

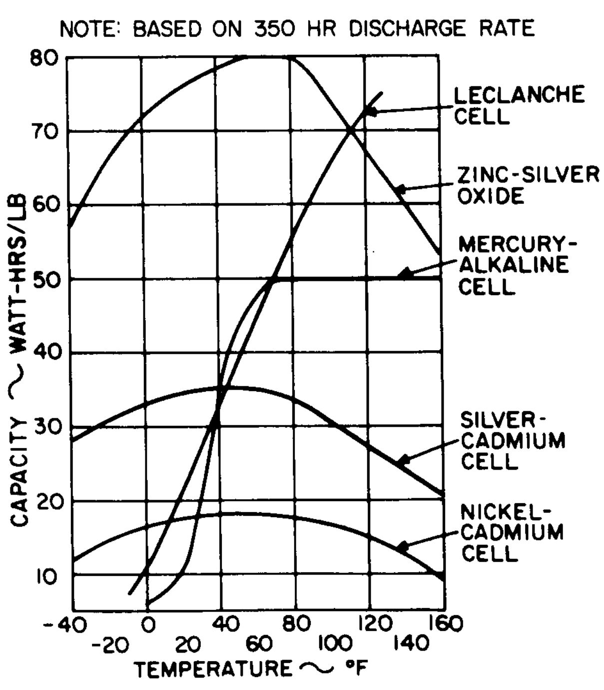

Figure 4.3-4 Capacity vs Temperature for Various Batteries

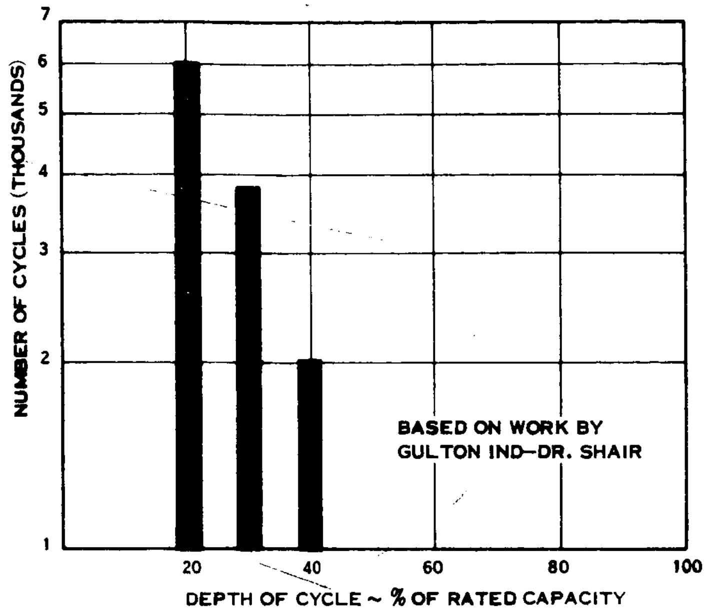

Figure 4.3-5 Ag Zn Battery Cycle Life

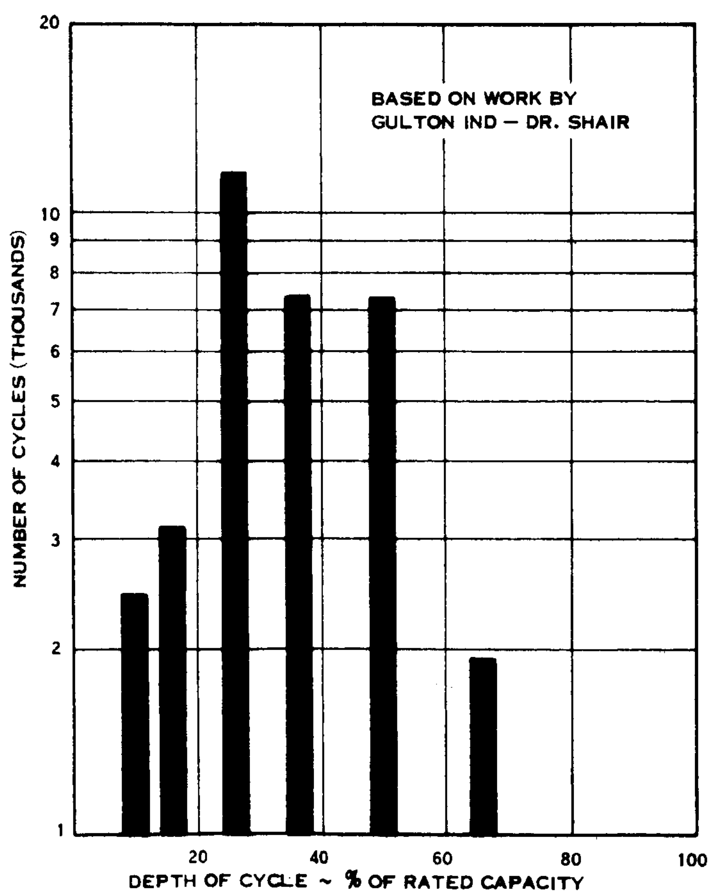

Figure 4.3-6 Ag Cd Battery Cycle Life

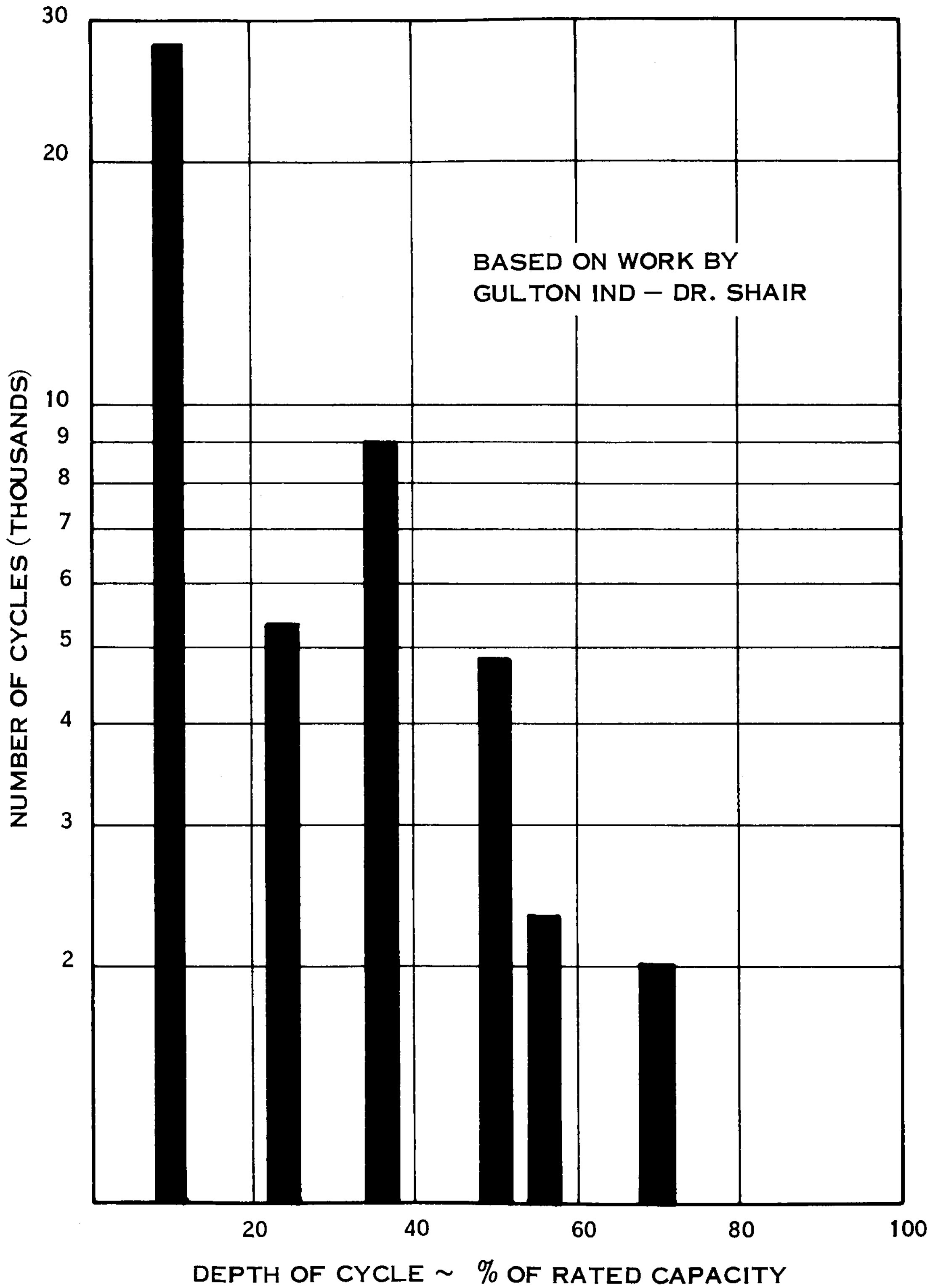

Figure 4.3-7 Ni - Cd Battery Cycle Life

The general trend for these three cell types is that the cycle life (beyond which the battery is unable to deliver rated capacity) is reduced with increased depth of discharge. The figures are based upon testing of production quality cells at Gulton Industries, Inc. The apparent low current density degradation of silver-cadmium cells for cycling depths below about 30% would constitute a disadvantage for lightly loaded systems; estimating the magnitude of this effect from the empirical data presented may not reflect a sufficient sample to be reliable. By contrast, the nickel-cadmium cell data indicates a maximum cycle life at the lowest cycle depth. Satellite experience with nickel-cadmium batteries tends to validate this Gulton data. For example, the three PEGASUS satellites launched in 1965, have operated at 11.5% cycle depth without failure. The first of the series has experienced about 9000 cycles over a period of 18 months.

The choice of battery type must be based upon several factors: cycle life, specific energy and volume, reliability, charge rate, discharge rate, temperature effects, overcharge rate. Assuming that a maximum of 5 discharges per 24 hours are made from the battery system for a period of 2 years and including the requirements of four occult phases (approx. 40 days each up to 67 minutes/day, see Figure 4.3-8) a total cycle requirement of approximately 4,000 is required. From the charts of Figure 4.3-6 and 4.3-7 it can be seen that both the silver-cadmium and the nickel-cadmium will satisfy the cycle life requirements at a 50 percent depth of discharge or less (50% depth of discharge selected as a practical limit to preclude possibility of cell reversal damage). If the per day cycle requirement increases to 10 discharges per 24 hours (8000 per 2 years) the use of silver-cadmium becomes highly marginal at any depth of discharge. The 2 year orbit life plus the additional "wet life" involved in battery manufacturing and pre launch storage and fabrication is a very severe requirement on the silver-cadmium battery due to the separator problem as stated in the brief description of the silver type batteries. Two years is well into the marginal life of the Ag-Cd batteries due to the silver migration. If the cycling or 2 year life requirements were increased at all, the silver-cadmium battery would be unsatisfactory at its present state of development.

Recommendation - The ATS-4 life and cycling requirements (4000 maximum for 2 years is best satisfied by the nickel-cadmium battery. The considerable amount of experience with nickel-cadmium battery and the associated charging and control circuits enhance the confidence that it is the best system to successfully satisfy the ATS-4 performance requirements. In accordance with this selection, the following sections use 12.5 watt-hrs. per pound at a recharge efficiency of 66%.

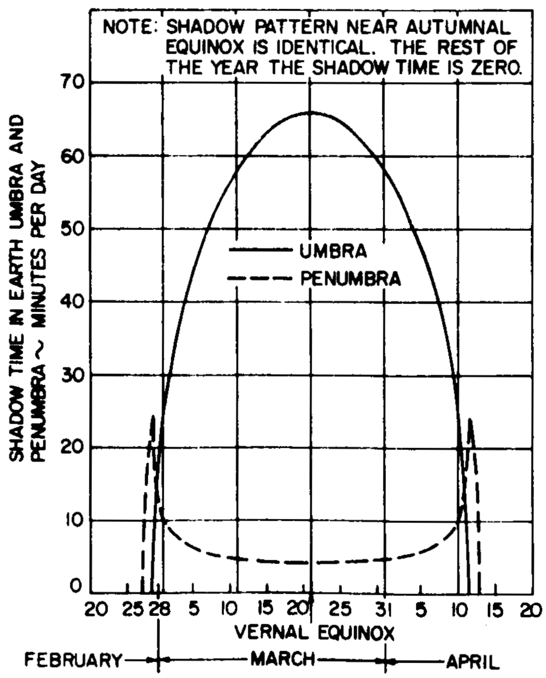

Figure 4.3-8 Umbra and Penumbra Patterns for a Synchronous Equatorial Satellite

4.4 BATTERY CHARGING AND CONTROL

Several battery charging and control approaches have been utilized with the sealed Ni-Cad battery, the most often selected approaches are:

- constant current
- constant voltage
- modified constant voltage
- tapered charge

With each of the above methods of charging, several approaches to charge termination can be utilized singly or in combination. The control parameters are:

- pressure
- voltage
- third electrode voltage
- watt-hours
- temperature

4.4.1 Constant Current Charging

Constant current charging is the fastest method of recharging a battery. This method can be used very successfully when the charge-discharge times and rates as well as temperature are firmly established. The time for recharge must be sufficiently long that the recharge rate will be low enough that it does not exceed the allowable continuous over-charge rate. At the same time the temperature must not vary greatly since there is a minimum current (function of cell capacity) below which the battery will never recharge completely. The amount of energy that must be returned increases very rapidly as temperatures exceed 70°F (see Figure 4.4-1). Thus with variations of temperature and/or loading and duty cycle the battery can be subjected to serious under or overcharging;

therefore, if a simple constant current charger is to be economically employed, the electrical and physical environment must be closely controlled or else a gross oversizing of battery capacity will be required to tolerate a continuous overcharge rate sufficiently high to compensate for all contingencies.

4.4.2 Constant Voltage Charging

A constant voltage charging is a slow method of complete recharging. Essentially, the battery is "floated" directly across a constant potential voltage source. The voltage level of the source is selected to provide a safe maximum voltage while still providing complete recharge. The rate of gassing, hence internal pressure, is a function of temperature as illustrated at the two temperatures (40^{o} and 77^{o} F) shown in Figure 4.4-2. The low temperature pressures are many times the pressure developed at room temperature. Excessive pressure results in mechanical failure of the cells. The effect of temperature upon cell voltage is shown in Figure 4.4-3 which is equally applicable to constant potential charging. Thus a fixed potential is not practical unless the temperature range is limited closely. A temperature compensating circuit can be added to vary the limiting voltage according to Figure 4.4-3. However, the recharge time is still long enough to preclude multicycling daily without excessive depth of discharge. This means that if only 10% capacity is removed, the battery cannot be cycled between 90% and 100% capacity because the high terminal voltage prevents recharge in the time allotted. The battery must cycle at some lower capacity level (i.e. 55% to 65%) at which point the terminal voltage is sufficiently low to permit a charge current high enough to return sufficient ampere-hours to replace the ampere-hours removed. This forces the system to operate at a depth of discharge associated with a lower cycle life and reserve capacity (see Characteristics, Section 4.3).

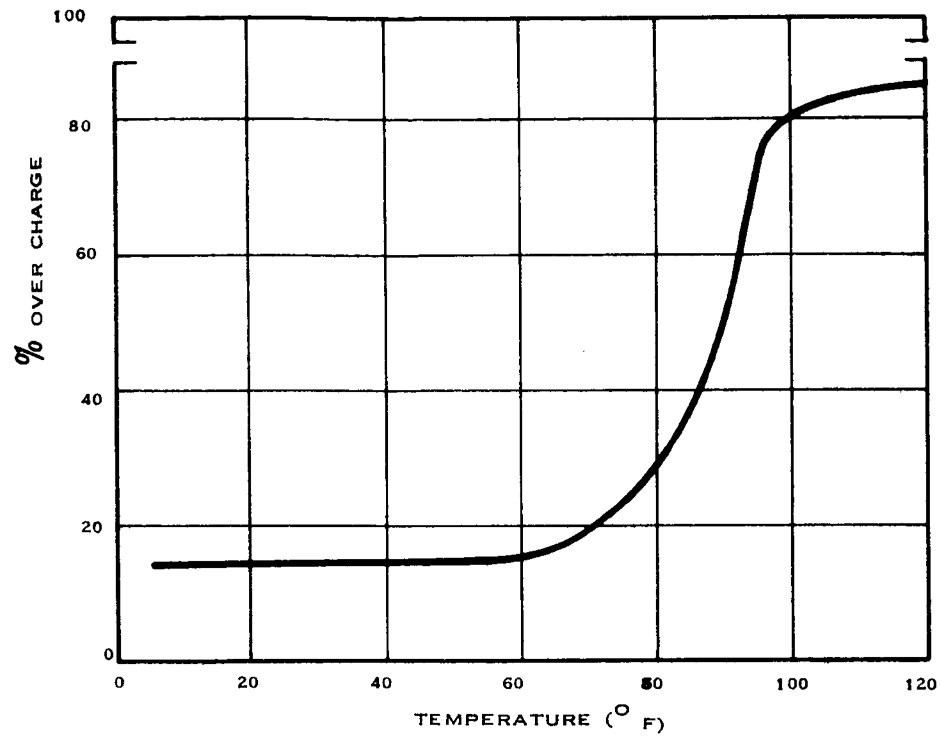

Figure 4.4-1 Recommended Percentage Overcharge vs. Temperature

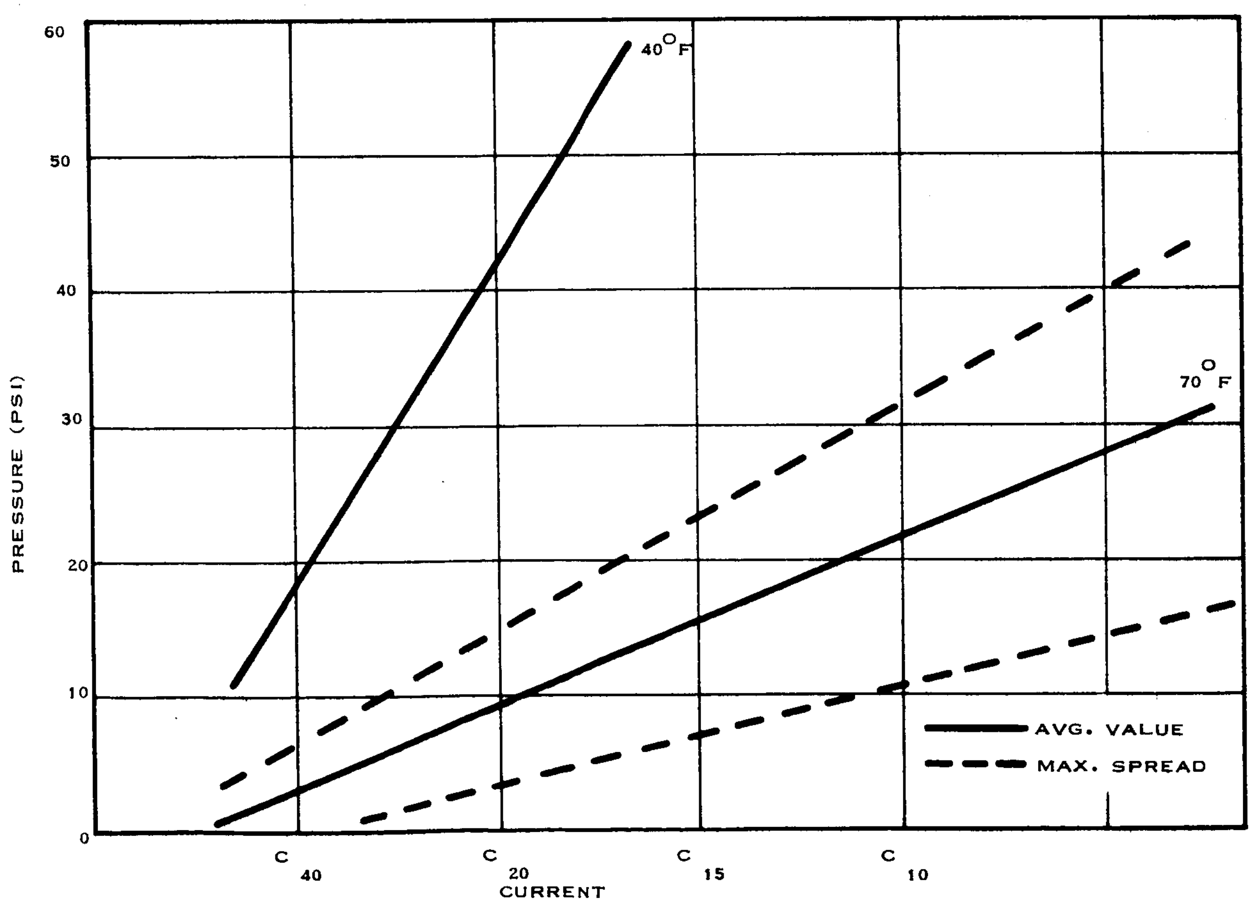

Figure 4.4-2 Overcharge Pressure vs. Current

4.4.3 Modified Constant Voltage Charging

The modified constant potential charger is similar to the constant potential charger and shows its general charging characteristics except at initial charging or at low voltage operation. Whereas the current into the battery for a constant potential charger with a "stiff power system" (not current limited) is limited only by the battery impedance, a modified constant potential system has a current limiter (series resistor) in series with the battery to protect the battery from high currents when its voltage is low. As the battery charges and its voltage increases the current decreases and the IR drop across the current limiting resistor becomes negligible.

4.4.4 Tapered Chargers

The tapered charger combines the advantages of both systems. During the initial recharge a constant current is supplied to the battery and thus provides rapid recharge up to a predetermined voltage at which point the charging current is tapered back approaching that of a constant potential charging system. The break point voltage at which it departs from the constant current mode is a function of battery temperature and is sensed by thermistors buried in the battery pack. The effect of the thermistor on a typical set of voltage-recharge current is shown in Figure 4.4-4. These curves are from measurements on a tapered charger design which has accumulated 46 months of space flight time for more than 33,000 charge-discharge cycles.

4.4.5 Recommendation

It is concluded that the tapered charging approach is best suited to the ATS-4. Not only does the past experience with the tapered charger show the approach to be very satisfactory but it also incorporates the best features of both the constant current and the modified constant potential chargers while providing sufficient inherent protection for the battery. Supplemental protection can be provided by sensors (thermal, voltage, pressure, etc.) to initiate battery change over as described in Section 4.5.

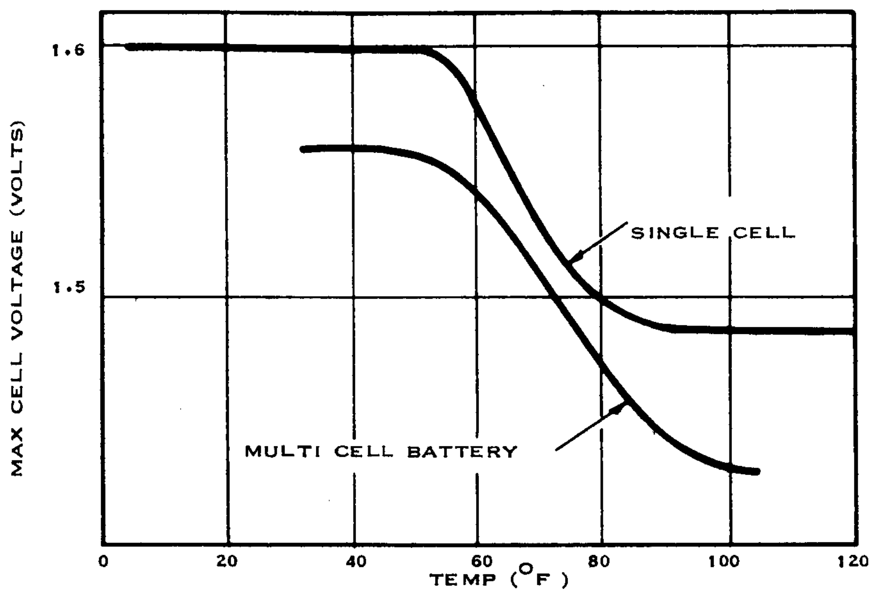

Figure 4.4-3 Maximum Limiting Voltage vs Temperature (For Tapered Charge)

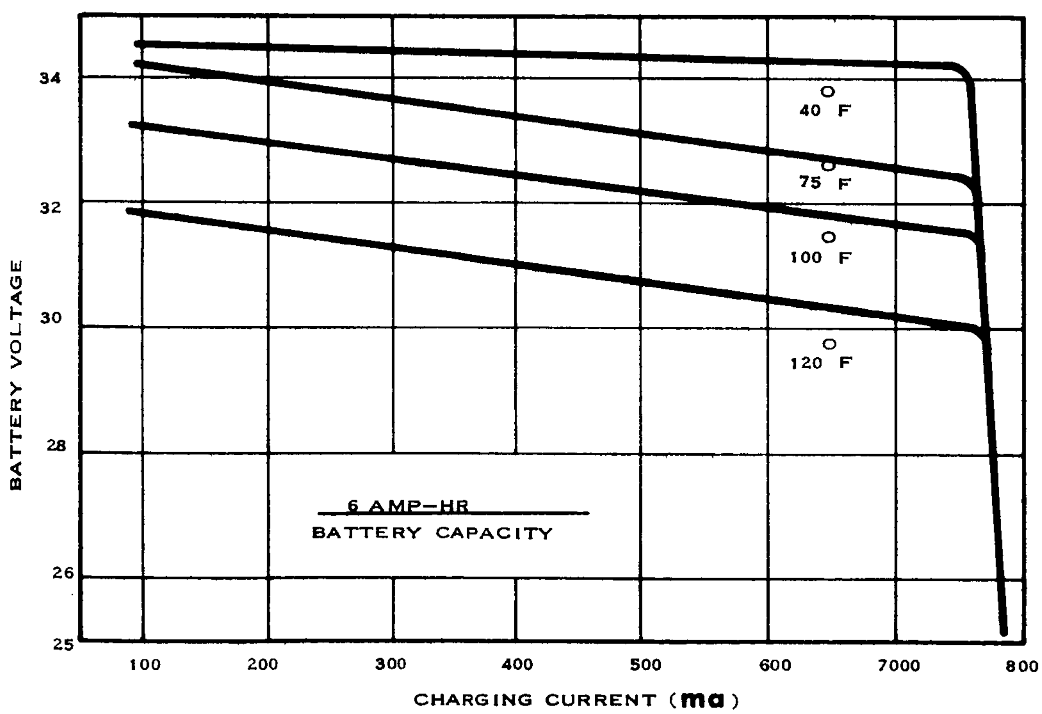

Figure 4.4-4 Tapered Charge Characteristic

4.5 Concept Power Subsystem

The power sybsystem design objective is realization of a minimum weight system satisfying the mission demands discussed in Section 2.3. The estimated power demands (Table 4.5-1) and power profiles (Figure 4.5-1, -2 and -3) previously discussed are repeated here for completeness. To summarize, the pre-orbital demand is estimated to be 100 watts, for the 16 hour duration between shroud ejection and array deployment. The on-station standby or occultation demand is 175 watts; peak experiment demand is estimated at 350 watts.

4.5.1 Design Approach

The minimum weight design approach involves analysis of load dynamics followed by apportionment of battery capacity and solar array output to produce the minimum weight combination. Total weight, W_T (lb) is composed of battery, panel, and power conditioning component weights. This total is related to battery energy to weight ratio and panel power to weight ratio by the expression:

$$W_T = \left(\frac{1}{12.5\ D} + \frac{1}{13.2\ T}\right)\sum_{i=1}^{m} \tau_i\,(a_i - r) + \frac{r}{6.6} + 15$$

where the symbols are defined as follows:

- D = Repetitive fractional discharge depth of 12.5 watt-hour per pound battery.
- T = Load cycle period (hours);
- τ_i = Duration of i^{th} load (hours);
- a_i = Magnitude of i^{th} load (watts);
- r = Main load bus input from 6.6 watts per square foot array.

The 15 pound constant accounts for power conditioning, regulation and switching circuitry. Figure 4.5-4 is a graphical presentation of the weight equation which shows the minimum total weight is a function of load

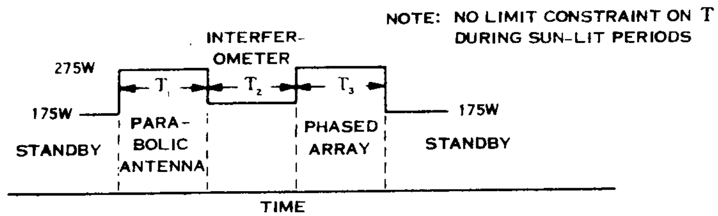

Figure 4.5-1 Typical Experiment Evaluation Power Profile

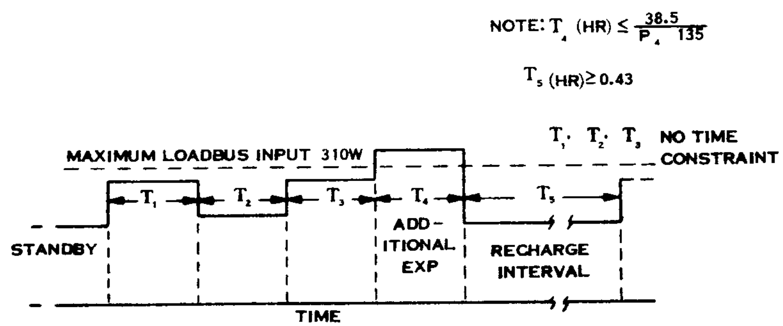

Figure 4.5-2 Power Profile with Additional Experiments

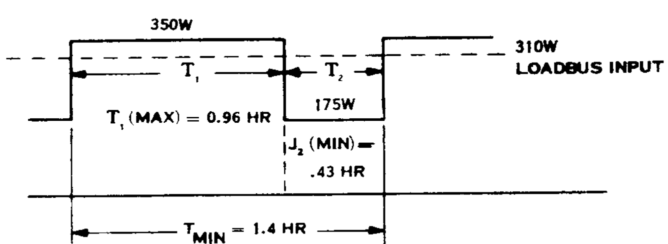

Figure 4.5-3 Experiment Demonstration Maximum Demand Profile

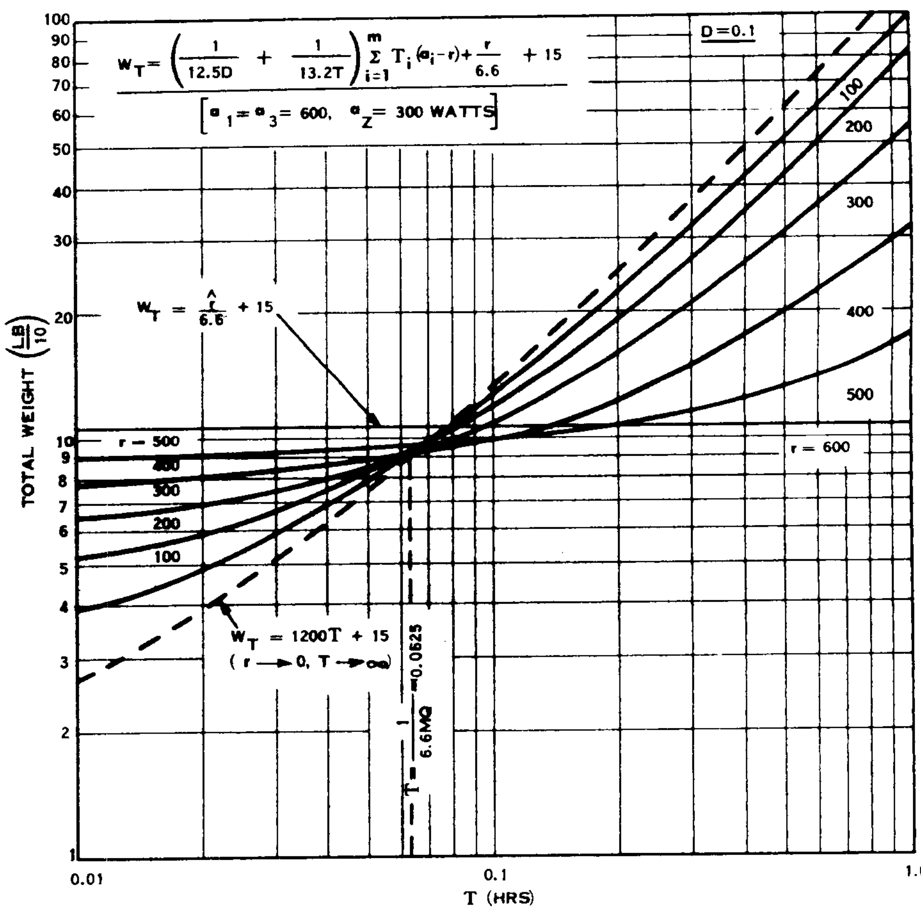

Figure 4.5-4 Power System Weight vs Load Duration

TABLE 4.5-1 ESTIMATED POWER DEMAND - EVALUATION TESTS

SUBSYSTEM	Preorbital	Standby and Occultation	Deployment and Structural Evaluation	Interferometer	Parabolic Antenna Patterns	Phased Array Patterns	Occultation Parabola X-Band Pattern	Occultation Phased Array Pattern
I Parabolic Antenna								
1. Transmitters					42.7	0	42.7	0
7.3 GHz	0							
2.3 GHz	0				1.4	0		
800 MHz	0				36.0	0		
100 MHz	0				18.0	0		
2. Receivers								
8.0 GHz	0.6	4.6						
1.7/2.1 GHz	0.4	3.4						
II Phased Array								
1. Transmitters	0					85.2	0	42.7
2. Receivers	0.4	2.4						
III Orientation and Control	29.5	88.0						
IV Radio Interferometer	3.0	8.0		34.0	8.0			
V Command Subsystem	2.2							
VI Telemetry and R Ṙ	34.6		69.1	32.3				
VII Instrumentation	5							
VIII LO-Mult. Chain	13.7							
Total Load: (watts)	89.4	161.9	196.4	185.6	257.7	244.8	202.3	202.3
Design Loads:	100	175	225	200	275	275	225	225
Design Margin	12%	8%	14%	8%	7%	12%	11%	11%
2 Year Operating Margin	-	-	85	110	35	35	85	85
Initial Operating Margin	-	-	131	156	81	81	131	131

TABLE 4. 5-1 ESTIMATED POWER DEMAND - DEMONSTRATION TESTS

SUBSYSTEM		PARABOLIC ANTENNA				PHASED ARRAY		
	Up Frequency	1.7/2.1 GHz	8.0	8.0	8.0	8.0	8.0	8.0
	Down Frequency	2.3 GHz	7.0	0.8	0.1	7.3	7.3	7.3, 0.8, 0.1
I Parabolic Antenna								
1. Transmitters								
7.3 GHz		0	42.5	0				
2.3 GHz		1.4	0					
800 MHz		0		36.0	0			36.0
100 MHz		0			18.0	0		18.0
2. Receivers								
8.0 GHz		4.6						
1.7/2.1 GHz		3.4						
II Phased Array								
1. Transmitters		0				42.5	85.0	
2. Receivers		2.4						
III Orientation and Control		88.0						
IV Radio Interferometer		34.0						
V Command Subsystem		2.2						
VI Telemetry and R $\dot{R}$		32.3						
VII Instrumentation		5.0						
VIII LO-Mult. Chain		13.7						
Total Load: (watts)		187.0	228.1	221.6	203.6	228.1	270.6	324.6
Design Loads		200	250	250	225	250	300	350
Design Margin		7%	9%	13%	11%	9%	11%	8%
2 Year Operating Margin		110	60	60	85	60	10	-40
Initial Operating Margin		156	106	106	131	106	56	6

duration, τ_i, and apportionment between panel output and battery capacity; the numerical values are ficticious and chosen for illustration only.

It can be shown that below a certain τ value, the minimum weight system will utilize minimum panel area; i.e., just sufficient to provide for battery recharge within the load period, T. Likewise, above this certain value of τ, minimum weight is realized for a minimum battery capacity configuration; i.e., just sufficient to support the occultation load.

For state-of-the-art battery and solar panel constants, the "cross-over" value of load duration τ is 0.16 hr. As ATS-4 experiment evaluation test routines are expected to require on the order of an hour, it is evident that the concept power design should be based on minimum battery capacity consistent with occultation demands, and of course, structural or other constraints on the panel area and weight.

Power subsystem constants are summarized in Table 4.5-2. The concept power system weights are tabulated in Table 4.5-3.

4.5.2 Battery Complement

The required mission battery capacity may be determined from the occultation requirement, which is an estimated 175-watt load for a maximum occultation duration of 1.1 hours. Utilizing the Ni-Cd cells described in Section 4.3, with a packaged specific energy of 12.5 watt-hours per pound, the required battery capacity and weight is determined from

$$\text{capacity} = \frac{(\text{load}) \times (\text{duration})}{(\text{allowable depth of discharge}}$$

$$= \frac{175 \times 1.1}{0.5} = 385 \text{ watt-hr}$$

$$\text{weight} = \frac{(\text{load}) \times (\text{duration})}{(\text{allowable depth of discharge}) \times (\text{energy to weight ratio})}$$

$$= \frac{(175)(1.1)}{(.5)(12.5)} = 31 \text{ pounds}$$

TABLE 4.5-2 POWER SYSTEM CONSTANTS

SOLAR PANELS		
Silicon N-on-P Cell Output	-	11.5 watts/ft^2 initially (@ 25°C)
Panel Output	-	7.8 watts/ft^2 after 2 yrs. (@ 50°C)
Two-year Degradation Factor	-	Total Radiation 13%
		Thermal 14%
		Area Efficiency 90%
		Aggregate 32.5%
Cruciform Panel Weight	-	0.66 lb/ft^2 of cell area
Normalized Effective Area	-	0.3 (Cruciform)
		0.9 (One Deg. of Freedom)
POWER CONDITIONING		
Efficiency	-	85%
BATTERIES		
Redundant Ni-Cd	-	12.5 watt-hr/lb
Cycle Life	-	>4400 cycles
Discharge Depth	-	10% during sun-lit periods
	-	50% during occulted periods

TABLE 4.5-3 MINIMUM WEIGHT ATS-4 POWER SYSTEM

LOADS		
Pre-orbital	-	100 watts, nominal
Standby/Occult	-	175 watts
Peak Experiment	-	350 watts
Max. Duration	-	1 hour
BATTERIES		
Mission Main Battery	-	385 watt-hr; 31 lb
Mission Redundant Batt.	-	385 watt-hr; 31 lb
SOLAR PANELS		
Min. Output @ 2 yrs.	-	310 watts
Min. Cruciform Area	-	155 square feet
Est. Cruciform Weight	-	103 pounds
POWER CONDITIONING		
Weight	-	15 pounds
POWER SYSTEM		
Total Weight	-	180 pounds

For the comparatively small number of occultations in 2 years at synchronous altitude (about 160), 50% discharge depth is acceptable. Allowing for 100% redundancy, the total mission battery weight is 62 pounds. No preorbital battery is required for launch 8 months of the year; launch at equinox ± 2 months requires a separate battery of 10 pounds, maximum

4.5.3 Solar Array

The minimum power input to the main load bus, p_A, is related to the peak power demand, $\hat{a}$, its duration, τ, battery capacity, C, and permissible fractional discharge depth, D.

$$p_A = \hat{a} - \frac{CD}{\tau}$$

For a 385 watt-hr. battery, 10% depth of discharge, and 350 watt peak load duration of 1 hour, the minimum input to the load bus is thus 311.5 watts.

Array size and weight are related to this power input by the following expression:

$$\text{Area} = \frac{p_A}{f \epsilon \sigma_0 (1 - d_{rad})(1 - d_{th})},$$

where

ϵ: Power conditioning efficiency (85 - 90% typical)

σ_o: Initial matched panel output per unit area for given cell conversion efficiency, temperature, and packaging;

d: Degradation factor for radiation (d_{rad}) and thermal (d_{th}) effects.

f: Array factor (effective normal area per ft^2)

Using 12.4% efficiency N-on-P cells (AM1 @ $25^{\circ}C$), 85% conditioning efficiency, 13% radiation degradation at the end of two years, 14% thermal derating for operation at 55°C, yields 7.34 watts per ft^2 cell area. A panel area utilization efficiency of 90% results in 6.6 watts delivered to the main load bus per square foot of panel area operating at 55°C and normal to the solar vector (at the end of 2 years).

From the results of Section 4.1, the cruciform array normalized effective area is 0.3. The total surface area required is thus $\frac{311.5}{0.3 \times 6.6} = 158\ ft^2$. The preferred spacecraft concept allots a total of 155 ft^2 to two double faced panels of 38.8 ft^2 frame area each.

Utilizing a single degree of freedom rotating single faced panel would require $\frac{311.5}{0.9 \times 6.6} = 53\ ft^2$, or two single faced panels of 26 ft^2 each. Since an actuator is required, the weight advantage of this arrangement is not as great as indicated by the area ratio.

Lightweight aluminum honeycomb construction single face panels are approximately $\frac{2}{3}$ structure, $\frac{1}{3}$ solar cells by weight; a typical panel weighs about 1 lb/ft^2. Hence, the single degree of freedom array would weigh about 53 pounds. Double face cruciform panels will weigh about $\frac{2}{3}$ lb/ft^2. The panels for the referenced concept will weigh about 103 pounds.

Growth potential may be an important design consideration in the initial choice of panel size and structural support. In this connection, it is to be noted that the 77.5 ft^2 frame area in a rotatable array provides 455 watts to the load bus at the end of 2 years, 522 watts initially.

4.5.4 Power Conditioning and Control

A simplified block diagram of the power subsystem is shown in Figure 4.5-5. The solar array is shown as four groups of diode isolated panels. Each of the series - parallel modules will be isolated by a pair of derated blocking diodes thus protecting the power system from self dissipation into a shorted or shadowed module.

POWER SYSTEM BLOCK DIAGRAM

Figure 4.5-5

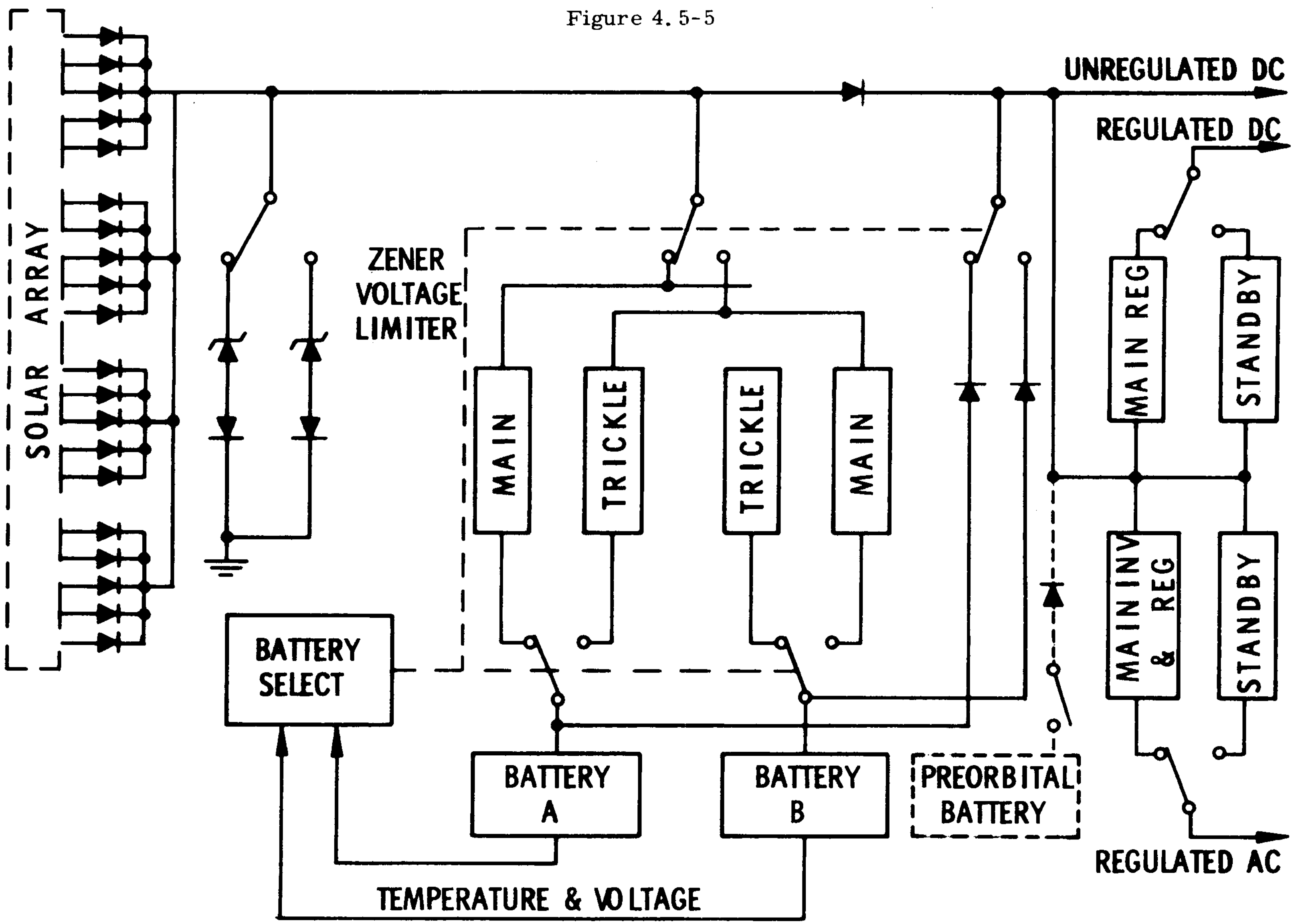

F-7A

Redundant zener voltage limiters are provided with automatic or ground commandable over-voltage changeover. The function of the zener voltage limiters is to establish an upper voltage limit for the unregulated bus so that when the solar array is fully illuminated and the connected load is reduced the bus voltage will not exceed a permissible level. Temperature compensating diodes are included to maintain a 1 volt tolerance on the voltage limit. This precludes the necessity for adding loads when other loads are removed in order to maintain a voltage tolerance. In addition, the voltage limited input to the regulators and inverters reduces the demand upon these units thereby lowering the thermal dissipation and reducing the complexity and weight of the power conditioning equipment. A major benefit of the zener voltage limiter approach is realized by simplifying the thermal control function. Since the solar array output is time dependent, considerable power is normally dissipated in regulation and conversion at start of life and reduced to a minimum at the end of life. Varying thermal input is eliminated by permitting the zener package to dissipate this excess energy outside of the thermally controlled area.

Battery charging is accomplished by a redundant system. System "A" selection places battery "A" on a main charger and standby battery "B" on a low rate trickle charger. A reversal of status, "B" battery as main and "A" battery on standby, can be accomplished by ground command or by the on-board automatic system sensing an over or under voltage condition and/or excessive battery temperature. The redundant main chargers will be of the tapered charge type. The battery will be charged at a constant rate until a predetermined voltage is reached. This voltage level is a function of battery temperature and is sensed by one or more thermistors buried in the battery package. Once the cut-back voltage is reached, the charging current is reduced proportional to any further increase in voltage. A lower limit is established as a minimum charge rate to maintain the battery charge (a temperature dependent value). The trickle charger is similar to the main charger except that the constant current level is much lower, the cutback voltage limit is higher, though it is also responsive to the battery temperature sensing thermistor.

Another source of energy is available to the main power bus. The pre-orbital battery will be required to supplement the folded array output for a solstice launch. This 12-pound, 608.5-watt-hour silver zinc primary battery is connected to the main bus through a commandable relay and a series blocking diode. This is done to prevent the battery from becoming a load on the main bus in case of relay failure, or shorting the main bus after separator break down of the dissipated battery.

Both the solid state dc regulators and inverters utilize the energy conserving pulse width modulation approach. The use of an active redundant standby unit is provided with automatic change-over upon over or under voltage or frequency. The selection of main or standby unit may also be accomplished by ground command based upon ground observation of telemetry. The ground command has the capability of over-riding the spacecraft selection unit.

It has been found that this described approach provides a highly reliable, low weight and volume power subsystem. The use of automatic internal control within the ATS-4 provides for quick reaction system protection and correction with a minimum amount of ground surveillance. The ground telemetry and command link provides an over-ride capability if a malfunction should occur plus the additional flexibility of operating the power subsystem in any desired configuration.

5.0 ORBITAL ANALYSIS

5.1 GENERAL

This section of the ATS-4 final report presents the results of studies relating to trajectory and orbital analyses; including launch vehicles, apogee injection stages, ascent trajectories and injection stations, orbit payloads, orbit injection errors, orbit perturbations, orbit guidance, (including injection error correction, station keeping and station repositioning) and auxiliary propulsion systems.

Three (3) boost vehicles have been specified by NASA for consideration in the ATS-4 mission study: the SLV3A/Agena, the SLV3C/Centaur, and the Titan IIIC. Nominal payload capabilities to synchronous orbit altitude for the first two boosters were defined by NASA based on the following conditions:

- A due-East launch from ETR
- A standard Agena shroud for the SLV3A/Agena and a standard Surveyor shroud for the SLV3C/Centaur
- Use of an initial 100 nautical mile parking orbit
- No orbit plane change by booster upon injection of its designated payload into the inclined Hohmann transfer orbit from the initial parking orbit to the final synchronous orbit.

The corresponding synchronous apogee payload for the SLV3A/Agena was given as 2300 lbs. and for the SLV3C/Centaur as 4000 lbs.

Further ground rules were established by NASA for the SLV3C/Centaur, namely that the factor to be used to relate increases in Surveyor shroud weight to desired increases in shroud length is 5.4 lb/in. and coast time for the Centaur in the parking orbit (between first and second burns) shall not extend beyond the 1st descending node in this orbit.

5.2 APOGEE INJECTION STAGES

An Apogee Injection Stage (AIS) must be employed with the SLV3A/Agena and the SLV3C/Centaur launch vehicle to provide the impulse required at apogee of the transfer orbit to inject the ATS-4 into a synchronous equatorial orbit. Two types of AIS's were found which meet these requirements with minimum modifications, both incorporating versions of the Surveyor main retro rocket motor as the propulsion engine. These are: the 3-axis stabilized Burner II (References 5-1 and 5-2) and spin-stabilized AIS's.

The main elements of the Burner II consist of a Thiokol TE 364 solid propellant motor, a preprogrammed strapped-down inertial guidance, a combination hot and cold gas reaction control system, a battery powered electrical system, a destruct system, a stage structure, and an airborne data telemetry system. The Burner II, also designated the Boeing Model 946 is supplied in several versions as follows:

946-025	Current Burner II stage using the TE 364- 2 motor with a 200 pound payload support capability and a 43 minute coast capability
946-027B	Same as current Burner II stage except has new payload support structure to handle 1400 pound payloads, uses the TE 364-3 motor with up to 1440 pounds of propellant, and has increased batteries and N_2 control propellant for 5.5 hour coast capability.
946-128B	Same as 946-027B except payload support capability is 4000 pounds, and uses the TE 364-4 motor which has a cylindrical insert permitting propellant loadings of up to 2100 pounds.

Spin-stabilized AIS's using the same TE 364-3 and 364-4 motors (Reference 5-3) were also considered. Small solid rocket motors would be used for spin-up, and control of the spin axis orientation and coneing motions provided during the coasting period in the transfer orbit and during the apogee maneuver. Passive yo-yo mechanisms appear most effective for despin, although despin rockets could be employed. The attitude control techniques considered for the spin-stabilized AIS's are discussed further in Section 6.6.1 of this report.

The weight characteristics of the various Burner II and spin-stabilized AIS's are included in the summary data of Table 5.4-3 presented later in this section. The velocity impulses which must be supplied by the AIS's for the different types of ascent trajectories under consideration are presented in Table 5.4-1. The approximate thrust levels and burn times for the subject AIS's are 9000 pounds and 40 seconds, respectively.

5.3 ASCENT TRAJECTORIES

5.3.1 Requirements and General Considerations

In the choice of an ascent trajectory and injection station (ie, the Earth longitude associated with the final 24-hour synchronous orbit) consideration must be given to factors such as the following:

- Operational flexibility of the launch vehicle
- Ground tracking facilities for status monitoring and possible control during ascent and orbit injection and for identification and command correction of orbit injection errors
- Favorable satellite orientation relative to the sun during the transfer orbit, enabling power requirements to be met using the solar paddles rather than launch battery packs.
- Ease and effectiveness of initial satellite checkout and experimentation following injection and orbit correction
- Ground tracking facilities for identification and command-control of required station keeping operations and of desired station repositioning operations

Ground tracking facilities considered for the ascent and orbit injection operations included the STADAN network and the ATS-4 stations at Rosman and Mojave, as discussed in paragraph 2.1.2.

Various classes of ascent trajectories and associated longitude injection stations were studied for the three (3) launch vehicles under consideration in accordance with the preceding mission requirements. All of the ascent trajectories assumed a near-East launch from ETR (off-East launches to modify the injection longitude station are briefly considered herein) and injection into a 100 nautical mile parking orbit. At the first (descending) or second (ascending) node of this parking orbit, a second burn of the launch vehicle is employed to inject into an inclined Hohmann transfer orbit to synchronous orbit altitude. In some cases for the Centaur launch vehicle, in order to maximize the final orbit payload, the 28.5^{o} inclination of the parking orbit -- associated with a due-East launch from ETR at a latitude of 28.5^{o} -- is reduced as the transfer orbit is initiated. At first or second apogee of the transfer orbit (the choice dictated by consideration of the desired injection longitude) the ATS-4 is injected into the final synchronous, circular, equatorial orbit by means of an apogee injection maneuver. By under-injecting at this point into a slightly-elliptical high altitude parking orbit, different longitude injection stations are available as will be discussed subsequently.

A graphic representation of these various ascent trajectories, together with an indication of the final injection longitudes based on a due-East launch from ETR, is presented in Figure 5.3-1. The SLV3A/ Agena and Titan IIIC launch vehicles can be permitted to coast to the second node of the low altitude parking before second burn to initiate the transfer orbit. Such a procedure would permit the ATS-4 satellite to be injected into the final synchronous orbit at first apogee of the transfer orbit with an associated longitude station of 87^{o} West. This is an advantageous station from the standpoint of mission experiment command-control from the ATS-4 ground stations at Rosman (83^{o} West) and Mojave (117^{o} West).

Since coasting to the second node of the parking orbit cannot be considered for Centaur, two (2) ascent trajectories have been studied for it. The preferred approach involves initiation of the transfer orbit at the first descending node of the low altitude parking orbit, coasting for 1-1/2 revolutions (15.75 hours) in the transfer orbit, and injecting into the final synchronous orbit at second apogee of the transfer orbit. Initial orbit correction (as necessary) and vehicle checkout and experimentation would be accomplished near the injection longitude of 54^{o} West. The vehicle would

Figure 5.3-1

ASCENT TRAJECTORES

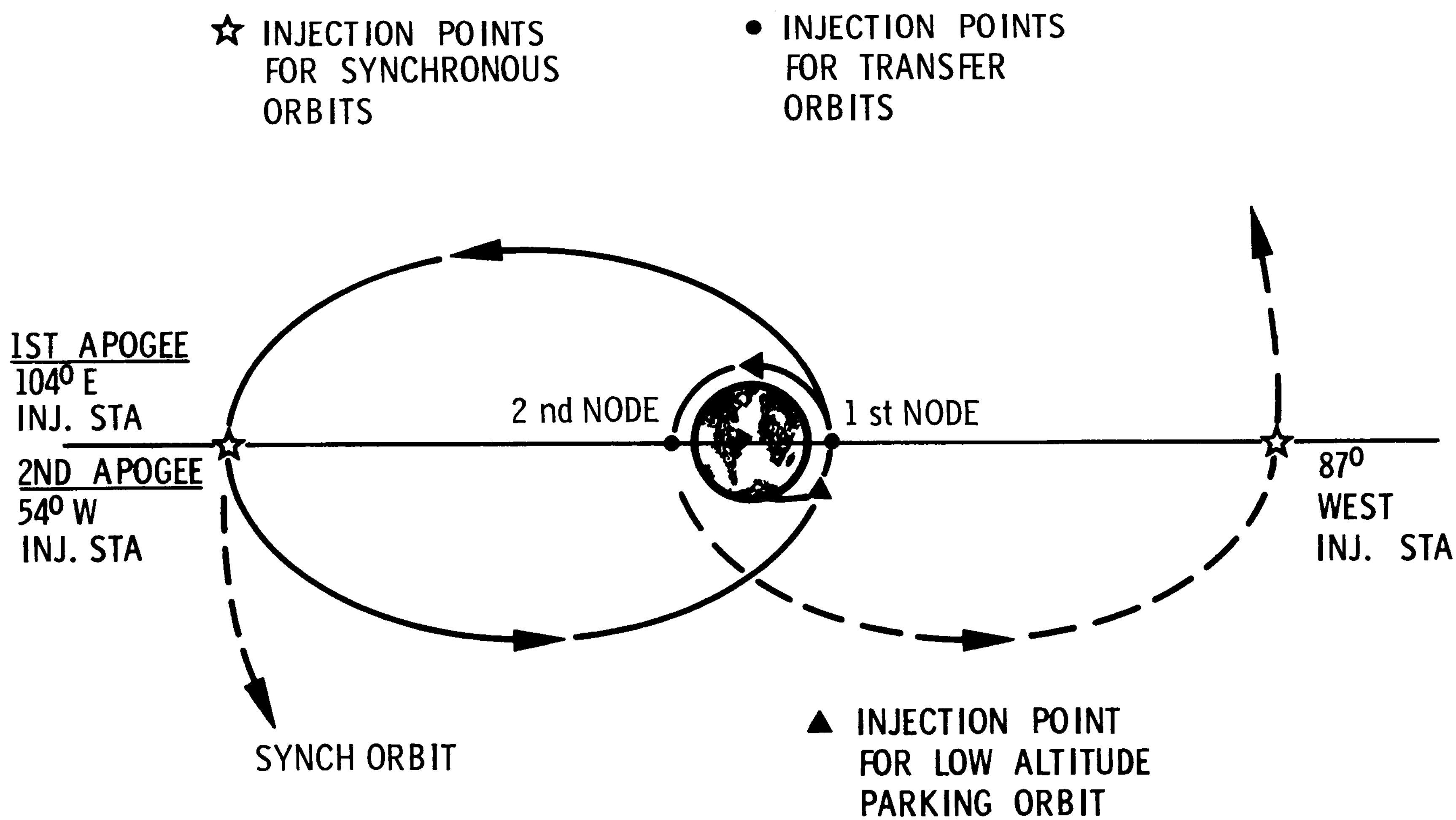

E-1

then be caused to drift Westward (if the initial period were greater than 24 hours due to orbit injection errors this could automatically provide a drift in the desired direction) to a more advantageous location central to the Rosman and Mojave station longitudes.

The second ascent trajectory approach involved subsynchronous injection of the ATS-4 at first apogee of the transfer orbit (at a longitude station of 104^{o} East), and a consequent Eastward "walk" in the high altitude parking orbit to a final acceptable longitude station. As will be shown, this approach involves extended waiting periods, and, hence, it is not favored.

5.3.2 Synchronous Injection - Single Apogee Impulse

Launch vehicle operations and payload optimization considerations dictate an essentially fixed-launch trajectory into a low altitude (taken as 100 n.m.) parking orbit. This phase is based on a powered ascent trajectory launched eastward from ETR. The powered ascent phase terminates in a low altitude waiting orbit inclined 28.5^{o} to the equator. An elliptical transfer orbit to synchronous altitude can be initiated at any equatorial nodal crossing and permit injection into a final synchronous orbit at an equatorial station with a single impulse. This initiation time (t_1) is given by

$$t_1 = t_o + (j - 1) \frac{P_w}{2}$$

where

t_o = time at first nodal crossing

P_w = period of parking orbit, 1.47 hours

Integer j describes each successive nodal occurrence. Odd integers denote descending node positions, while even integers denote ascending node transfer positions.

The parameter t_o is the time of the first nodal crossing. This includes the powered launch ascent trajectory as well as some orbit coasting time. Both burning time and range angle achieved during the powered phase are dependent on the launch vehicle characteristics. It will be shown that these parameters only have a small influence on the phasing requirements necessary to establish a given station longitude.

When the appropriate node of the low altitude parking orbit is reached, the second burn commences, and the vehicle is transferred to a Hohmann path having an apogee altitude which is coincident with the synchronous orbit altitude. The characteristic velocity required to perform this maneuver is 8069 ft/sec, assuming no change to the orbit plane inclination.(1)

A high altitude node (1st apogee) is attained at time t_2 given by:

$$t_2 = t_1 + \frac{P_H}{2}$$

where

P_H = period of the Hohmann orbit, 10.5 hours

At this instant, the satellite longitude (λ)is given by

$$\lambda = (i+j)\,\pi - (GHA_o + \omega_E\, t_2)$$

where

ω_E = rotational velocity of the earth

GHA_o = Greenwich hour angle at launch measured from the first descending node.

The right ascension between the descending node and ETR at launch is independent of booster characteristics. This angle is dependent on launch azimuth only. For a due east launch, the right ascension is essentially -90^o;

(1) Table 5.4-1 of subsection 5.4 summarizes the velocity requirements associated with orbit plane changes from 0 to 10 degrees

hence

$$GHA_o = -90 - \lambda_{ETR} = -9.5^o$$

Booster burnout conditions (time, t_b, and inertial range angle, R_b) have only a small influence on the ability to establish a desired equatorial station position when a low altitude parking orbit is employed. The final station position is shifted by the time difference between given boosters in transversing a given powered ascent range angle. Consider a nominal powered ascent to orbit specified by a boost time (t_b) of 0.15 hour and an inertial range angle (R_b) of 17.94^o. Let the Hohmann transfer be initiated at the 2nd (ascending) node as for the Agena or Titan launch vehicles. Then (since P_W = 1.47 hours):

$$t_1 = 0.15 + \frac{P_W}{360}(72.06) + \frac{P_W}{2} = 1.18 \text{ hour}$$

and:

$$\lambda_{24} = 2\pi - \left[-9.5 + 15.03\,(6.43)\right] = 87.2^o \text{ W}$$

Note that the time in the Hohmann transfer orbit is 5.25 hours and that λ_{24} is the satellite longitude at injection into a synchronous orbit. If burnout were assumed to occur directly over ETR at time zero, then t_1 would equal 1.10 hour and λ_{24} = 86.0^o W. Thus, the phasing requirements essentially do not vary between the launch vehicles under consideration.

In the absence of injection errors, both circularization and orbit plane reorientation, as desired, are accomplished by the injection maneuver at Hohmann apogee altitude. (The Titan 3C would provide this impulse itself, but the SLV3A/Agena would require the use of a separate apogee injection stage.) A 6030 ft/sec velocity impulse is required to perform this maneuver for the case of a final equatorial orbit. This impulse is applied in the plane of the horizon at an azimuth angle of 52.7^o measured from the local direction of motion for this ascent trajectory (departing from 2nd node of parking orbit with no plane change; injection at 1st apogee).

Figure 5.3-2 presents the ground track associated with this ascent trajectory while Table 5.3-1 summarizes some of its pertinent characteristics.(2) Data are also presented in this summary table for an ascent trajectory with a Hohmann transfer initiated at the first (descending) node of the low altitude parking orbit. The final longitude station for this ascent trajectory is seen to be 104° East, while its total maneuver time is 5.69 hours.

For this latter ascent trajectory, if injection into the final synchronous orbit is delayed until 2nd apogee of the transfer orbit, then the injection longitude is shifted to about 54° West. This station results because of the 360° range angle transversed by the satellite in its 10.5 hour coast in the transfer orbit while the Earth rotates at 15.03°/hour for this same period, ie,

$$54^{\circ} \text{ West} \approx 104^{\circ} \text{ East} - (15.03)\,(10.5 \text{ hr})$$

$$= 104^{\circ} \text{ East} - 157.8 = -53.8^{\circ} \text{ E}$$

5.3.3 Subsynchronous Injection - High Altitude Parking Orbit

The ascent trajectory data previously presented has indicated that injection longitudes of about 104° E or 87° W are available using a low altitude parking orbit and a single impulse injection at 1st apogee of the transfer orbit. These stations are based on Hohmann transfers being initiated at the first or second nodes of the low-altitude parking orbit, respectively, following a due East launch from ETR.

(2) Corresponding velocity data for the cases where the Centaur vehicle is used to provide orbit plane inclination changes are given in Table 5.4-1 of the following subsection.

Changes in these injection longitudes for a synchronous, equatorial orbit can be effected by off-East launches (Figure 5.3-3). This effectively shifts the inertial position of the parking orbit nodes with respect to Greenwich at launch. Only moderate deviations from off-East

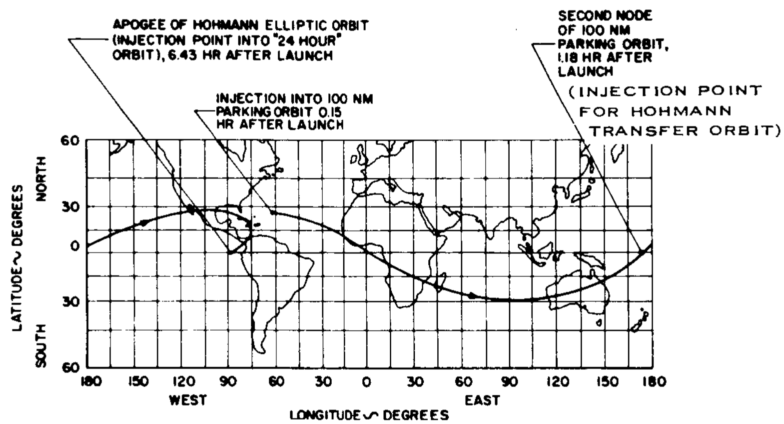

Figure 5.3-2 Earth Track of Ascent Trajectory (2^{nd} Node Departure)

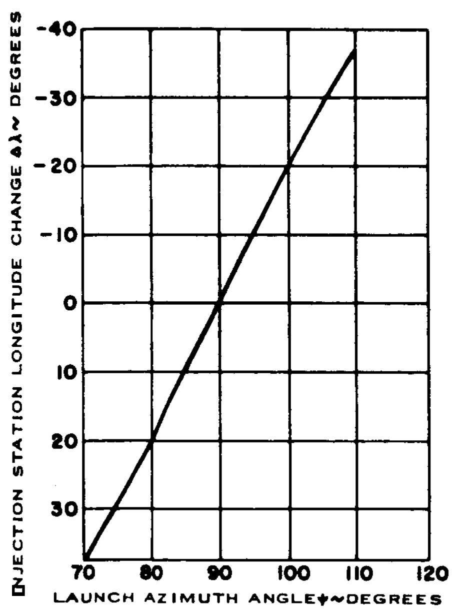

Figure 5.3-3 Injection Station Longitude Variation With Off-East Launch Azimuths

TABLE 5.3-1 ASCENT TRAJECTORY CHARACTERISTICS-SYNCHRONOUS INJECTION AT 1ST APOGEE

EVENT	DEPARTURE NODE	TIME (HRS)	ALTITUDE N.M.	SPEED (FT/SEC)	CHARACTERISTIC VELOCITY REQUIRED (FT/SEC)	INJECTION STATION WEST LONGITUDE (DEGREES)
LAUNCH DUE EAST FROM ETR		0		1,340(1)		80.5
INJECTION INTO PARKING ORBIT		0.15	100	25,567		
INJECTION INTO HOHMANN TRANSFER ORBIT	2 (1)	1.18(2) (0.44)	100 (100)	33,636 (33,636)	8069 (8069)	
APOGEE OF TRANSFER ORBIT	2 (1)	6.43(3) (5.69)	19,327 (19,327)	5,232 (5,232)		
INJECTION INTO SYNCHRONOUS EQUATORIAL ORBIT	2 (1)	6.43 (5.69)	19,327 (19,327)	10,087 (10,087)	6030 (6030)	87.2 (256.0)

(1) EAST COMPONENT OF EARTH ROTATIONAL VELOCITY

(2) THE PERIOD OF THE PARKING ORBIT IS 1.47 HOURS

(3) THE TIME IN THE HOHMANN TRANSFER ORBIT IS 5.25 HOURS

launch azimuths (and hence moderate shifts in final longitude stations) can be permitted, however, without incurring excessive characteristic velocity penalties as illustrated in Figure 5.3-4.

As noted, the Centaur launch vehicle must initiate the transfer orbit at the 1st (descending) node of the low altitude parking orbit. One method of achieving a favorable longitude station following injection at 1st apogee of the transfer orbit is by means of an ascent trajectory incorporating a high altitude parking orbit as next described.

In the high altitude parking orbit method, the desired longitude station is established after a Hohmann transfer to an elliptical, equatorial parking orbit with apogee at the synchronous orbit altitude. The following launch procedure is assumed:

- A 90 degree East launch azimuth is used. (Variations from this procedure are discussed later.)
- An initial low altitude parking orbit is employed and departure from this orbit is always at the first node. (Direct ascent trajectories into a near-synchronous, elliptical parking orbit could also be considered.)
- A Hohmann transfer is effected to synchronous orbit altitude.
- The satellite is injected into an elliptical, equatorial high altitude parking orbit with apogee at synchronous orbit altitude using an apogee injection stage (AIS).
- The transfer from this parking orbit to a circular, synchronous orbit always occurs at the apogee of the parking orbit (after an integral number of revolutions in that orbit, which is assumed to have a period less than one sidereal day). This impulse would be provided by the auxiliary propulsion system of the ATS-4.

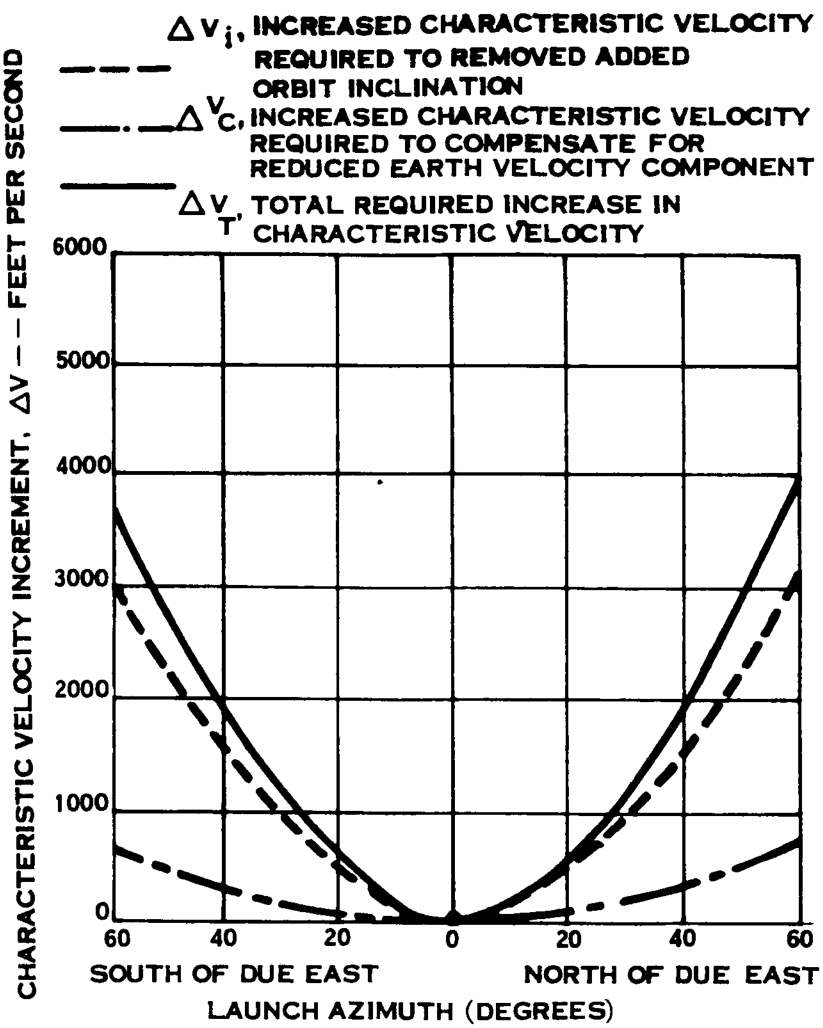

Figure 5. 3-4 Effect of Launch Azimuth on Required Increase in Characteristic Velocity

It is assumed that the velocity increment required to produce a 24-hour equatorial orbit is only partially provided at the apogee of the Hohmann transfer path. While a high altitude parking orbit with a period greater than 24-hours also could be employed, giving rise to a westward drift of the satellite, the total characteristic velocity required would be higher, which makes this approach less attractive.

The high altitude, elliptical parking orbit has its apogee at the altitude of the 24-hour orbit and its perigee at some lower altitude between the low altitude parking orbit and the 24-hour orbit. The limiting periods of the high altitude parking ellipse are the period of the Hohmann transfer orbit (10.5 hours) and the period of the 24-hour orbit (one sidereal day). Earth longitude shifts of the vehicle are eastward, relative to the initial longitude of the apogee point of the Hohmann orbit, during each revolution in the high altitude parking orbit.

Figure 5.3-5 depicts the eastward longitude shifts per revolution ($\Delta \lambda_H$) in the parking orbit as a function of the orbit period (P_H). The velocity increment (ΔV_c) that must be provided to circularize this orbit also is given as a function of P_H. Additionally, the initial longitude of the vehicle, when it next reaches apogee of this orbit (λ_0) also is given.

With the high altitude parking orbit method being discussed, transfer to the final synchronous orbit, again, is effected only at apogee of the parking orbit (that is, only after an integral number of revolutions in the parking orbit). This can involve extended waiting in the high altitude parking orbit to achieve a specified longitude and again only makes discrete longitude stations available with any given parking orbit. This situation is shown in Figures 5.3-6 which shows the satellite trajectory ground tracks. A high altitude parking orbit period of 0.945 sidereal day is assumed, corresponding to a synchronous velocity deficiency, ΔV_c, of

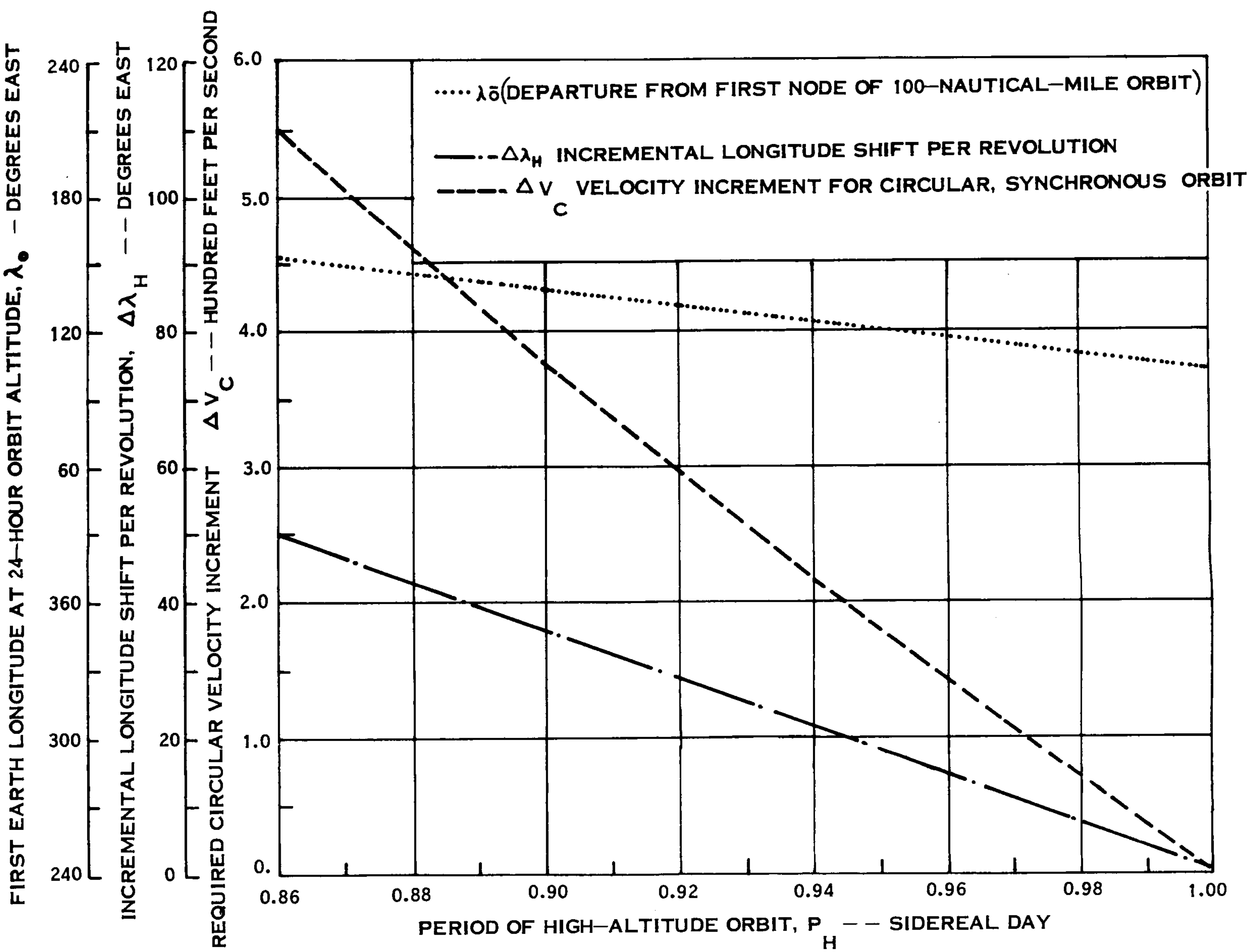

Figure 5.3-5 High-Altitude, Elliptic Parking Orbit Characteristics

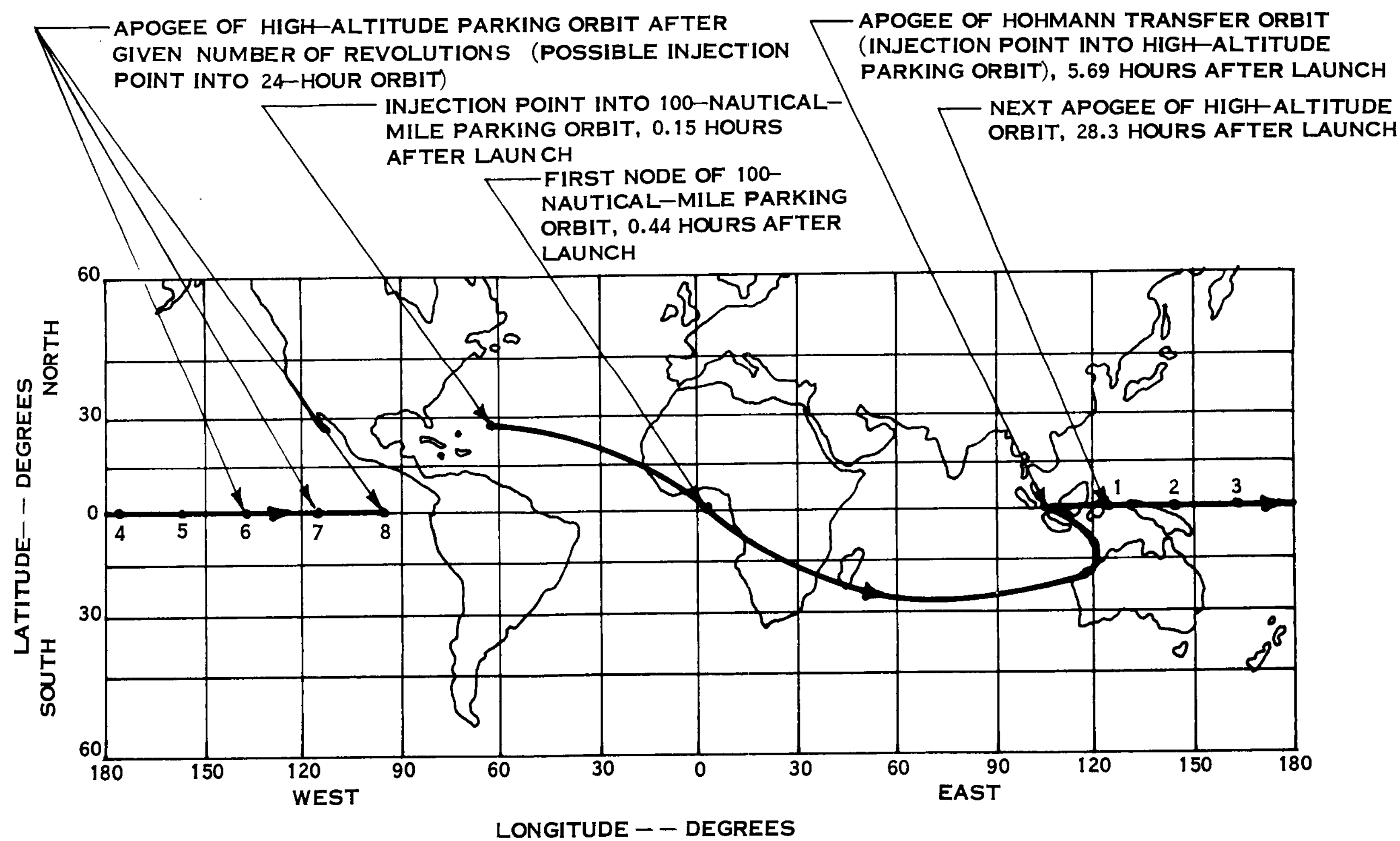

Figure 5.3-6 Earth Track of High-Altitude Parking Orbit Ascent Trajectory (Transfer from First Node of Low Altitude Parking Orbit)

200 feet per second. Approximately 8 days are required to reach a desired longitude station of about 100° W. Variations in launch azimuth could be used to add flexibility and permit intermediate longitude stations to be realized in the final, synchronous orbit with this given parking orbit.

It is noted that, for this method of injection longitude control, the final impulse, ΔV_c, required to bring the spacecraft to the circular, synchronous speed is assumed to be supplied by an auxiliary thrust device in the spacecraft. The launch vehicle would not then be required to function during the waiting period in the high altitude parking orbit. Therefore, its maximum mission time would be 5.69 hours, assuming that a first nodal departure from the initial low altitude parking orbit was used.

5.3.4 Recommended Centaur Ascent Trajectory

Figure 5.3-7 presents ground tracks of the ascent trajectories studied for the SLV3C/Centaur. The two optional techniques for arriving at a synchronous orbit injection station near the continental USA are shown. They are: (1) injecting at the second apogee of the transfer orbit and, (2) injecting at the first apogee with a synchronous orbit velocity deficiency of 200 ft/sec which causes the satellite to drift eastward until the desired final orbit station is reached. The former approach is preferred because the injection station is reached in about 16 hours as against about a week's delay for the latter. It may be desirable to somewhat "over-inject" for the preferred second apogee case in order to cause the satellite to drift a bit westward for a more favorable synchronous orbit station relative to the Rosman and Mojave ground stations.

For the reference ATS-4 concept using a spin-stabilized, Thiokol TE 364-3 solid rocket motor as an apogee injection stage (AIS), the Centaur would provide a 7.6° plane change at its second burn, initiating the transfer orbit. The ground track reflects this assumed plane change. The Centaur vehicle would then rotate (yaw) in essentially the local horizontal plane so

Figure 5.3-7

GROUND TRACK OF ASCENT TRAJECTORIES

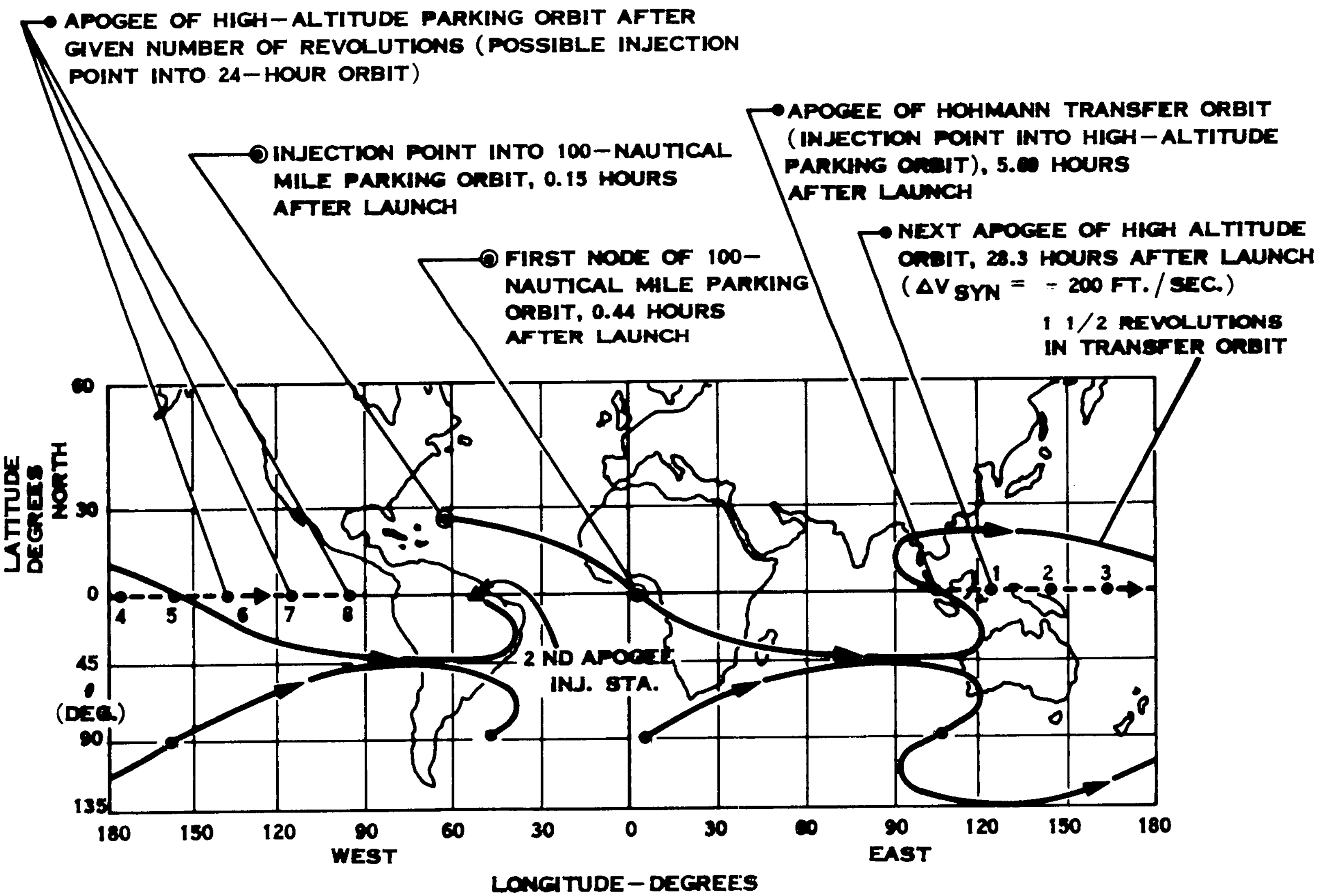

as to orient the thrust vector of the AIS in the required direction for the apogee injection impulse. The Centaur may then be caused to spin to about 1 RPM, at which point the spacecraft is separated and spun-up to about 60 RPM. During this process and throughout the transfer orbit, the pre-orbital spin control system acts to preserve the desired inertial orientation of the spin axis.

Also shown on Figure 5.3-7 is a plot of the magnitude of the corresponding space angle (θ) between the satellite spin axis and the instantaneous local vertical vector for the recommended second apogee injection case. It can be seen that this angle varies from a value of 90° at the nodal crossing down to a minimum value of about 45° at a true anomoly of 90° in the transfer orbit and up to a maximum value of about 135° at a true anomoly of 270°.

With the recommended ATS-4 configuration, the solar paddles are folded during the launch phase so as to permit the generation of solar power if a reasonably large angle can be preserved between the satellite spin axis and the sun vector. Hence, a study has been conducted of the preferred time of day for injection into the synchronous orbit (relative to the associated longitude subpoint) based on launch dates throughout the year.

For the reference ATS-4 concept, using a spin stabilized TE 364-3 as the AIS, the Centaur is used to provide a 7.6° orbit inclination change for the transfer orbit. Hence the apogee injection velocity impulse must be directed downward (toward the South Pole) at an angle of about 20° relative to the equatorial plane, to yield a synchronous equatorial orbit.

As depicted in Figure 5.3-8, by injecting at sunset into the synchronous orbit for a winter launch date (and at sunrise for a summer launch date) the angle between the spin axis and the sun vector is most favorable, up to a maximum value of 44°. (Acquisition of the nominal earth-pointing attitude

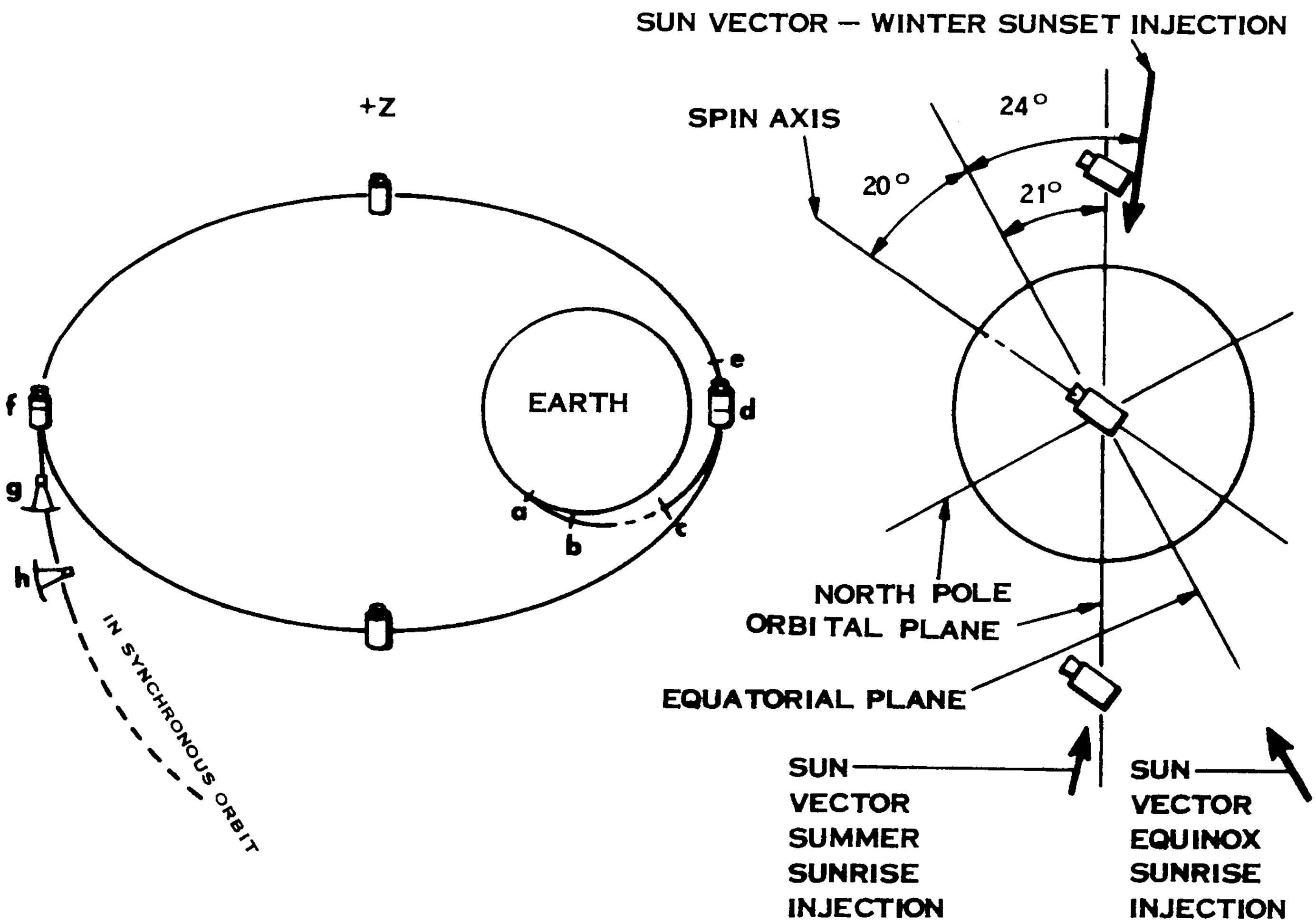

Figure 5.3-8 Spacecraft/Sun Orientation in Transfer Orbit

by the stabilization and control system is also facilitated by a sunrise or sunset injection into the final synchronous orbit.) At an equinox condition, either a sunrise or sunset injection can be employed, and the relative incidence angle can be as low as 20 degrees.

5.4 ORBIT PAYLOADS

5.4.1 General

Payload weight and volume have been treated as system parameters rather than fixed requirements. Thus, the studies have ranged from the minimum weight-volume capabilities of the SLV3A/Agena with several different Apogee Injection Stages (AIS), through various combinations of the SLV3C/Centaur with different shrouds and AIS's, through the Titan IIIC with shroud modifications to increase its payload volume capabilities.

5.4.2 SLV3A/Agena and SLV3C/Centaur

Analysis Procedure -- In calculating the orbit payload capabilities for the SLV3A/Agena and SLV3C/Centaur, the basic reference data were the payload-to-synchronous-apogee weights provided by the NASA, 2300 and 4000 pounds, respectively. The procedure used to determine the final orbit payload in the desired synchronous (24-hour) equatorial orbit was as follows:

The nominal payload-to-synchronous-apogee (W_{SAN}) was first reduced for those cases where a larger shroud was employed on the Centaur. For these calculations, the weight increase of the Surveyor shroud per inch of extension was taken as 5.4 pounds/inch (as specified by the NASA) and the change in the W_{SA} per pound change in the shroud weight (ΔW_s was taken as 1/13 (as specified by the vehicle contractor).

The nominal payload to synchronous apogee was also reduced for those cases where the Centaur vehicle was employed to effect an orbit plane change at the initiation of the transfer orbit. The associated change in W_{SAN} per foot/sec. of additional ΔV required of the Centaur was indicated to be 0.632 pound per foot/sec. by the vehicle contractor.

The modified payload-to-synchronous-apogee (W_{SA}) as thus obtained was then reduced by the weight of the attitude control expendables during the transfer orbit (W_{EX_C}). For the case of the 3-axis stabilized

Burner II Apogee Injection Stage (AIS) with only 5.25 hours (1/2 revolution) in the transfer orbit, this weight was taken as 5 lbs. (For the cases where a second apogee injection was employed, with an associated 15.75 hour coast time in the transfer orbit, then a final orbit payload weight reduction of 100 lbs. was assumed based on data supplied by the Burner II contractor, Reference 5-1.)

For the spin-stabilized AIS's, the control expendable weights were taken as 25 lbs., including spin-up and control for up to 15.75 hours in the transfer orbit(*).

Further reducing W_{SA} by the weight of the adaptor mating the launch vehicle to AIS/ATS-4 (W_A), the start-burn weight (W_{SB}) for the apogee injection maneuver was obtained. The end-burn weight (W_{EB}) was then calculated using the standard formula:

$$\ln \frac{W_{SB}}{W_{EB}} = \frac{\Delta V}{g I_{SP}}$$

where:

ΔV = characteristic velocity required of the AIS to achieve the synchronous equatorial orbit

g = acceleration of gravity

I_{SP} = specific impulse of the AIS

The end-burn weight (W_{EB}) was then reduced by the weights of the expended rocket motor inerts of the AIS (W_{EX_R}) the attitude control expendables (W_{EX_C}, including despin elements for the spin-stabilized AIS's), the AIS to ATS-4 spacecraft adaptor (W_A), and the empty weight of the AIS (W_E). In this way, the final synchronous equatorial payload weight (W_{PL}) was obtained.

(*) Later control analyzes revealed these weights to be conservative; control expendable weights could be as low as 10 pounds.

Orbit Plane Change by Centaur - In order to maximize W_{PL}, in some cases the Centaur was employed to provide an orbit plane inclination reduction (Δi_c) at injection into the transfer orbit. Table 5.4-1 summarizes as a function of Δi_c, the associated characteristic velocity which must be provided by the Centaur (ΔV_C), the deviation of this ΔV_C value from the nominal value for $\Delta i_c = 0$ ($\Delta\Delta V_C$), the associated change in synchronous apogee payload (ΔW_{SA}), the residual inclination of the transfer orbit which must be removed by the AIS based on an initial inclination of 28.5° for an Eastward launch from ETR (Δi_{AIS}), the characteristic velocity thus required of the AIS to yield a synchronous, equatorial orbit (ΔV_{AIS}), and the related start-burn to end-burn weight ratio, (W_{SB}/W_{EB}). The bottom half of Table 5.4-1 corresponds to the case where the ATS-4 is injected with a velocity deficiency from synchronous speed of 200 ft/sec.

The accompanying vector diagrams depict how the ΔV values were calculated for the transfer orbit and the apogee maneuvers for the synchronous injection case. The start-burn velocities (V_{SB}) and end-burn velocities (V_{EB}) are shown for each of these maneuvers.

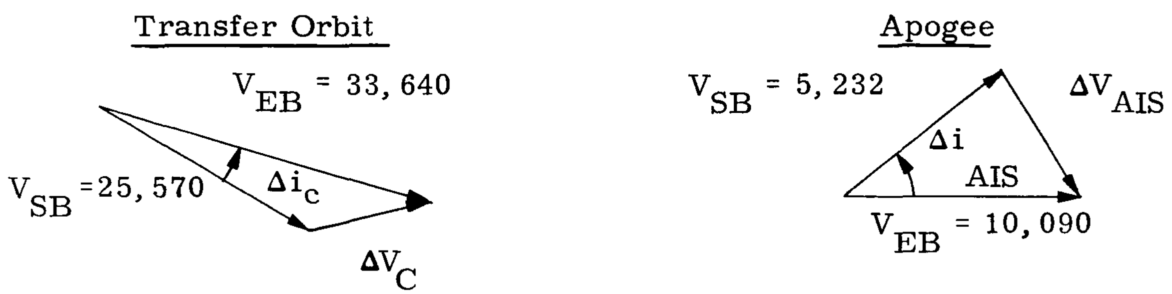

Maneuver Velocity Vector Diagrams

In considering use of the TE 364-3 motor (with its maximum propulsion loading of 1440 lbs.) for either the Burner II or spin-stabilized AIS's, it was established that, by using the Centaur to provide some of the

TABLE 5.4-1. TRANSFER ORBIT AND APOGEE MANEUVER DATA

Δi_C (deg.)	ΔV_C (ft./sec.)	$\Delta\Delta V_C$ (ft./sec.)	ΔW_{SA} $\approx .632 \Delta\Delta V$ (lbs.)	Δi_{AIS} (deg.)	ΔV_{AIS} (ft./sec.)	W_{SB}/W_{EB}
SYNCHRONOUS INJECTION						
0	8069	0	0	28.5	6030	1.9087
3	8216	147	95	25.5	5820	1.8661
4	8319	250	160	24.5	5753	1.8527
6	8637	568	360	22.5	5624	1.8273
8	9044	975	615	20.5	5503	1.8057
10	9534	1465	925	18.5	5390	1.7820
SUBSYNCHRONOUS INJECTION (Speed Deficiency = -200 ft/sec)						
0	8069	0	0	28.5	5854	1.873
6^o	8637	568	360	22.5	5430	1.790
8^o	9044	975	615	20.5	5320	1.770

required cancellation of the initial orbit inclination of 28.5°, the final orbit payload (W_{PL}) could be increased.

In order to determine the optimum value for the inclination change to be provided by the Centaur (Δi_c), plots were obtained of W_{PL} and AIS propellant weight (W_P) as a function of Δi_c, using the indicated analyses procedure and the data of Table 5.4-1. These plots are presented in Figures 5.4-1 and 5.4-2 for the SLV 3C/Centaur/Burner II-027B and the SLV 3C/Centaur/Spin-Stabilized TE 364-3, respectively. (These and all subsequent Centaur cases assume the use of a 10 ft. extended Surveyor Shroud as required by payload volume considerations.) From Figure 5.4-1 (Burner II case), it can be seen that a value for Δi_c of 7.7° corresponds to the maximum realizable propellant loading of 1440 lbs. For this Δi_c value, a W_{PL} of 1365 lbs. is achieved. Figure 5.4-2 for the spin-stabilized TE 364-3 case correspondingly indicates a Δi_c of 7.6° and a W^*_{PL} of 1615 lbs. Reducing W^*_{PL} by 10 pounds, the preliminary weight estimate for despin elements, the final payload weight (W_{PL}) is 1605 pounds.

Orbit Payload Data -- A summary of the orbit payload data obtained by the analysis procedure just presented is given in Table 5.4-2. The current Burner II with an extended coast capability (BII-025B) is considered as an AIS with the SLV3A/Agena, as is a spin-stabilized AIS using the same rocket motor, the TE 364-2. The advanced Delta motor, the TE 364-3, and the extended motor, the TE 364-4, are considered for the SLV 3C/Centaur, both as incorporated in Burner II AIS's and in spin-stabilized AIS's. Also indicated are the data for Centaur cases where the ATS-4 is under-injected with a final velocity deficiency from synchronous speed of 200 ft/sec. The notation for the various intermediate weight items is the same as that presented in the preceding paragraphs.

It can be seen that the SLV 3A/Agena payload weight for the BII-025B is 730 lbs. and for the spin-stabilized TE 364-2 is 965 lbs. Since these

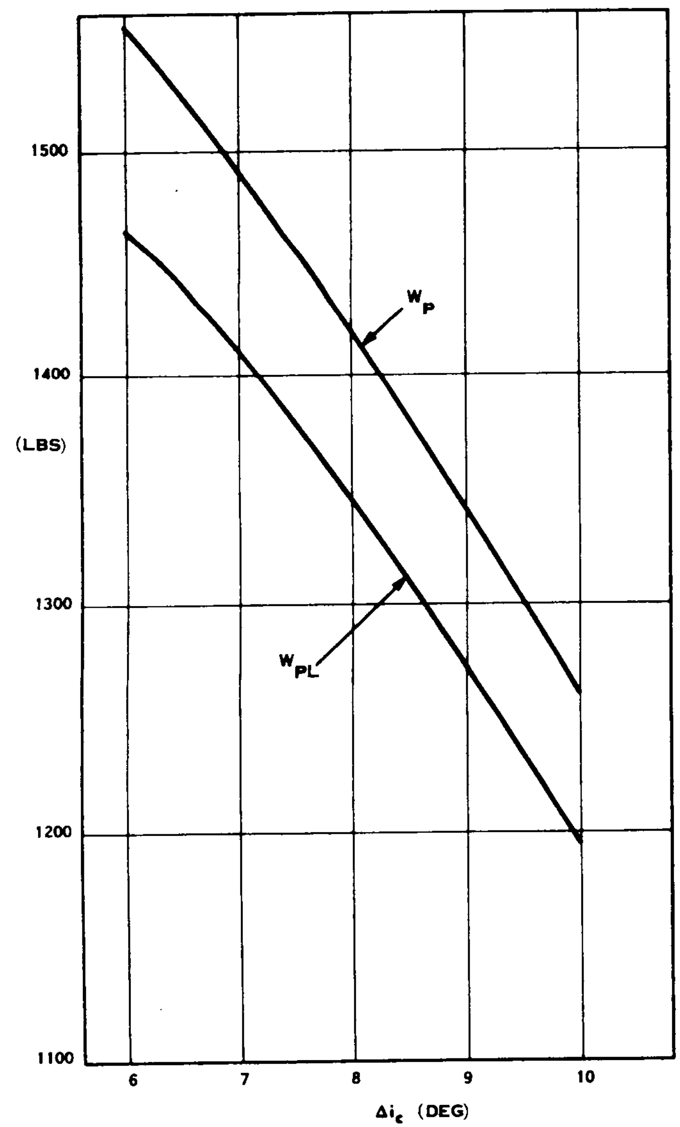

Figure 5.4-1 Payload and AIS Propellant Weight vs Δi_c (SLV3C/Centaur/Burner II-027B with 10-ft Ext. Surveyor Shroud)

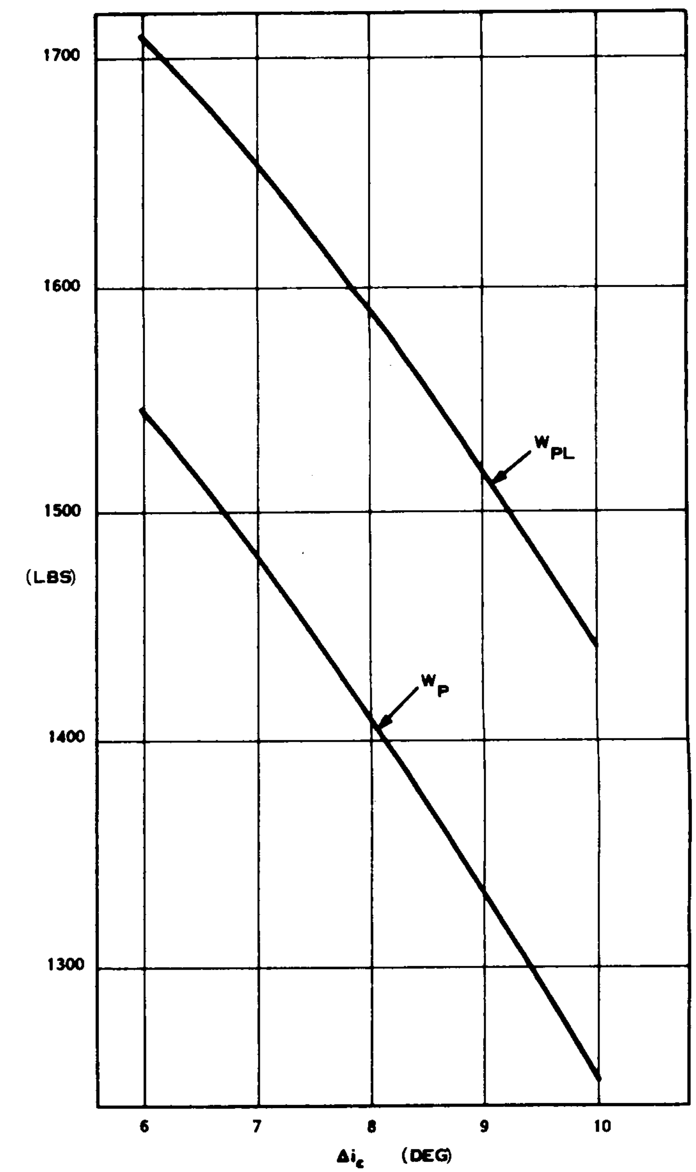

Figure 5.4-2 Payload and AIS Propellant Weight vs Δi_c (SLV 3C/Centaur/Spin Stab TE 364-3 with 10-ft Ext. Surveyor Shroud)

TABLE 5.4-2 ORBIT PAYLOAD DATA -AGENA AND CENTAUR (1ST APOGEE INJECTION)

Item	SLV 3A/Agena/TE 364-2		SLV 3C/Centaur/TE 364-3 (10 Ft. Ext. Shroud)				SLV 3C/ Centaur/TE 364-4 (10 Ft. Ext. Shroud)			
	BII	Spin Stab.	BII		Spin Stabilized		BII		Spin Stabilized	
ΔV_{SYN}	0	0	0	-200	0	-200	0	-200	0	-200
W_{SAN}	2300	2300	4000	4000	4000	4000	4000	4000	4000	4000
ΔW_{SA} (ΔW_S)	- -	- -	-50	-50	-50	-50	-50	-50	-50	-50
ΔW_{SA} (Δi_C)	- -	- -	-575	-500	-560	-490	- -	- -	- -	- -
Δi_C	0	0	7.7	7.1	7.6	7.0	0	0	0	0
W_{SA}	2300	2300	3375	3450	3390	3460	3950	3950	3950	3950
W_A	-115	-125	-150	-150	-150	-150	-150	-150	-150	-150
W_{EX_C}	-5	-25	-5	-5	-25	-25	-5	-5	-25	-25
W_{SB}	2180	2150	3220	3295	3215	3285	3795	3795	3775	3775
W_P	-1040	-1020	-1440	-1440	-1440	-1440	-1805	-1770	-1795	-1760
W_{EB}	1140	1130	1780	1855	1775	1845	1990	2025	1980	2015
W_{EX_R}	-15	-15	-15	15	-15	-15	-20	-20	-20	-20
W_{EX_C}	-15	-10	-15	-15	-10	-10	-20	-20	-10	-10
W_A	-30	- -	-35	-35	- -	- -	-50	-50	- -	- -
W_E	-350	-140	-350	-350	-145	-145	-400	-400	-160	-160
W_{PL}	730	965	1365	1440	1605	1675	1500	1535	1790	1825

NOTE: All units are pounds except for ΔV_{SYN}, (FT/SEC)and Δi, (DEG) payloads (and associated shroud volume constraints) were found incompatible with those required to meet mission objectives, the SLV 3A/Agena was dropped from further consideration as a launch vehicle for the ATS-4.

5.4.3 Titan IIIC

Based upon data obtained from the vehicle contractor (Reference 5.4), the Titan IIIC payload capability in a synchronous, equatorial orbit is 2100 lbs. based upon use of a standard shroud and a nominal ascent trajectory. This assumes as Eastward launch from ETR, that the transfer orbit is initiated at the first or second node of the parking orbit, and that final injection occurs at first apogee of the transfer orbit.

The additional weight associated with a modified OAO shroud to meet ATS-4 volume requirements is 1400 lbs. The factor relating decrement in payload weight to increase in shroud weight (ΔW_S) is 0.06. Hence, the final synchronous payload would be reduced by 85 lbs. with the use of a modified OAO shroud.

In addition, an adaptor section weighing 125 lbs. would be required to mate the OAO shroud with the Titan IIIC transtage. Therefore, the final synchronous orbit payload capability (W_{PL}) is reduced to 1865 lbs.

5.4.4 Payload Data Summary

Table 5.4-3 presents a summary of the final orbit payload capabilities of the launch vehicles under consideration, including the appropriate shrouds and AIS's. For the Centaur vehicle, the payload weights associated with under-injection (ΔV = -200 ft/sec) at first apogee of the parking orbit are indicated, as well as payload weights for synchronous injection at 2nd apogee of the transfer orbit.

As previously noted, for the recommended SLV 3C/Centaur/Spin-Stabilized TE 364-3, the orbital payload weight capability is 1605 pounds. For the corresponding SLV 3C/Centaur/BII-027B (same rocket motor for the AIS) the payload weight for 2nd apogee injection is 1265 pounds. This represents a 100 pound reduction from the 1st apogee payload weight as previously indicated.

TABLE 5.4-3

ORBIT PAYLOAD DATA SUMMARY

BOOSTER	SHROUD	BOOSTER INCLIN CHANGE	PAYLOAD TO SYN. APOGEE	ΔV FROM SYN.	APOGEE STAGE NAME	APOGEE STAGE FULL WT	APOGEE STAGE PROP WT	ORBIT PAYLOAD 1ST APOGEE	ORBIT PAYLOAD 2ND APOGEE
		(DEG)	(LB)	(FT/SEC)		(LB)	(LB)	(LB)	(LB)
SLV3A/ AGENA	NIMBUS	0	2,300	0	BII-027B	1,450	1,040	730	—
		0	2,300	0	SPIN STAB (TE 364-2)	1,175	1,020	965	—
SLV3C/ CENTAUR	SURVEYOR (10 FT EXT)	7.7	3,375	0	BII-027B	1,855	1,440	1,365	1,265
		7.1	3,450	-200	SAME	SAME	SAME	1,440	—
		7.6	3,390	0	SPIN STAB (TE 364-3)	1,600	1,440	1,605	1,605
		7.0	3,460	-200	SAME	SAME	SAME	1,675	—
		0	3,950	0	BII-128B	2,295	1,805	1,500	1,400
		0	3,950	-200	SAME	2,260	1,770	1,535	—
		0	3,950	0	SPIN STAB (TE 364-4)	1,975	1,795	1,790	1,790
		0	3,950	-200	SAME	1,940	1,760	1,825	—
TITAN 3C	MOD OAO			0	—			1,865	—

5.5 ORBIT INJECTION ERRORS

5.5.1 Error Values

Because of guidance inaccuracies inherent in the various phases of the ascent and orbit injection maneuvers, the final orbit will deviate from the desired synchronous, circular, equatorial orbit. This subsection describes the estimates that were obtained of the three sigma (σ) values for the significant orbit element errors, how these errors affect the deviations in satellite subpoint latitude and longitude (the quantities of greatest interest from a mission standpoint) and the velocity impulse requirements associated with correcting these errors.

One error of particular concern in the transfer orbit was the possible lowering of the second perigee altitude when final injection was delayed until second apogee. It was established that when the Centaur was used to initiate the transfer orbit from a parking orbit altitude of 100 n-mi., then a 3 sigma minimum value for the perigee altitude during the second revolution in the transfer orbit is 95 n-mi. This fully acceptable orbit error effect was corroborated with the vehicle contractor.

The orbit element errors of concern for the final, synchronous orbit are those which have a dominant effect on variations in the satellite subpoint latitude and longitude; these element errors include orbit inclination, eccentricity and period errors.

Because of the general nature of this ATS-4 mission investigation, extensive study efforts were not expended to obtain a precise definition of expected orbit element error values. Only the general magnitudes of these errors are required to define an acceptable guidance approach for their correction and to establish the associated, component velocity impulse requirements for the auxiliary propulsion system. (Comparable velocity impulses are also needed to meet station keeping and repositioning requirements.)

Various sets of error data were analyzed in order to arrive at reasonable estimates for final orbit element errors. The cases studied included the 3 launch vehicles under consideration; the SLV 3A/Agena, the SLV 3C/Centaur and the Titan 3C, with both Burner II and spin-stabilized AIS's being investigated for the Agena and Centaur launch vehicles.

Table 5.5-1 summarizes the 3 sigma values for final orbit element errors thus obtained from the various data sources and indicates the design values chosen for the ATS-4 mission study.

5.5.2 Associated Latitude-Longitude Deviations

As noted, the aspect of the orbit element errors of greatest concern is the associated variation in satellite subpoint latitude ($\Delta\phi$) and longitude ($\Delta\lambda$). With regard to eccentricity error (e), the approximate expression for the relationship between e and $\Delta\lambda$ can be obtained by first expressing the true anomaly, ν (See Figure 5.5-1) as a power series in the mean anomoly, M. (The satellite is assumed to be initially injected near the line of apsides of its final orbit.)

$$\nu = M + 2e \sin M + (5/4) e^2 \sin 2M + \ldots$$

Therefore; $\Delta\lambda = \nu - M \approx 2e \sin M = 2e \sin \eta\,(t-T)$

Where: η = mean angular motion

T = time of perigee passage

Hence, $\Delta\lambda_{max}$ (degrees) = $\pm$ (57.3) 2e = $\pm$ 115e, with a daily oscillation between these extreme values. Should the satellite be injected at positions far removed from the line of apsides, then the $\Delta\lambda$ values may range from 0 to 230e or 0 to -230e.

As an example of the realizable values for longitude deviations ($\Delta\lambda$), the reference launch vehicle -AIS (SLV3C/Centaur/Spin-Stabilized AIS) is considered. For the 3 sigma value of 0.003 for e as indicated in Table 5.5-1, the $\Delta\lambda$ values could oscillate daily between $\pm$ 3.5 degrees, or 0 to +7.0 degrees, or 0 to -7.0 degrees depending on the satellite injection

TABLE 5.5-1 ORBIT INJECTION ERRORS

Launch Vehicle	Apogee Stage	Injection Technique	3σ Error Value Eccentricity e	Inclination i (deg)	Period ΔP (Min)	Remarks (Source And/Or Chosen Value)
SLV 3A/ Agena	Attitude Stab.	At 1st Apogee	0.008	± 0.25	± 55	Lockheed - Theoretical Kick Stage
	Burner II	At 1st Apogee	0.0199	± 0.35	± 36	Boeing - COMSAT Data
	Attitude Stab.	At 1st Apogee	0.025	± 0.60	± 57	Fairchild Hiller - SMS Study
	Burner II	At 1st Apogee	0.025	± 0.5	± 55	Chosen Design Values
	Spin- Stab.	Timed	0.0266	+ 1.8 - 1.74	+ 59.5 - 54.4	NASA - Lewis - Sagge Mission
	Spin - Stab.	At 1st Apogee	0.0425	± 1.18	± 57	Boeing - COMSAT Data
	Spin - Stab.	At 1st Apogee	0.042	± 1.25	± 60	Chosen Design Values
SLV 3C/ Centaur	Burner II	At 1st Apogee	0.017	± 0.33	± 36	General Dynamics - REF 5-1
		At 2nd Apogee	0.017	± 0.40	± 36	Boeing
		At 1st Apogee	0.017	± 0.35	± 36	Chosen Design Values
		At 2nd Apogee	0.017	± 0.40	± 36	Chosen Design Values
	Spin - Stab.	At 1st Apogee	0.03	± 0.9	± 45	Chosen Design Values
		At 2nd Apogee	0.03	± 1.1	± 45	Chosen Design Values
TITAN - 3C	--	At 1st Apogee	0.01	± 0.3	± 3.5	3 Times Realized Errors For Near-Synchronous SSLV #11

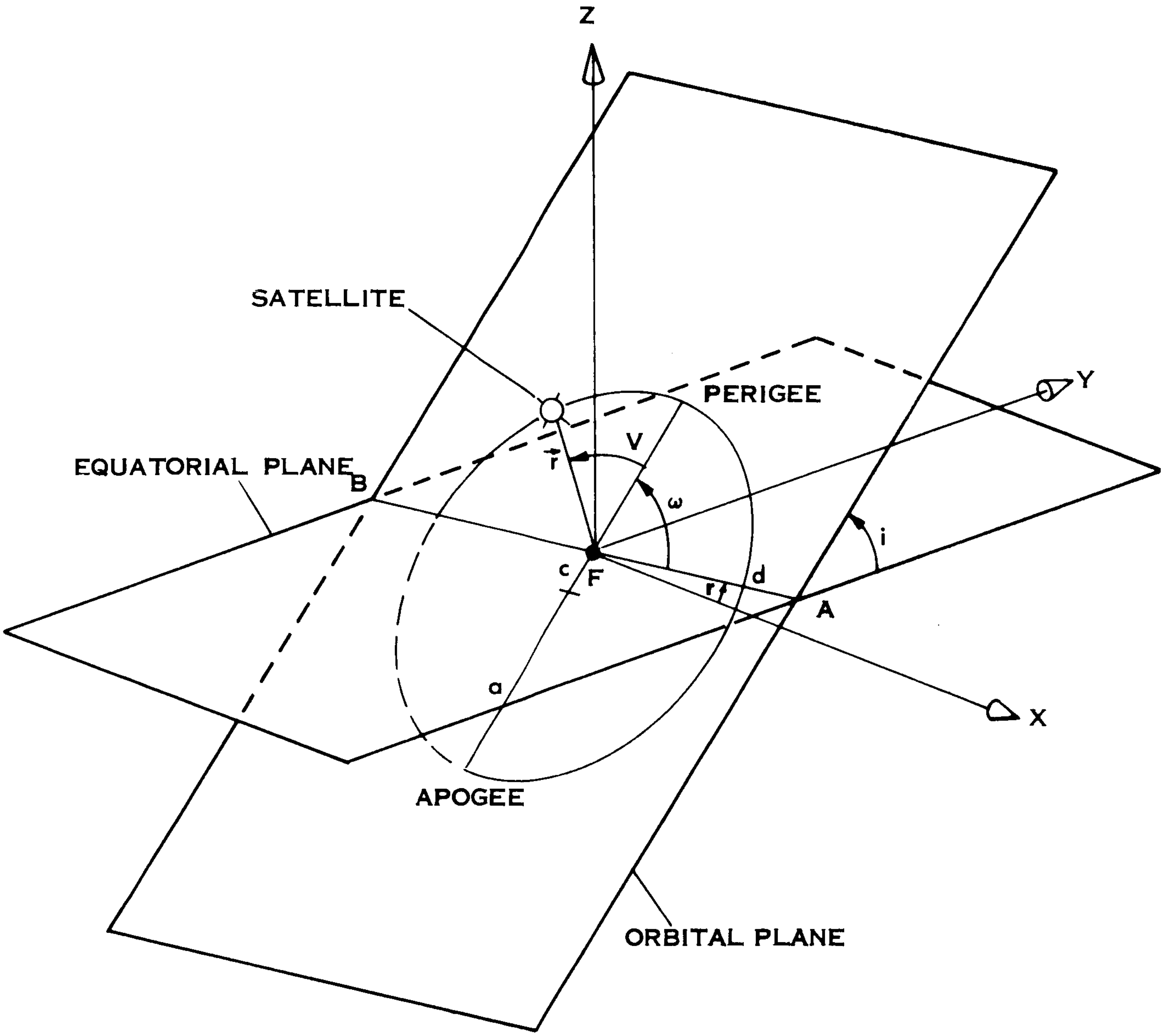

F = CENTER OF EARTH

a = SEMIMAJOR AXIS

e = ECCENTRICITY = c/a

d = ASCENDING NODE

Ω = LONGITUDE OF THE ASCENDING NODE

ω = ARGUMENT OF PERIGEE

u = ARGUMENT OF LATITUDE = v + w

v = TRUE ANOMALY

i = INCLINATION OF THE ORBIT PLANE TO THE EQUATORIAL PLANE

$\vec{r}$ = RADIUS VECTOR TO THE SATELLITE

V = ORBITAL VELOCITY OF THE SATELLITE

AB = LINE OF NODES

Figure 5.5-1 Orbital Geometry and Definitions of Symbols point relative to the line of apsides of its final orbit. Longitude oscillations of this magnitude would be excessive based on mission considerations; and, hence, orbit eccentricity must be corrected to relatively low levels.

The period error is even more critical as regards the associated longitude deviations. Thus, since the satellite has a mean angular motion (η) of about 360 degrees/day, a period error of 1 minute would result in an average longitude drift rate relative to the Earth ($\Delta\bar{\lambda}$) given by $\Delta\bar{\lambda} = \Delta\eta = \frac{360}{(24)(60)} = 0.25$ deg/day. For the case of the reference launch vehicle -- AIS configuration, with an indicated 3 σ period error of ± 45 min., the initial longitude drift rate could thus be as high as 11.3 deg/day. In order to prevent excessive off-station drift, this initial period error must be corrected as soon as possible after orbit injection.

An orbit inclination error (i) would cause a daily, periodic oscillation in latitude ($\Delta\phi$), with $\Delta\phi_{max}$ values equal to ± i. Thus, for the reference case with a 2nd apogee injection, the $\Delta\phi_{max}$ values would be ± 1.08 degrees. Oscillations of this magnitude would not necessarily be excessive from a mission experiment standpoint. However, velocity impulse requirements for correcting orbit injection errors have been predicated upon compensating the initial inclination error as well. This will facilitate demonstration of the specified North-South station keeping capability. However, since such a capability can be demonstrated even in the presence of initial inclination errors, the elimination of guidance maneuvers for inclination error correction (with a resultant reduction in impulse requirements for the auxiliary propulsion system) should be considered.

5.5.3 Associated Corrective Velocity Impulse Requirements

The chosen 3 sigma design values for the 3 orbit element errors under consideration were next related to the velocity impulses required to correct them. The formulas relating the associated corrective velocity impulses (ΔV) to the orbit element errors are given by:

- <u>In-plane (IP) Errors</u>

  Period error: $\Delta V_{\Delta P}$ (ft/sec) = 2.36 ΔP (min)

  Eccentricity error: ΔV_e (ft/sec) = 5045e

- <u>Out-of-plane (OP) Error</u>

  Inclination error: ΔV_i (ft/sec) = 176 Δi (deg)

Table 5.5-2 summarizes the associated corrective velocity impulse values for the various error cases of interest. In establishing the final total value for ΔV_{IP}, it was assumed that the eccentricity and period error would be corrected in concert to minimize the required ΔV. Hence ΔV_{IP} is taken as the upper bound of the ΔV_e and $\Delta V_{\Delta P}$ values. Independent correction of the out-of-plane error is assumed, so that ΔV_{OP} is taken equal to ΔV_i. The three - σ values for V_{1P} and V_{OP} for the reference launch vehicle - AIS configuration (SLV3C/Centaur/Spin Stabilized TE364-3 with 2nd apogee injection) are indicated to be 150 ft/sec and 195 ft/sec, respectively.

TABLE 5.5-2 INJECTION ERROR VELOCITY IMPULSE REQUIREMENTS

Booster	Apogee Stage	Injection Point	In Plane Errors					Out Of Plane Errors		
			ΔP (min)	$\Delta V_{\Delta P}$ (ft/sec)	e	ΔV_e (ft/sec)	ΔV_{IP} (ft/sec)	Δi (deg)	ΔV_i (ft/sec)	ΔV_{OP} (ft/sec)
SLV 3A/ Agena	B-II	1st Apogee	55	130	0.025	126	130	0.5	88	90
	Spin Stab.	1st Apogee	60	142	0.042	211	210	1.25	220	220
SLV 3C/ Centaur	B-II	1st Apogee	36	85	0.017	86	85	0.35	62	65
	Spin Stab.	1st Apogee	45	106	0.030	151	150	0.90	158	160
	B-II	2nd Apogee	36	85	0.017	86	85	0.42	77	80
	Spin Stab.	2nd Apogee	45	106	0.030	151	150	1.08	193	195
Titan 3C	--	1st Apogee	3.5	8.3	0.010	50	50	0.3	55	55

5.6 ORBIT PERTURBATIONS

5.6.1 General

The ATS-4 is to be established in a synchronous equatorial orbit. For the purposes of the following discussion, it is assumed to be injected near a 90° W longitude station. The concept of a "stationary position" relative to the earth is limited to two-body mechanics. Inclusion of noncentral and/or non-Newtonian forces cause the satellite to drift from its "ideal position". Knowledge of satellite deviations becomes essential for defining station keeping propellant and guidance requirements.

The more important perturbation influences relative to the ATS-4 mission therefore are discussed. Earth oblateness and extraterrestrial perturbations are included in Subsection 5.6.2 while perturbations resulting from the earth's equatorial ellipticity are discussed in Subsection 5.6.3.

5.6.2 Earth Oblateness and Extraterrestrial Perturbations

General - The perturbative influences due to earth oblateness, lunar-solar gravitational forces, and solar radiation pressure forces were developed in studies of synchronous meteorological satellite system problems (Reference 5-5). These results were based on general perturbation theory (References 5-6 to 5-13) and verified by special perturbation techniques (References 5-14 to 5-17). Orbital perturbation forces ascribed to solar winds, interplanetary dust, solar reradiation from the earth, and electrostatic and magnetic drag may be neglected, since these forces are many orders of magnitude less than the perturbations mentioned above.

Guidance system limitations preclude the achievement of an exact circular orbit. Hence, for the initial perturbation studies under discussion, an initial orbit eccentricity of 0.005 was assumed.[4] The initial location of

4. An increase in initial eccentricity to the maximum reference value, 0.030, would have no significant effect on the subsequent perturbation analysis results.

the argument of perigee (ω) has a moderate influence on the maximum osculation of the elements. This effect was considered in determining the perturbations of the orbital elements of concern for the ATS-4 mission, namely semimajor axis, eccentricity, and inclination.

Semimajor Axis - The semimajor axis "a" is the most crucial element with regard to longitude drift. Solar, lunar, or earth oblateness gravitational perturbations cannot produce a secular change in a semimajor axis. Also, to the accuracy of the subject analysis, Δa experiences no long period motion from the aforementioned gravitation sources. Solar radiation pressure forces, however, induce a semimajor axis change each time the satellite enters the shadow. This change, based on 78 hours of shadow time for the most critical perigee orientation of an assumed 0.005 eccentric orbit, amounts to about 70 ft/year Δa reduction.[5] Accordingly, secular Δa perturbations can be safely neglected.

Short period perturbations due to lunar-solar gravitational effects are shown in Figure 5.6-1 for two moon-sun-satellite initial configurations. A 12°/yr steady easterly subsatellite drift occurs when the sun, moon, and satellite are all initially aligned along a common radius.

Altering the initial configuration (sun and moon located along a common radius and positioned 90° from the satellite; $\nu = -90^{\circ}$; $g_{s_o} = g_{m_o} = 0$; $\Omega_m = \Omega_s = 0$) alters the osculating level.

It is emphasized that relative drift, ascribed to Δa, can be nullified completely by injecting the satellite at the "correct altitude" regardless of sun-moon-satellite orientation or the earth's polar shape. Specifically, once the correct mean motion is established, there will be no secular drift.

Eccentricity - The earth's oblateness contribution to long-period eccentricity perturbations is approximately two orders of magnitude less than

5. Based on a disturbing acceleration of 1.6×10^{-6} ft/sec^2.

perturbations arising from other sources. Solar pressure forces exert the dominant perturbing influence on eccentricity. Nevertheless, the Δe perturbations caused by the foregoing effects over the course of a year will be much smaller than the possible residual eccentricity following injection error correction.

Inclination - Inclination excursions result primarily from lunar-solar gravitational accelerations. These excursions were computed from the planetary equations (Reference 5-9) using Musen's disturbing function (Reference 5-6) and subsequently were corroborated by special perturbation techniques (References 5-16 and 5-17).

The accumulation of inclination perturbations after one year is small, about 0.75°, as shown in Figure 5.6-2. Nevertheless, this causes a gradual expansion in the latitude deviations from the ideal subsatellite position. The "apparent secular growth" in inclination is attributed to long period perturbations dependent on $\dot{\Omega}$ and $\dot{\omega}$. This long period contribution produces a maximum inclination change of 6.5° and has an associated period of approx-mately 54 years.

5.6.3 Terrestrial Perturbations - Equatorial Ellipticity

Longitude station keeping requirements for a 24-hour equatorial satellite largely stem from the dominant perturbations induced by the earth's triaxial shape. Considering only the associated second order sectorial gravitational harmonic, a satellite in an equatorial, circular orbit at synchronous altitude will exhibit pure harmonic motion about the nearest end of the earth's minor axis. The amplitude of this motion is equal to $\pm\Delta\lambda_{m_o}$, where $\Delta\lambda_{m_o}$ is equal to the initial satellite longitude (λ_o) minus the longitude of the minor axis (λ_m). Simultaneously, the satellite will trace out periodic radial excursions (Δr) with maximum amplitude occurring at the crossing of the minor axis.

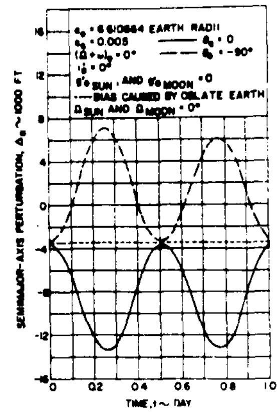

Figure 5.6-1 Satellite Semimajor Axis Perturbation

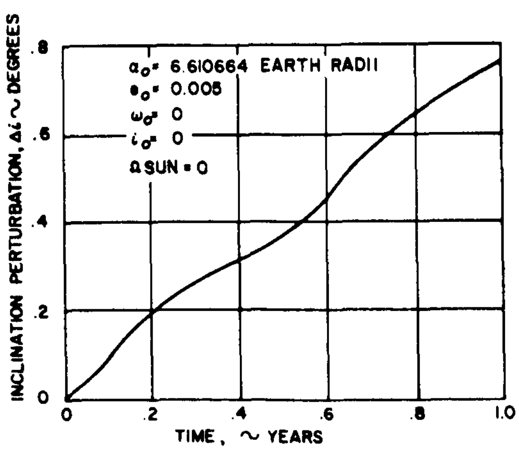

FIGURE 6.10
SATELLITE INCLINATION PERTURBATION

Figure 5.6-2 Satellite Inclination Perturbation

An approximate relationship between radial excursion (Δr, measured in earth radius) and satellite longitudinal excurisions measured from the minor axis ($\Delta \lambda_m$) is given by (Reference 5-16):

$$\Delta r = 4 \sqrt{J_2^{(2)}} \sin \lambda_{m_o} \left[1 - \frac{\sin^2 \Delta \lambda_m}{\sin^2 \Delta \lambda_{m_o}} \right]^{1/2}$$

where

$J_2^{(2)}$ = coefficient of the second sectorial harmonic of the earth's gravitational potential function

Reference 5-15 indicates that $J_2^{(2)} = -2.32 \times 10^{-6}$ and $\lambda_m = 127.5$ degrees west. Based on these data, Figure 5.6-3 presents the expected radial and longitudinal excursions for a satellite injected at 90° W longitude ($\Delta \lambda_{m_o} = 37.5^\circ$). In the absence of injection errors the satellite initially moves toward the minor axis at longitude 127.5°W and experiences an increase in radial displacement. The period of this osciallation is 2.22 years. After 1.11 years, the satellite is displaced about 75°W from the desired subsatellite station.

Table 5.6-1 indicates the range in values for $J_2^{(2)}$ as determined by various investigators in recent years. Also, shown are calculated values for the longitude of the equatorial major axis, $\varphi_2^{(2)}$.

More recent data on the earth's triaxial shape have been derived from SYNCOM II orbit observations (Reference 5-18). These data indicate that the nearest end of the earth's minor axis, about which a satellite at 90 degrees west longitude will oscillate, is at 109 ±6 degrees west; further, the value of $J_2^{(2)}$ is calculated as $-(1.70 \pm 0.05) \times 10^{-6}$. These data are in reasonable agreement with those presented in Table 5.6-1 as published since 1963 by Kaula, Izsak, Newton, Kozai and Guier, and represent an adequate basis for designing a station keeping system for a 24-hour satellite.

TABLE 5.6-1 EARTH EQUATORIAL ELLIPTICITY DATA

	Investigator	$-J_2^{(2)} \times 10^6$	$\phi_2^{(2)}$
1.	Izsak (1961)	5.35	33° W
2.	Kaula (1961)	1.68	38.5° W
3.	Kozai (1961)	2.32	37.5° W
4.	Newton (1962)	4.0	11° W
5.	Kaula (1963 a)	3.89	22° W
6.	Kaula (1963 b)	3.43	21.5° W
7.	Newton (1963)	2.2	10° W
8.	Kozai (1963)	1.97	19.5° W
9.	Izsak (1963)	1.05	11.2° W
10.	Guier (1963)	1.80	10.4° W

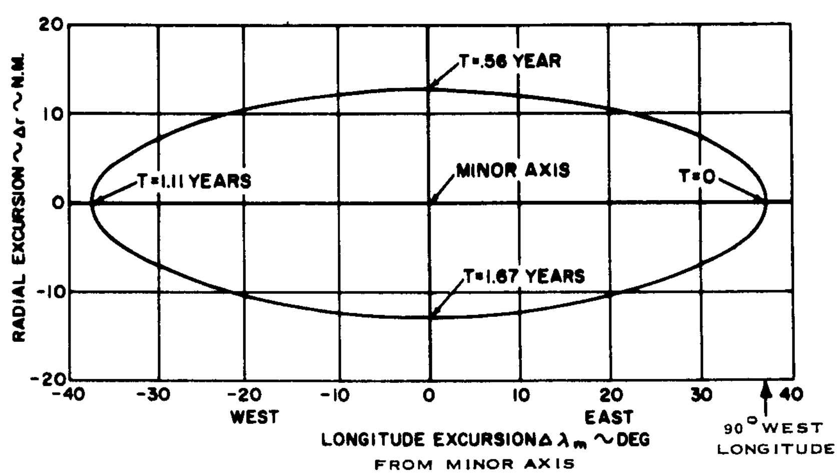

Figure 5.6-3 Long Period Oscillation for a Satellite Injected into a Synchronous Orbit at 90° W Longitude

$(J_2^{(2)} = -2.32 \times 10^{-6}$; $\Delta \lambda m_o = +37.5$ Degrees)

5.6.4 Associated Corrective Velocity Impulse Requirements

In summary, the major orbit perturbation necessitating a North-South station keeping operation is the long-period buildup in orbit inclination caused by solar-lunar gravitational perturbations. The indicated 0.75 degree/year inclination change would require a velocity impulse of about 130 feet/second for its correction.

The major longitudinal orbit disturbance effect, giving rise to a requirement for East-West station keeping, is that associated with the Earth's gravitational perturbation caused by its equatorial ellipiticity, i.e., its second sectorial gravitational harmonic. The longitudinal perturbing forces associated with this effect must be countered in order to provide east-west station keeping. The maximum perturbing accelerations, and associated required corrective velocity impulses, will occur at longitude stations 45 degrees removed from the earth's minor and major axes. Based on SYNCOM II orbit data (Reference 5-18), these longitudes are at 154 degrees West, 64 degrees West, 26 degrees East and 116 degrees East. For the associated $J_2^{(2)}$ value of -1.7×10^{-6}, the associated maximum characteristic velocity required for a year of east-west station keeping above a triaxial earth at any of these longitudes is 5.36 feet/second.

Figure 5.6-4 presents a corresponding plot of the characteristic velocity required per year for east-west station keeping as a function of the synchronous, equatorial longitude station. At a longitude of 90 degrees West, the ΔV required is seen to be about 3 ft/sec per year. It is noted that these required characteristic velocity values may be low by as much as 15 percent because of higher order tesseral harmonics that were neglected in the reduction of SYNCOM II orbit data (Reference 5-18).

Also shown on Figure 5.6-4 for comparison are the characteristic velocity requirements per year of east-west station keeping based on the

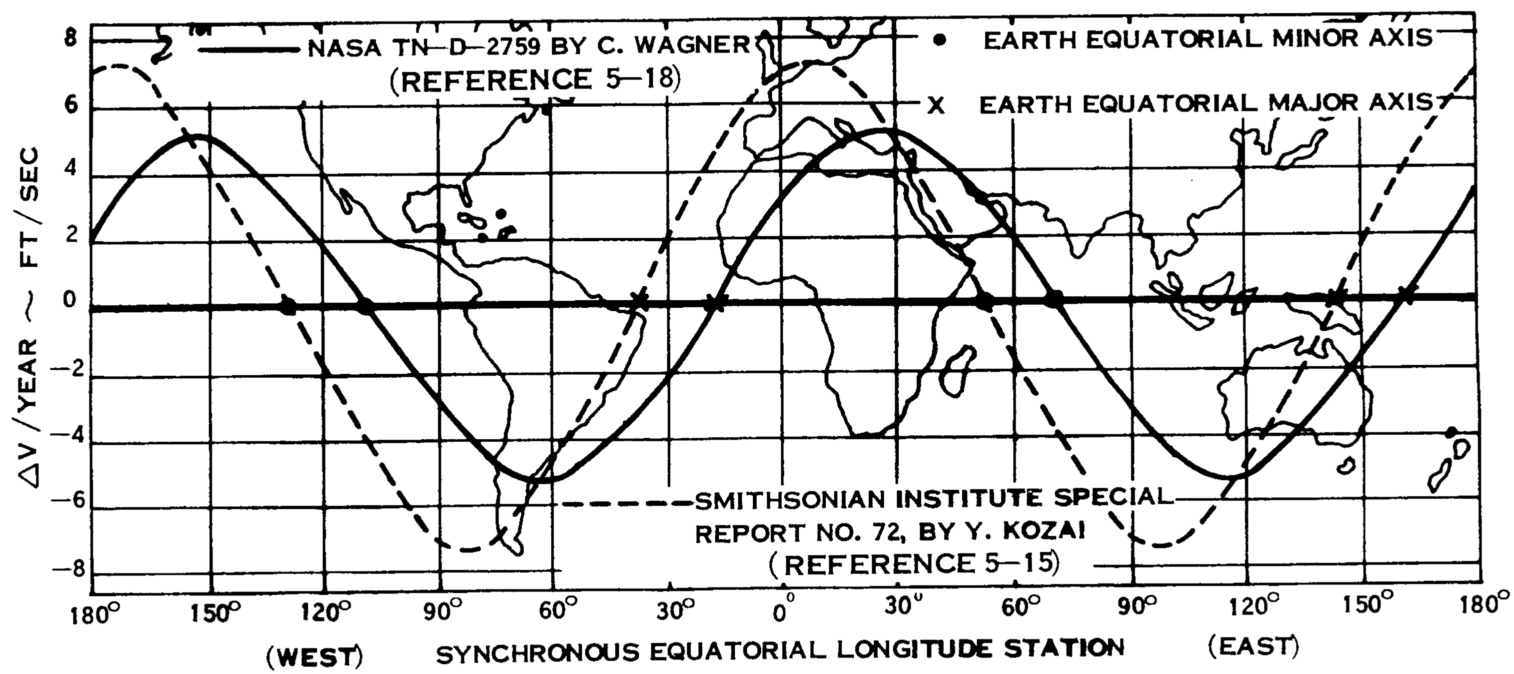

Figure 5.6-4 Required Velocity Impulse (ΔV) Per Year of East-West Station Keeping as a Function of Synchronous Equatorial Longitude Station

earth triaxial gravity data of Reference 5-15 ($J_2^{(2)} = -2.32 \times 10^{-6}$ and $\lambda_m = -127.5$ degrees). A ΔV of about 7 feet/second is indicated to be required for one year of station keeping for a satellite located at 90 degrees West longitude.

5.7 AUXILIARY PROPULSION SYSTEM

5.7.1 Velocity Impulse and Thrust Requirements

Table 5.7-1 summarizes the velocity impulse requirements which must be satisfied by the auxiliary propulsion system (APS). The data of this table incorporate the velocity impulse requirements previously given in subsection 5.5 for injection error correction and in subsection 5.6 for compensation of orbit perturbations. The 120 ft/sec velocity impulse indicated for East-West station keeping and repositioning includes the 100 ft/sec repositioning capability specified by NASA. It also provides approximately a 100% margin on the maximum ΔV value of 10.6 ft/sec required for 2 years of East-West station keeping. Also included in Table 5.7-1 is a ΔV impulse requirement of 200 ft/sec for final orbit speed compensation for those cases where a subsynchronous injection is considered.

Initially, thrust levels of from 1 to 5 pounds were considered for the APS; a 1-pound level was later specified based on consideration of attitude stabilization requirements. Various nozzle configurations were also considered, ranging from 1 to 5 pound thrusters aligned along the satellite Z-axis to several 1 to 5 pound thrusters aligned transverse to the Z-axis i.e., along the roll axis (parallel to the direction of motion) and the pitch axis (perpendicular to the orbit plane). The final nozzle arrangement for the reference ATS-4 configuration has two 1-pound thrusters aligned fore-aft along the roll axis and one along the pitch axis (thrusting North).

5.7.2 Initial APS Comparison Study

Various propulsion systems were studied as candidates for the APS. The two most promising were a hypergolic bipropellant system, using a 50-50 fuel mixture of hydrazine and UDMH with N_2O_4 as the oxidizer, and a monopropellant hydrazine system, using the Shell 405 catalyst.

In order to conduct a weight comparison study of these two

TABLE 5.7-1

APS VELOCITY IMPULSE REQUIREMENTS

BOOSTER	APOGEE STAGE	INJ APOGEE	REQUIRED ΔV (FT/SEC)					
			SYN SPEED DEFICIENCY	INJECT ERROR (3σ)		N-S STA KEEP	E-W STA KEEP & REPOS	TOTAL
				IN PLANE	OUT PLANE			
SLV/3C CENTAUR	BURNER II	2ND	0	85	80	130	120	415
		1ST (-200 FT/SEC)	200	85	65			600
	SPIN STAB	2ND	0	150	195			595
		1ST (-200 FT/SEC)	200	150	160			760
TITAN 3C	—	—						
		1ST	0	50	55	130	120	355

E-5

candidate systems, preliminary total impulse requirements for the APS were established. Thus, based upon the velocity impulse requirements of Table 5.7-1 and preliminary orbit payload data, the APS total impulse requirements given in Table 5.7-2 were calculated for the launch vehicle configurations of strongest interest.

Preliminary designs for hypergolic bipropellant and monopropellant hydrazine propulsion systems to meet the three total impulse levels of Table 5.7-2 were established. All of these early APS's assumed the use of a single 5-pound thruster aligned along the Z axis. Summary data for these systems are presented in Table 5.7-3. Implicit in these data are assumed specific impulse (I_{sp}) values of 275 seconds and 230 seconds for the bipropellant and monopropellant systems, respectively. It is noted that nitrogen is used as the pressurant for both systems, and that equivalent oxidizer and fuel tanks are required for the bipropellant system.

The data of Table 5.7-3 indicate that the hypergolic bipropellant system has a weight advantage over the monopropellant hydrazine system. However, the latter type of APS has been recommended for the ATS-4 application because of consideration of such additional factors as:

- Long-term reliable operation for a 2-year mission
- Development status
- Cost
- Safety

In order to even further improve the simplicity and reliability of the monopropellant hydrazine system, a simple blow-down system is proposed. Thus, the propellant tank pressure will not be regulated; it will be allowed to decay as propellant is expended. While a consequent reduction in thrust level will be experienced, no loss in specific impulse will result.

TABLE 5.7-2 PRELIMINARY APS TOTAL IMPULSE REQUIREMENTS

Launch Vehicle	Total Impulse (lb - sec)
SLV3C/Centaur/BII-027B (2nd apogee)	17,100
SLV3C/Centaur/Spin Stabilized TE 364-3 (2nd apogee)	27,200
Titan 3C	19,400

TABLE 5.7-2 PRELIMINARY APS DATA

Total Impulse (lb-sec)	APS	Fuel Weight (lbs)	Oxydizer Weight (lbs)	Prop. Tank Wt. (lbs)	Prop. Tank Diam. (ins)	Nitrogen Weight (lbs)	Nitrogen Tank Wt. (lbs)	Nitrogen Tank Diam. (ins)	APS Weight (lbs)
17, 100	Bi-Prop.	24.4	39.1	6.9 (2)	11.7 (2)	1.1	1.3	6.6	95
	Mono-Prop.	76.0	--	11.5	16.1	1.4	1.6	7.2	104
27, 200	Bi-Prop.	38.8	62.1	8.8 (2)	12.2 (2)	1.8	2.0	7.4	138
	Mono-Prop.	120.8	--	14.6	18.8	2.3	2.7	8.2	153
19, 400	Bi-Prop.	27.7	44.4	7.4 (2)	13.6 (2)	1.3	1.5	6.9	105
	Mono-Prop.	86.1	--	12.2	16.8	1.6	1.9	7.5	115

Status monitoring of tank pressure and temperature will enable the current thrust level to be calculated to an accuracy compatible with orbital guidance requirements. This is based upon the guidance system concept of using ground-initiated on-off thrust commands to execute the required orbital maneuvers.

Figure 5.7-1 presents a schematic of a blow-down, hydrazine APS configuration as proposed by Hamilton Standard. It is noted that squib valves can be actuated on command to shut off the propellant flow should a thruster-on type failure occur. Further discussion of system development is provided in paragraph 6.4.2. Since a similar propulsion approach is recommended for the thrusters for the attitude stabilization and control system, system weight economies can be effected through the use of common propellant tanks.

Refined orbit payload data were used to arrive at final weight estimates for the recommended APS. Thus, the final payload data of Table 5.4-3 were combined with the total APS velocity impulse requirements given in Table 5.7-1, to yield the final total impulse requirements listed in Table 5.7-4. A lower I_{sp} value of 220 sec, corresponding to the reduced (1-pound) thrust levels for the 3 nozzles of the APS, was used to calculate the associated fuel weights. The total APS weights which are tabulated for the various study cases include tank weights, nozzles, plumbing, fuel residuals, etc.

The "net payload" data of Table 5.7-4 are included so as to provide a more direct comparison of the actual orbit payload capabilities associated with the various apogee stages. These payload data were obtained by reducing the nominal payload weights by the APS fuel weights required for correcting the maximum anticipated (3σ) orbit injection errors and for compensating the synchronous speed deficiency for the Centaur 1st apogee injection cases. It can be seen that despite the greater injection

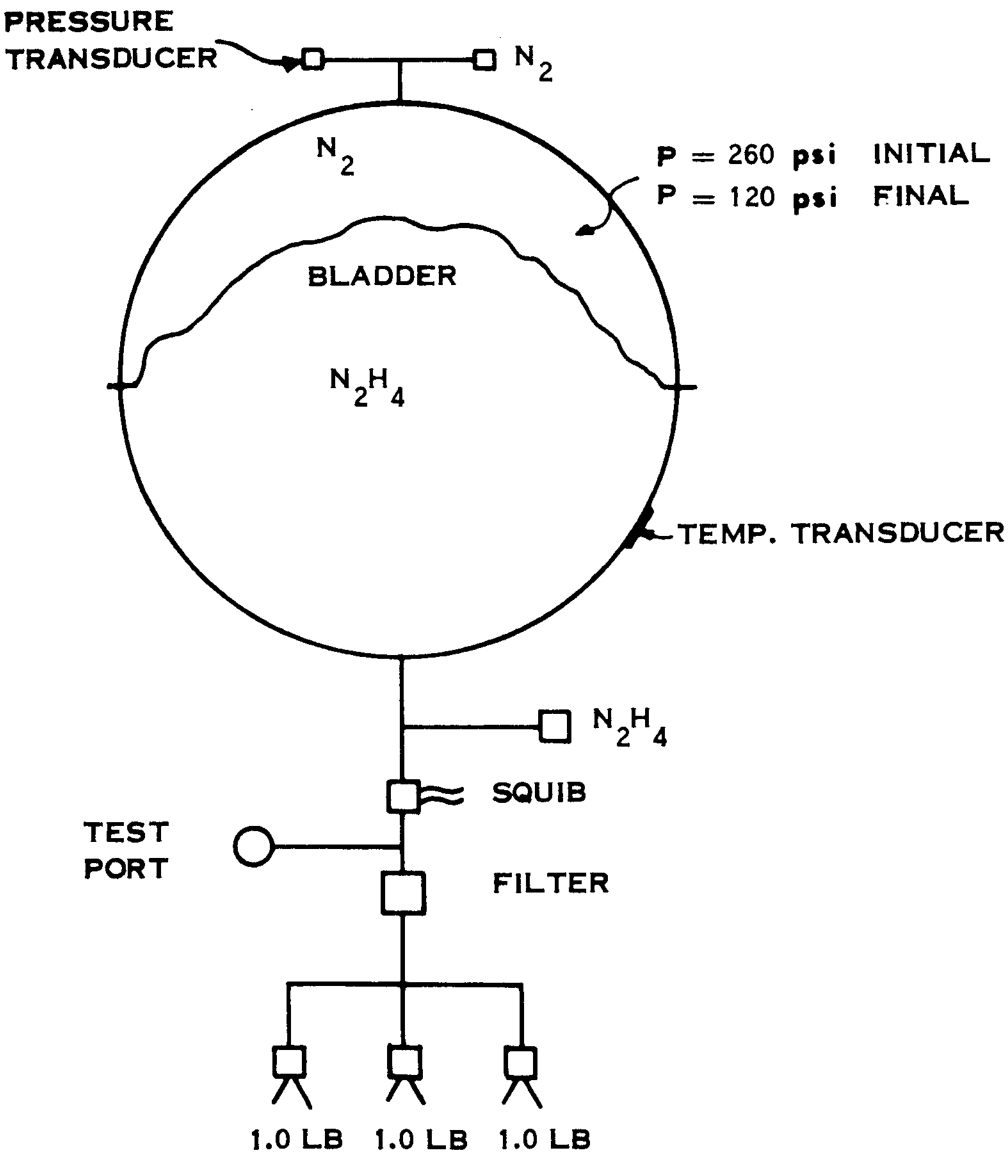

Figure 5.7-1 Blow Down Hydrazine APS

TABLE 5.7-4

APS WEIGHT DATA

(MONOPROPELLANT HYDRAZINE; Isp = 220 SEC)

BOOSTER (SHROUD)	APOGEE STAGE	INJ APOGEE	ΔV TOTAL (FT/SEC)	ORBIT PAYLOAD (LB)	TOTAL IMPULSE (LB-SEC)	FUEL WEIGHT (LB)	TOTAL APS WEIGHT (LB)	NET PAYLOAD* (LB)
SLV3C/ CENTAUR	BII-027B	2ND	415	1,265	16,300	74	106	1,235
		1ST	600	1,440	26,800	122	157	1,370
(10 FT EXT SURV)	SPIN STAB (TE 364-3)	2ND	595	1,605	29,600	135	172	1,525
		1ST	760	1,675	39,500	180	240	1,555
	BII-128B	2ND	415	1,400	18,100	82	112	1,365
		1ST	600	1,535	28,600	130	166	1,460
	SPIN STAB (TE 364-4)	2ND	595	1,790	33,000	150	194	1,705
		1ST	160	1,825	43,100	196	266	1,695
TITAN 3C (MOD OAO)	——	1ST	355	1,865	20,500	93	124	1,840

*NET PAYLOAD = ORBIT PAYLOAD-FUEL WEIGHT FOR CORRECTION OF SYN SPEED DEFICIENCY AND INJ ERRORS.

E-6

errors associated with the spin-stabilized apogee injection stages, they still provide a "net" payload advantage.

A breakdown of the indicated APS weight figure of 172 pounds for the reference case (SLV 3C/Centaur/Spin Stabilized TE 364-3 with 2nd apogee injection) is provided in Table 5.7-5.

TABLE 5.7-5 APS WEIGHT BREAKDOWN
Reference Case
(Blow-down Monopropellant Hydrazine)

Item	Weight (lbs)
Fuel	135
Fuel Tank (Tank diam = 23.5 inches)	25
Nozzles (3)	3
Miscellaneous (Valves, tubing, pressurant, residuals)	9
TOTAL	172

5.8 ORBITAL GUIDANCE

5.8.1 General Requirements

There are a number of separate accuracy requirements imposed on the various guidance operations which must be accomplished during the ATS-4 mission; including initiation of the thrusting period for the apogee injection maneuver, identification and correction of orbit injection errors, North-South station keeping and East-West station keeping and repositioning. In addition, in order to be able to command the attitude control system to provide the proper pitch and roll offset angles for the satellite to point at a designated ground station, the ephemeris of the satellite (relative to the Earth) must be accurately known. This includes the requirement to identify the daily periodic variations in satellite subpoint latitude and longitude, caused by the existing orbit inclination and eccentricity errors, so that these can be compensated by the SCS during fixed offset pointing mode.

In order to suitably restrict the associated contribution to orbit injection errors, it is required to identify the argument of apogee and the instantaneous satellite angular position relative to apogee in the transfer orbit to within a central angle accuracy of 0.01°. Appropriate initiation of the apogee injection maneuver can then be commanded from the ground command-control station.

For the purpose of identifying final orbit injection errors so they can be corrected, the orbital elements should be measured to the following accuracies (maximum allowable error): Period, ±0.025 min; eccentricity, 0.00005; inclination, $\pm 0.025^{\circ}$; right ascension, $\pm 0.025^{\circ}$; argument of perigee, $\pm 0.025^{\circ}$; true anomaly, $\pm 0.025^{\circ}$. Deviations in the orbit elements from the desired synchronous, 24-hour, circular equatorial orbit shall be corrected to within the following accuracies: Period, ±0.25 min. (corresponding to a longitude drift rate of 0.0625 deg/day); eccentricity, 0.0005 (corresponding to a total periodic daily longitude oscillation of 0.115°); and inclination error, ±0.10 (corresponding to a periodic daily oscillation in latitude of ±0.10°). Coarse corrections of the initial period error shall be initiated within 2-4 hours after orbit injection so as to prevent excessive off-station drift due to the effect of this error.

During North-South station keeping, the same inclination measurement and correction accuracies shall be achieved. During East-West station keeping operations, deviations in the satellite subpoint longitude from its nominal value (due to longitude drift rates caused by orbit perturbations) of up to ±1° can be tolerated. Orbit eccentricity shall be kept within 0.001, corresponding to a total maximum daily longitude excursion of 0.23°.

5.8.2 Orbit Injection Error Correction

A study has been conducted to establish the accuracy to which the ATS-4 synchronous orbit elements can be determined as a function of track time after injection, using the ATS-4 stations at Rosman and Mojave. While the study assumed an orbital longitude station of 90° West, it is not expected that the results would be substantially different for the reference injection longitude of 54° West (second apogee injection with the SLV3C/Centaur/Spin-stabilized TE 364-3).

The final orbit after injection was assumed to be nominally circular. The ATS radar characteristics were taken as described in document S2-0000, Appendix A, 5.0 Ground Stations. This document indicated that the ATS radar has the following error model:

Range	±1.5 meters
Range Rate	±.01 meters/sec
Elevation	±1.0 milliradian
Azimuth	±1.0 milliradian

These errors values were considered to be representative of both random and bias type errors.

It was also assumed that the effective data rate is one set of range, range-rate, azimuth and elevation measurements per hour. The chosen data processing scheme or navigation filter was an extended state Kalman filter. The extended state included the radar bias terms as well as the usual position and velocity states.

The results of the filter error analysis were transformed into one sigma values for period, inclination and eccentricity measurement errors as a function of time after injection. Table 5.8-1 presents the results of these analyses.

It can be seen that the orbit element measurement accuracies that are attainable after four (4) hours of tracking are essentially consistent with the required measurement accuracies given in the previous subsection.

Any existing inclination error (Δi) in the final orbit will be corrected independently of the in-plane errors, using the APS thruster with the North-oriented thrust vector (when the ATS-4 is stabilized in the nominal Earth-oriented attitude). Positive (negative) inclination errors will be removed by ground-initiated on-off thrust commands that bracket satellite passage through the descending (ascending) node.

Direct ground control of the proper thrust initiation time and thrust termination time for the APS will be based on a calculated current thrust level in accordance with received APS status data such as tank pressure and temperature. (It is noted that a simple blow-down system is predicated for the monopropellant hydrazine APS; hence, its thrust level will decay as the system pressure drops with propellant utilization.)

The satellite's central angle travel in orbit during these corrective maneuvers will be restricted to about 10^{o}. This will ensure most effective use of the thrust impulse for correction of the inclination error. Assuming a maximum satellite weight of 1600 lbs., the 1-lb. thrust level of the APS

TABLE 5.8-1 SYNCHRONOUS ORBIT MEASUREMENT ERRORS VERSUS TIME AFTER INJECTION

Time	One Sigma Error Value		
	Period (min.)	Inclination (deg.)	Eccentricity
Injection	43.0	0.6	.20
Injection plus 1 hr	11.1	0.575	$.528 \times 10^{-2}$
Injection plus 2 hrs.	.128	0.0196	$.6 \times 10^{-4}$
Injection plus 3 hrs.	.015	0.0127	$.773 \times 10^{-5}$
Injection plus 4 hrs.	.0118	0.0116	$.585 \times 10^{-5}$
Injection plus 5 hrs.	.0085	0.0102	$.425 \times 10^{-5}$

thruster can effect a ΔV change of about 48 ft/sec during the 40 minutes associated with the indicated angular travel in orbit.

A 3σ value of 195 ft/sec for the required out-of-plane corrective velocity impulse ΔV_{OP} was given in Table 5.5-2 for the reference launch vehicle-AIS configuration. Hence, as many as four corrective velocity impulses of the 48 ft/sec magnitude could be required for correction of the initial inclination error.

The in-plane orbit injection errors of concern, period error ΔP (or equivalently semi-major axis error Δa) and eccentricity error e, will be corrected in concert to minimize ΔV requirements. To do this, the East-West oriented thrusters of the APS will be used to provide appropriate tangential velocity impulses upon command from the master ground station.

The differential changes in the orbital elements of interest (semi-major axis (a) and eccentricity (e) caused by small circumferential impulsive velocity corrections, are given by:

$$\frac{\Delta a}{a} = \frac{2V^2 a}{\mu} \cos\gamma \frac{\Delta V}{V}$$

$$\Delta e = \frac{1}{\cos\gamma} \left[2\cos\theta + e\left(1 + \cos^2\theta\right) \right] \frac{\Delta V}{V}$$

where

γ = flight path angle

θ = true anomaly

μ = gravitational constant

The maximum flight path angle (γ) occurs at a true anomaly given by $\theta = \cos^{-1}(-e)$; hence, $\cos\gamma \approx 1$, since $\cos\gamma_{max} = \sqrt{1 - e^2} \approx 1$. Therefore for the nearly circular orbit under consideration, Δa may be further approximated as

$$\frac{\Delta a}{a} = \frac{2}{3} \frac{\Delta P}{P} \approx \frac{2\Delta V}{V}$$

A velocity impulse to correct the semi-major axis error Δa will alter the eccentricity as follows:

$$\Delta e \approx \frac{\Delta a}{2a} \left[2 \cos\theta + e\,(1 - \cos^2\theta) \right]$$

In order to jointly correct both types of in-plane errors, if the satellite drifts Eastward ($\Delta a < 0$) after injection then a forward corrective velocity impulse should be imparted at apogee. A Westward drift ($\Delta a > 0$) requires a braking correction at perigee. If either Δa or Δe should prove to be zero following injection, then the use of two appropriate tangential velocity impulses 12 hours apart will permit correction of one element without affecting the other.

By jointly correcting both the period and eccentricity errors, the required in-plane corrective velocity impulse ΔV_{IP} is never more than the maximum velocity impulse value required to correct eccentricity (ΔV_e) or period error ($\Delta V_{\Delta P}$). A 3σ value for ΔV_{IP} of 150 ft/sec, is given in Table 5.5-2 for the SLV3C/Centaur/Spin-stabilized TE 364-3. Hence, several corrective velocity impulses equivalent to the 48 ft/sec value previously discussed for the out-of-plane error case may be required to reduce the in-plane injection errors to acceptable levels.

5.8.3 Station Keeping and Repositioning

Based on the orbit perturbation studies previously described, the North-South station keeping mode must be designed to correct the long period inclination perturbations caused by lunar-solar gravitational effects. The East-West station keeping mode is concerned primarily with countering the disturbing tangential accelerations caused by the second order, sectorial gravitational harmonic associated with the Earth's equatorial ellipticity.

It was previously indicated that a change in orbit inclination of about 0.75^{o} would occur during the course of a year. Hence, to demonstrate a complete North-South station keeping capability for this period, a ΔV of about 130 ft/sec would be required to compensate the inclination buildup.

On-off thrust commands initiated near the appropriate orbital node by the master ground station are planned to effect the desired North-South station keeping. Using ΔV impulses of up to the indicated maximum value of 48 ft/sec, essentially three such maneuver commands executed every four months will be adequate.

In choosing an East-West station keeping or guidance technique for maintaining the ATS-4 above a desired longitude station, strong emphasis was placed on the following criteria. The technique should be highly reliable, simple to implement and require a minimum of ground track data. As has been noted, the perturbing accelerations acting on the satellite are very small (about 1.7×10^{-7} ft/sec^{2}). Hence, an intermittent, differential mean motion guidance concept has been chosen as being simple to implement but adequate to meet all requirements.

This mean motion correction technique operates basically as follows: (It is assumed that a synchronous, circular, equatorial orbit has been attained for the desired satellite position.)

(1) The disturbing force associated with the equatorial ellipticity of Earth causes the satellite to drift Westward relative to Earth.

(2) When this longitude drift ($\Delta\lambda$) is observed to equal the preselected limit value ($\Delta\lambda = -\Delta\lambda_{LIM}$), the Westward oriented thruster of the APS will be activated by ground command. (A $\Delta\lambda_{LIM}$ value of 1^{o} is compatible with the East-West station keeping accuracy requirements.)

(3) This corrective velocity impulse, which is actually a Westward braking impulse, will increase the mean motion of the satellite and cause it to drift Eastward relative to the Earth.

(4) By properly controlling the magnitude of this impulse, the satellite will be caused to drift Eastward to $\Delta\lambda = + \Delta\lambda_{LIM}$ before the gravitational perturbing forces stop its relative motion and again cause it to drift Westward.

(5) When the satellite again drifts to its control boundary ($\Delta\lambda = \Delta\lambda_{LIM}$), another corrective velocity impulse is applied, and the sequence is repeated.

Only one longitude boundary is used to trigger a corrective thrust during the subject station keeping mode; this is the boundary toward which the terrestrial gravitational disturbing forces cause the vehicle to drift. Because there is a steady disturbing acceleration field, a station keeping guidance method based on dual control boundaries on each side of the desired longitude station (with possible attendant stability problems) is not required. (A modification of this guidance logic could be required if the satellite were located near an extension of the equatorial major axis.)

As previously indicated in subsection 5.6 of this report (Figure 5.6-4) a corrective velocity impulse of at most 5.4 ft/sec is required to provide one year of East-West station keeping above the most unfavorable longitude stations (longitude 64° West is such a location). By providing 1/4 of this velocity impulse every three months, the associated longitude excursions can be kept within $\pm 1^{\circ}$ as desired.

East-West station repositioning will be accomplished using ground-initiated on-off commands for the East-West thrusters of the APS. Longitude drift rates of up to 5.35 deg/day can be employed to transfer the satellite to a new synchronous longitude station, based on a 100 ft/sec ΔV.

5.9 REFERENCES AND SYMBOLS

5.9.1 References

5-1 "Atlas/Centaur/Burner II Design Study," General Dynamics Report No. RKS-1022, 1 August 1966.

5-2 Boeing Letter of 22 July 1966, File No. 2-6815-331.

5-3 "Space Technology Presentation," Thiokol Report

5-4 Martin Letter of 7 July 1966, File No. 6-Y-34230

5-5 "Proposal for Studies of Synchronous Meteorological Satellite System Problems," Republic Aviation Corporation Report No. RAC 826, Volume III, 23 July 1962

5-6 Munsen, P., Bailie, A., and Upton, E., "Development of the Lunar and Solar Perturbations in the Motion of an Artificial Satellite," NASA TN-D-4941, January 1961

5-7 Kozai, Y., "On the Effects of the Sun and the Moon Upon the Motion of a Close Earth Satellite," Smithsonian Institution Astrophysical Observatory Special Report No. 22, March 1960

5-8 Republic Aviation Corporation Proposal, "Radio-Microwave Powered 24-Hour Communication Satellite System," RAC 648-500, December 21, 1959

5-9 Brouwer, D., and Clemence, G. M., "Methods of Celestial Mechanics," Academic Press, New Yori, New York, 1961

5-10 Smart, W. M., "Celestial Mechanics," Longmans, Green and Company, London, 1953

5-11 Wyatt, S. P., "The Effects of Radiation Pressure on the Secular Acceleration of Satellites," Simithsonian Institution Astrophysical Observatory, Special Report No. 22, March 1961

5-12 Kozai, Y., "The Motion of a Close Earth Satellite," The Astronomical Journal, Volume 64, No. 9, November 1959

5-13 Issak, I. G., "A Determination of the Ellipticity of the Earth's Equator from the Motion of Two Satellites," Astronomical Journal, Volume 66, No. 5, June 1961

5-14 Pines, S., and Wolfe, H., "Interplanetary Trajectory by the Encke Method Programmed for the IBM 707 and 7090," Republic Aviation Corporation Report No. RAC 656-451, 12 December 1960 (prepared under Contract NASA-109).

5-15 Kozai, Y., "Tesseral Harmonics of the Potential of the Earth as Derived from Satellite Motions," Smithsonian Institution Astrophysical Observatory Special Report No. 72, August 1961

5-16 Frick, R. H. and Garbey, T. B., "Perturbations of a Synchronous Satellite Due to Triaxiality of the Earth," Journal of Aerospace Sci., Volume 29, No. 9, September 1962

5-17 Pines, S., Wolfe, H., and Richman, J., "Orbit Determination and General Purpose Differential Correction Program," Republic Aviation Corporation Report No. RAC 696, 25 April 1962 (Contract NAS 5-293).

5-18 Wagner, Carl A., "Determination of the Ellipticity of the Earth's Equator for Observations on the Drift of the SYNCOM II Satellite," NASA TN D-2759, May 1965

5.9.2 List of Symbols

a	=	Semimajor axis
a_e	=	Earth's mean equatorial radius, 2.0926×10^7 feet
e	=	Eccentricity
GHA	=	Equivalent Greenwich hour angle
g'	=	True anomaly of disturbing body
h	=	Altitude
i	=	Inclination
i'	=	Relative inclination with respect to plane of disturbing body
$J_2^{(2)}$	=	Earth-shape constant related to the second order sectorial gravitational harmonic associated with equatorial ellipticity
m	=	Mass
P	=	Period
R_b	=	Range angle
r	=	Satellite orbit radius
t	=	Time
t_I	=	Impulse time, seconds
V	=	Velocity
ΔV	=	Incremental or impulsive velocity addition
γ	=	Flight path angle
Δ	=	Incremental change
η	=	Mean notion
λ	=	Longitude
λ_m	=	Minor axis longitude
$\Delta\lambda_{m_o}$	=	Initial satellite longitude with respect to minor axis

$\Delta\lambda$	=	Longitude excursion
$\Delta\lambda_m$	=	Satellite longitude excursion measured from minor axis
μ	=	Mass gravitational constant for the earth, Gm_E, 1.4077×10^{16} ft^3/sec^2
$\phi_2^{(2)}$	=	Longitude of equatorial major axis
$\theta\gamma$	=	Satellite true anomaly
Ω	=	Right ascension of ascending node
ω	=	Angular velocity or argument of perigee
ω_o	=	Angular velocity of earth, 7.29×10^{-5} radian/sec

Subscripts

C	=	Circularization
K	=	Apogee kick
m	=	Moon or minor axis of earth equator
o	=	Initial or constant value
S	=	Sun or synchronous value
W	=	Wait orbit
24	=	Synchronous orbit value